GENE REGULATION DURING CENTRAL NERVOUS SYSTEM DEVELOPMENT AND POST-INJURY REGENERATION

By

YING LI

A dissertation submitted to the

Graduate School-New Brunswick

Rutgers, the State University of New Jersey

and

The Graduate School of Biomedical Sciences

In partial fulfillment of the requirements

For the degree of

Doctor of Philosophy

Graduate Program in Biomedical Engineering

Written under the direction of

Li Cai, Ph.D.

And approved by

_____

_____

_____

_____

New Brunswick, New Jersey

January 2016

ABSTRACT OF THE DISSERTATION

Gene Regulation during Central Nervous System Development and Post-Injury Regeneration

By Ying Li

Dissertation Director:

Li Cai, Ph.D.

Central nervous system (CNS) development and post-injury neurogenesis require accurate coordination of neural stem cell proliferation, progenitor cell differentiation, neuron, glia migration and maturation, and synapse formation between axons and dendrites. Such systems with high complexity require strict temporal and spatial control via several levels of regulation, in which the transcription regulation is one of the most critical steps. The developmental and injury-repair process involves over 18,000 genes, for majority of which the molecular mechanism governing their transcription remains largely unknown. In an attempt to address this question, four projects were conducted focusing on two levels of transcription regulation: i.e., chromatin modification, and the interaction of *cis*-acting regulatory sequences with *trans*-acting protein factors. Computational methods were adopted to analyze the sequences of the *cis*-elements and

make predictions for their interacting transcription factors (TFs). The functional roles of these *cis*- and *trans*-elements were further determined *in vivo* and *in vitro*. The following findings are presented: 1) the function of DNA topoisomerase II beta (Top2b) in proper laminar formation and cell survival during retinal development; 2) the development of computational method for identifying gene regulatory networks involving enhancers and master TFs that are important in retinal cell differentiation; 3) the mechanism of Notch1 regulation in neural stem/progenitor cells via the interaction between Nkx6.1 and a CNS specific enhancer CR2 during the development of the spinal cord interneurons; and 4) the role of CR2 in aNSC activation after injury. Findings from this dissertation provide new insights into the molecular mechanisms underlying transcription regulation during CNS development and post-injury neurogenesis. They can also serve as a basis for future development of gene therapies and regenerative medicine for neurological disorders including spinal cord injury.

ACKNOWLEDGEMENTS

I would like to first thank my mentor, Dr. Li Cai, for his guidance, support and excellent training. I won't be able to make all the progress and achievements without his generous support. I would also like to thank my committee members, Dr. Martin Grumet, Dr. Bonnie Firestein, Dr. Roko Rasin and Dr. Kelvin Kwan, for their helpful advices on my research, presentation and manuscripts. I also want to thank all the previous and current Cai lab members, for their help with the experiments and discussions. Finally, I would like to thank my parents, who are the greatest parents in the world and have always been supportive. I am truly grateful to be around with so many nice people and have the opportunity to study here at Rutgers.

TABLE OF CONTENTS

LIST OF TABLES

Chapter II

Chapter III

Chapter IV

LIST OF FIGURES

Chapter II

Chapter III

Chapter IV

Chapter V

LIST OF CHARTS

Chapter V

ABBREIVATIONS

aNSC	adult neural stem cell
CNS	central nervous system
CR	conserved region
d	day
dP1	dorsal progenitor layer 1
dpi	days post injury
FP	floor plate
GFP	green fluorescence protein
h	hour
min	minute
MN	motor neuron
NSC	neural stem cell
OPC	oligodendrocyte progenitor cells
pMN	motor neuron progenitor layer
pV2	ventral progenitor layer 2
RFP	red fluorescence protein
RP	roof plate
SCI	spinal cord injury
TF	transcription factor
TFBS	TF binding site
Top2b	Topoisomerase II beta
VZ	ventricular zone

ACKNOWLEDGEMENT OF SOURCE MATERIAL

All relevant chapters, subsections, and figures are accompanied by references to their original publication source, which exclusively includes work where I am a first author.

These references accompany the chapter/subsection titles in the main text, are within figure legends, and also can be summarized:

Chapter II: Topoisomerase II beta is required for proper retinal development and survival of postmitotic cells (Li et al., 2014). It is available from DOI: 10.1242/bio.20146767.

Chapter III: Transcriptional regulatory network for retinal development (Li et al., 2011). It is available from http://www.intechopen.com/articles/show/title/prediction-of-transcriptional-regulatory-networks-for-retinal-development .

It should be noted that Chapters IV and V are work in submission or in preparation of this thesis:

Chapter IV: Nkx6.1 regulates notch1 expression during interneuron development.

Chapter V: Molecular mechanism of neural stem cell activation after spinal cord Injury.

Chapter I

Introduction

In the field of biomedical engineering, the central nervous system (CNS) has always been one of the most prevailing topics. Researchers study how the brain, spinal cord and retina are constructed, how do the neurons in each organ function, how do they communicate with each other, and most importantly, how do we diagnose and cure the CNS disease. Here in my study, I tempted to answer some of these questions regarding CNS development and disease from the aspect of gene regulation.

As the headquarter that sends out commands to our body, the CNS itself is controlled by the genetic codes that are embedded in every cell of our body. The approximately 25,000 different genes in human genome precisely produce RNAs and proteins to coordinate the development, functioning and repair of the CNS and other organs. These genes are active or inactive in particular cells at particular time according to the intrinsic clock and the extrinsic information received from the environment. Transcriptional regulation is triggered first to either activate or block the binding of the transcriptional starting complex to the promoter region, and consequentially activates or silences the target gene. During this process, two important steps are included: a) release of DNA from the highly coiled chromatin structure; and b) send out a signal to RNA polymerase II by the interaction of the proteins (TFs) and the non-coding regulatory elements (enhancer, silencer, insulator, etc.). Both steps are critical and can be utilized to manipulate the expression of specific gene. My study focused on both steps in the transcription regulation involved in the development of CNS, including a) the function of a topoisomerase protein that helps release of DNA in the retina development (Chapter II); b) a transcription network that involves multiple master TFs and cis-elements (Chapter

III); c) the transcriptional regulation of Notch1 gene that is important to many major development events (Chapter IV); and d) neural regeneration after CNS injury (Chapter V).

One peer reviewed paper and a book chapter describing the first two studies have been published (Li et al., 2014; Li et al., 2011). One manuscript about the third study has been submitted and another one for the forth study is current in preparation.

The following paragraphs review the literatures concerning the background of these studies and discuss the significance.

1. Transcriptional regulation of gene expression

As first established in bacterial systems (Jacob and Monod, 1961), the concept of transcriptional regulation has been developed and included the control of gene transcription on multiple levels. Such mechanisms include the epigenetic regulators that modifies chromatin structure to indirectly affects gene expression, and the *cis*-element-*trans*-factor system that directly influence the efficiency of RNA polymerase II (Bannister and Kouzarides, 2011; Bonasio et al., 2010; Conaway and Conaway, 2011; Spitz and Furlong, 2012). The former usually includes chromatin modifications on histone structure and is vulnerable to external cues (Bannister and Kouzarides, 2011), while the latter emphasizes on the interaction between the TF and the regulatory DNA sequences which are precisely encoded in the genome (Spitz and Furlong, 2012). Topoisomerases are one of the enzymes that help to change the topo-structure of DNA and aid DNA transcription, modification or repair (Berger et al., 1996). A study focused on the function of Topoisomerase II beta (Top2b) during retinal development is described in Chapter II.

To study the intrinsic signal of gene regulation, researchers intensively focused on the non-coding regions of mammalian genome, which is approximately 98% of the whole

DNA sequence (Vavouri et al., 2007). Many of the gene-regulating *cis*-elements reside in these non-coding regions. They contribute to the regulation of genes through interaction with the *trans*-elements or production of non-coding RNA regulators such as miRNAs, snRNAs and siRNAs (Lee and Young, 2013). The *trans*-elements, or TFs usually function in a cooperative fashion and form a complex with the RNA polymerase to control the start and end of transcription. DNA loops to allow such transcription initiation complex to interact both the enhancer and the core promoters of nearby or distant genes (Krivega and Dean, 2012).

Cis-elements like enhancers can be identified by testing the highly evolutionally conserved regions of non-coding DNA sequences and exam their ability to drive report expression in a enhancer-reporter vector (Bucher, 1999). Large number of putative enhancers have been identified and available in multiple databases, such as Ensembl (Flicek et al., 2012) and VISTA Enhancer Browser (Visel et al., 2007). These enhancers provide a good resource for identifying the TFs that bind on them for the regulatory function. For this purpose the TF binding weight matrices can be used by mapping programs such as MatInspector to predict the potential factor binding sites on targeting enhancer sequence, as described in Chapter III. Master TFs that bind to multiple enhancers of genes specific to developing mouse retina were identified. A gene regulatory network was built base on these master TFs and enhancers. Although this method only identifies the TFs that direct bind to enhancer, it provides a reliable pipeline for study of gene regulatory when combined with experimental verification. In Chapter IV, a Notch1 enhancer is validated and its interacting TF is identified using such pipeline.

As technology advances, experimental approaches for studying transcriptional regulation *in vivo* now extend from single-molecule techniques to genome-wide measurements (Coulon et al., 2013). Massive whole genome sequencing results are

widely used in identifying chromatin modification sites, active enhancer loci and putative TFs (Core et al., 2008; Gamsiz et al., 2012; Lee and Young, 2013). In Chapter II, RNA-seq was used to identify the targets of Topoisomerase II beta (Top2b) in retina and further study the different role of Top2b at different stage of retinal development.

2. Development of the retina and spinal cord

Brain, spinal cord and neural retina are the three major components of the CNS. They are all highly organized organs with complex physiologic and functional structures which require coordinated temporal and spatial regulation during embryonic development. In this study I first focused on the gene regulatory in neural retina, as the retina is like a window to the brain not only in the literal sense but also in structural and pathologic aspects (London et al., 2013). Then the focus moved to spinal cord, which is the relay station for communication of brain and other parts of our body.

The neural retina presents a excellent model for investigating the molecular mechanism of neural cell proliferation, differentiation and migration in the CNS. The six types of neurons and one type of glia cells are sorted out in three layers and form complex pathways for proper transduction of vision signals to the brain (Harada et al., 2007). They were derived from a common progenitor cells which reside in the inner layer of the optic cup, and differentiated in an orderly manner which is conserved in vertebrates (Marquardt and Gruss, 2002). The TFs from basic helix-loop-helix (bHLH) and homeobox families contribute largely to the lineage determination of retinal progenitor cells and guide them to distinct destinies (Hatakeyama et al., 2001; Marquardt and Gruss, 2002). In Chapter II I discussed the influence of DNA topo-structure modulator Top2b on the transcription regulation during retina development. The consequences of deleting Top2b in mouse retina is shown and discussed.

Spinal cord has been another model for studies of neural development and diseases. The definition of spinal cord cell identities is achieved by a two-dimensional coordination between Sonic hedgehog (Shh) and bHLH gradients (Bae et al., 2000; Ericson et al., 1997). TFs are expressed in distinct domains, promoting the specific types of spinal cord cells while suppressing the cells from adjacent domains to preventing cells from developing into hybrid identities (Alaynick et al., 2011). These progenitor cells later will further differentiate into oligodendrocytes, astrocytes, motor neurons and 26 types of interneurons, in which more complicated transcriptional regulation is involved (Alaynick et al., 2011). Notch1 and Nkx6.1 are both regulators that are involved in the interneuron fate determination. Notch1 specifies the V2b interneurons (Del Barrio et al., 2007; Yang et al., 2006b) while Nkx6.1 is important for all ventral interneurons (Briscoe et al., 2000). In Chapter IV, I described how Nkx6.1 was found to be interacting with an enhancer of Notch1 (CR2) and regulated Notch1 expression. This finding revealed the upstream regulator of Notch1, and added a missing link in the network of TFs that regulates ventral spinal cord development.

3. Gene regulation and activation of adult neural stem cells after spinal cord injury

Injury to the brain and spinal cord typically leads to irreversible death of neurons and permanent loss of function since the ability of neural cells to regeneration is very limited (Farooque, 2000). Thus for treatment of spinal cord injury (SCI), transplantation of embryonic stem cells, induced pluripotent stem cells (iPSC) or neural progenitors with or without synthetic biomaterials have been prevailing. Evidence suggest that grafted fetal or iPSC were able to survive in the transplantation site, and achieve some growth in axons which can form a function relay (Kobayashi et al., 2012; Ogawa et al., 2002). However, challenges in timely transplantation, grafting and immune rejection remain

unsolved. In order to overcome these difficulties, researchers seeking alternative routes start to pay attention on promoting endogenous stem cells (Picard-Riera et al., 2004) or direct differentiation of astrocytes into neurons (Su et al., 2014).

Many studies have established that adult neural stem cells (aNSCs) exist in both parenchymal and ependymal regions in the spinal cord (Horner et al., 2000; Yamamoto et al., 2001). The ependymal cells are able to proliferate and predominantly differentiate into astrocytes and oligodendrocytes when they are triggered by injury (Barnabe-Heider et al., 2010; Meletis et al., 2008; Yamamoto et al., 2001). They are also capable of differentiate into neurons in vitro while growth factor is present (Ohori et al., 2006). However, the majority of ependymal cells will differentiate into astrocytes, which are the major component of scar tissue which prevents re-alignment of neural connections and obstruct the functional recovery (Yiu and He, 2006). The oligodendrocytes differentiated from ependymal cells are found to suffer from major death and cannot form myelin sheath around the exposed axons of surviving neurons (Meletis et al., 2008). Although all these results suggest that the resulting cells of the neurogenesis of ependymal cells are vulnerable to the adverse environment in injured tissue, these aNSCs are reliable source of regenerative medicine. Studies of facilitating the ependymal cell regeneration by isolating and culturing showed encouraging results of transplantation, with long-distance neural connection and recovery of motor activity (Moreno-Manzano et al., 2009). In Chapter V, cells collected from the injury site of specific transgenic mice are cultured and studied for their ability to proliferate and differentiate. These transgenic mice carry a reporter GFP gene following the Notch1 enhancer CR2. CR2 was proven to be involved in the interneuron differentiation in Chapter IV.

Chapter II

Topoisomerase II beta is required for proper retinal development and survival of postmitotic cells

1. Prologue

Topoisomerase II beta (Top2b) is a member of the Topoisomerase family which is known to be the catalyzer for unconstraining DNA supercoils in an ATP-dependent manner (Nitiss, 2009; Wang, 2002). It is important for releasing DNA and replacing histones during transcription initiation, DNA repair and DNA condensation (Meyer-Ficca et al., 2011). In mouse brain and other regions of the CNS, Top2b is expressed in the postmitotic neurons located in the cortical plate region which are undergoing terminal differentiation (Lyu and Wang, 2003a; Tsutsui et al., 1993; Tsutsui et al., 2001b). Evidences suggest that Top2b is involved in regulating several genes related to brain development (Lyu and Wang, 2003a) and neural degeneration diseases such as autism spectrum disorder (King et al., 2013).

In specific, deletion of Top2b in mouse brain leads to improper neurite outgrowth, abnormal migration of cerebral cortical neurons and defective lamination of cerebral cortex (Lyu and Wang, 2003a; Nur et al., 2007; Yang et al., 2000). In retina, Top2b is known to be involved in the laminar-specific targeting of retinal ganglion cell axons and dendrites (Nevin et al., 2011a). However, due to the ubiquitous expression pattern of Top2b, the traditional constitutive and brain-specific knock-out mice suffer from perinatal death. Such early death obstructs study of the *in vivo* function of Top2b, especially in the postnatal neural development. Since retina is an non-essential part of CNS that is not required for the survival of animals, it provides an excellent model for the study of neural development. Thus in this study, a retinal-specific Top2b knock-out mouse line was

utilized in additional to the traditional whole-body knock-out mouse line to reveal the consequences of lack of Top2b.

The specific hypothesis to be tested in this study is that Top2b is involved in proper development of neural cells in mouse retina. To test this hypothesis, eyeballs from several stages between embryonic day 17.5 (E17.5) to postnatal day 180 (P180) were collected and thorough analysis of the development, differentiation of the seven types of retinal cells was performed. Immunohistochemistry and Click-iT cell proliferation assays were used to study the proliferation, differentiation of the retinal progenitor cells and the migration, dendrite growth and axon path-finding of neurons. In addition, whole genome transcriptome analysis of P0 and P6 retinae was performed to analyze the genes respond to deletion of Top2b in order to construct a network that regulates retinal development.

Together, the analysis revealed that Top2b deficiency leads to delayed differentiation of all types of neurons, degeneration of the three plexiform layers, degeneration of the outer segments of both type of photoreceptor cells and a dramatic cell death which leads to decrease in the total number of cells in retina, while it is not involved in the temporal or spatial determination of cell differentiation. In addition, the genes identified in the genome-wide RNA-seq analysis can be categorized in two Gene Ontology groups: neuronal survival and neural system development. Thus the *in vivo* function of Top2b can be concluded as a factor required for the maintenance of postmitotic neurons and glia, and proper development of neural system.

The remainder of this chapter is reproduced verbatim from a manuscript published in Biology Open (Li et al., 2014) with minor modifications.

---

2. Abstract

Topoisomerase II beta (Top2b) is commonly known as an enzyme modulating DNA supercoiling by catalyzing the passage of DNA duplexes trough one another. It is ubiquitously expressed in postmitotic cells and known to function during the development of neuromuscular junctions in the diaphragm and the proper formation of laminar structure in the cerebral cortex. However, due to the perinatal death phenotype of the traditional constitutive and brain-specific Top2b knockout mice, the precise *in vivo* function of Top2b, especially during postnatal neural development, remains to be determined. Using both the constitutive and retina-specific knockout mouse models, we showed that Top2b deficiency resulted in delayed neuronal differentiation, degeneration of the plexiform layers and outer segment of photoreceptors, as well as dramatic reduction in cell number in the retina. Genome-wide transcriptome analysis by RNA sequencing revealed that genes involved in neuronal survival and neural system development were preferentially affected in Top2b-deficient retinas. Collectively, our findings have indicated an important function of Top2b in proper development and the maintenance/survival of postmitotic neurons in the retina.

3. Introduction

Type II DNA topoisomerases (topoisomerase II, Top2) are DNA machines that are capable of catalyzing an ATP-dependent passage of one DNA duplex through another (Wang, 1998). This activity is essential in removing unconstrained DNA supercoiling during various DNA transactions (Nitiss, 2009; Wang, 2002). In mammals, two evolutionally conserved Top2 isozymes (Top2a and Top2b) encoded by separate genes are present; and they possess similar in vitro catalytic activities (Nitiss, 2009; Wang, 2002). Top2a is expressed solely in proliferating cells, whereas Top2b is ubiquitously expressed in terminally differentiated cells including neurons and cardiomyocytes (Lyu et al., 2007; Lyu and Wang, 2003b; Tiwari et al., 2012; Tsutsui et al., 1993). While Top2a is essential in proliferating cells and has been linked to DNA replication and chromosome condensation/segregation, Top2b has been clearly indicated in regulating gene expression (e.g., Reln, Dab1, Catna2, Cdh13, Sst, Pbx3, and Epha7) during brain development (Lyu et al., 2006; Lyu and Wang, 2003b; Nur et al., 2007), autism spectrum disorder and other neurodegeneration disorders (King et al., 2013).

In the developing mouse cerebral cortex, Top2b is absent from proliferating neural progenitors located in the ventricular zone and subventricular zone, but expressed in postmitotic neurons undergoing terminal differentiation in the cortical plate region (Lyu and Wang, 2003b). A similar pattern of Top2b expression has also been observed in other regions of the central nervous system (CNS), e.g, the cerebellum (Tsutsui et al., 2001a; Tsutsui et al., 1993; Tsutsui et al., 2001c). Ablating Top2b in mice leads to neural developmental defects such as defective innervation of motor neurons in the diaphragm muscle (Yang et al., 2000), abnormal migration of cerebral cortical neurons, and aberrant lamination of the cerebral cortex (Lyu and Wang, 2003b; Yang et al., 2000). In addition, Top2b is required for proper neurite outgrowth and axon path-finding (Nevin et

al., 2011b; Nur et al., 2007). These findings indicate the importance of Top2b in neural development. Indeed, it has been shown that Top2b controls the expression of many developmentally regulated genes (e.g., Reln, Dab1, Epha gene family) during mouse embryonic brain development (Lyu et al., 2006), as well as gene activation in rat cerebellar granule cells (Sano et al., 2008; Tsutsui et al., 2001a). Furthermore, although Top2b is apparently nonessential in cultured cells, absence of Top2b in neural stem cell (NSC)-derived neurons results in premature cell death (Tiwari et al., 2012). However, in vivo evidence supporting an essential role of Top2b in survival/maintenance of postmitotic neurons is lacking.

To study the in vivo function of Top2b in postmitotic neurons, we have previously generated brain-specific Top2b knockout (KO) mice by breeding floxed Top2b mice (Lyu and Wang, 2003b) with Foxg1-Cre mice (Hebert and McConnell, 2000). Unfortunately, these mice showed a perinatal death phenotype, similar to that observed in the traditional constitutive Top2b KO mice (Lyu and Wang, 2003b; Yang et al., 2000). To circumvent this perinatal death problem, we have employed the developing mouse retina as a model to further analyze the in vivo function of Top2b. Retina is not essential for animal survival, and as a part of the CNS, it provides an excellent model for the study of neural development and pathogenesis. In vertebrate retina, there are six types of neurons and one type of glia interconnecting with one another to form a sophisticated neuron/glia network that relays visual input into the brain. The mature vertebrate retina is organized in a laminar structure composed of three cellular layers and two plexiform layers (basal to apical): ganglion cell layer (GCL), inner plexiform layer (IPL), inner nuclear layer (INL), outer plexiform layer (OPL) and outer nuclear layer (ONL). The genesis of mouse retinal cell types proceeds through an overlapping and yet temporal-controlled order: ganglion cells are born first around embryonic day 10 (E10), followed

by cone photoreceptors, horizontal cells and amacrine cells at around E13~E15, whereas the majority of rod photoreceptors, bipolar neurons, and Müller cells are generated after birth (Bassett and Wallace, 2012; Young, 1985a; Young, 1985c).

In this study, by employing both the traditional constitutive Top2b KO and retina-specific conditional Top2b KO (cKO) mouse models, we show that the initial specification of retinal progenitors into different retinal cell lineages was not affected by Top2b deficiency. However, retina lacking Top2b displays defects in the laminar structure and neurite outgrowth. In addition, Top2b deficiency led to a decrease in retinal thickness and an increase in apoptotic cell depth at later developmental stages. These results suggest a link between Top2b deficiency and retinal neurodegeneration and imply an essential role of Top2b in maintaining the function and survival of postmitotic neurons. Genome-wide transcriptome analysis of Top2b-deficient retinas using the RNA-seq method further confirms that Top2b regulate gene networks critical for neuronal survival and neurite outgrowth. Together, these results suggest that although it may have a minimal effect on retinal lineage specification, Top2b is vital in maintaining the postmitotic state and survival of retinal neurons.

4. Materials and Methods

Mouse strains

The traditional constitutive Top2b knockout (KO) mice were described in a previous publication (Lyu and Wang, 2003b). The retina-specific Top2b knockout (cKO) mice were generated by crossing the *Top2*b^{flox2} mouse strain (Lyu and Wang, 2003b) with the *Dkk3-Cre* mouse strain (Sato et al., 2007) (kindly provided by Dr. Hiromi Sesaki at the Johns Hopkins University). *Dkk3-Cre* mice showed restricted Cre expression to retinal progenitors starting from E10.5 (Sato et al., 2007). Based on our specific mating scheme (*Top2b*$^{flox2/flox2}$ X *Dkk3-Cre;Top2b*$^{+/flox2}$), the control mice used in this study had genotypes of *Dkk3-cre;Top2*b$^{+/flox2}$, *Top2*b$^{+/flox2}$, or *Top2*b$^{flox2/flox2}$ and the retina-specific Top2β knockout mice had the genotype of *DKK3-Cre*;*Top2*b$^{flox2/flox2}$. The *Dkk3-Cre*;*Top2*b$^{flox2/flox2}$ (cKO) mice were genetically *Top2*b$^{-/-}$ in retinal progenitors and all cells derived from them. PCR-based genotyping of the *Top2b*$^{+}$ (primers PR3 and PR1) and *Top2b*^{flox2} (primers PR3 and PR4, PR5 and PR6) alleles was performed using mouse tail DNAs as described previously (Lyu and Wang, 2003b) and the *Cre* allele was amplified using primers Cre3 (5'-CACCCTGTTACGTATAGCCG-3') and Cre4 (5'-GAGTCATCCTTAGCGCCGTA-3').

Tissue Preparation

Eyes of control or Top2b KO/cKO mice were dissected immediately after mice were sacrificed. They were washed in 1x PBS and fixed with 4% (w/v) paraformaldehyde for 1 hr. Fixed tissues were washed again and then cryopreserved in 30% (w/v) sucrose overnight. Images of the whole-mount eyes were taken with a microscope (Leica, MZ16FA) and eyeball diameter was measured. The eyeballs were embedded in cryo-preserving media (Tissue Tek® OCT compound) and kept frozen at -80ºC.

Immunohistochemistry

Frozen retinal tissues were sectioned sagittally (10-12 μm in thickness) using a cryostat (ThermoScientific) and air dried. Sections were blocked and permeablilized for 1 hr in blocking buffer containing 10% donkey serum, 0.1% TritonX, and 0.1% Tween® 20 at room temperature. Afterwards, they were incubated with primary antibodies overnight at 4ºC. Following three 10-min washes in PBS, sections were incubated in the blocking buffer containing corresponding fluorophore-conjugated secondary antibodies for 1 hr at room temperature. Slides were then washed three times with PBS (10-min each wash), and mounted with mounting media (Vector Laboratories) in the presence or absence of DAPI (to label the nuclei). The following primary antibodies were used: Top2b (1:300, sc-25330), Brn3 (1:300, sc-6026), Chx10 (1:300, sc-21692), Pkcα (1:300, sc-8393), EAAT1 (1:200, sc-7757), CRALBP (1:200, sc-59487) and PH3 (1:300, sc-8656-R) from Santa Cruz Biotechnology, Inc.; Lim1/2 (1:25) and Pax6 (1:15) from Developmental Studies Hybridoma Bank (DSHB); Brn3a (1:100, MAB1585), Calretinin (1:2500, MAB1568), Recoverin (1:1000, AB5585) and γ-H2AX (1:100, 05-636) from Millipore; Tuj-1 (1:1000, ab14545) from Abcam; cleaved-Casp3 (1:1600, #9661) from Cell Signaling; Prox1 (1:5000, prb-238c) from Covance; Rhodopsin 4D2 (1:100; gift from Dr. Robert S. Molday from University of British Columbia, Canada). Images were captured using a Zeiss Axio Imager M1 fluorescence microscope and AxioVision 4.8.

in vivo EdU labeling

To label proliferating cells *in vivo*, the thymidine analog EdU (5-Ethynyl-2′-deoxyuridine, 50 μg/g body weight, in PBS) was injected into pregnant female mice 2 hr before sacrifice and dissection. EdU labeling was detected using the Click-iT Edu Alexa

Fluor 647 Imaging kit (Invitrogen).

Whole genome transcriptome analysis using the RNA-seq method

Total RNA were isolated from retinas of the control and cKO pups at P0 and P6 (n=4 for each sample). The whole transcriptome RNA libraries were constructed, following by deep sequencing using the SOLiD System (Applied Biosystems). RNA-seq data analysis was performed according to the published protocol (Trapnell et al., 2012) with minor modifications. Briefly, raw 50 bp reads was aligned to the mouse genome (MGI, as of Feb 15, 2012) using Bowtie (Langmead et al., 2009). Gene expression level was analyzed with Cufflinks, with differentially expressed genes determined by Cuffdiff (Trapnell et al., 2010). Gene Ontology (GO) analysis of the gene expression data was performed using GSEA (permutation = 1000) (Subramanian et al., 2005) and visualized by the Enrichment Map tool (The Bader lab, University of Toronto) as a plug-in of Cytoscape (Merico et al., 2010).

Cell counting

Cell counting was performed manually on retina sections through the central regions at or directly adjacent to the optic nerve level. Either the whole section or a two 200 μm wide regions from the central part of the retina on each side of the optic nerve were counted, as indicated in the histograms.

Statistical analysis

Quantitative data were presented as mean ± standard deviation. Significance (*p*-value) was determined by Student's t-test.

5. Results

1) Top2b expression is only present in postmitotic cells during mouse retinal development

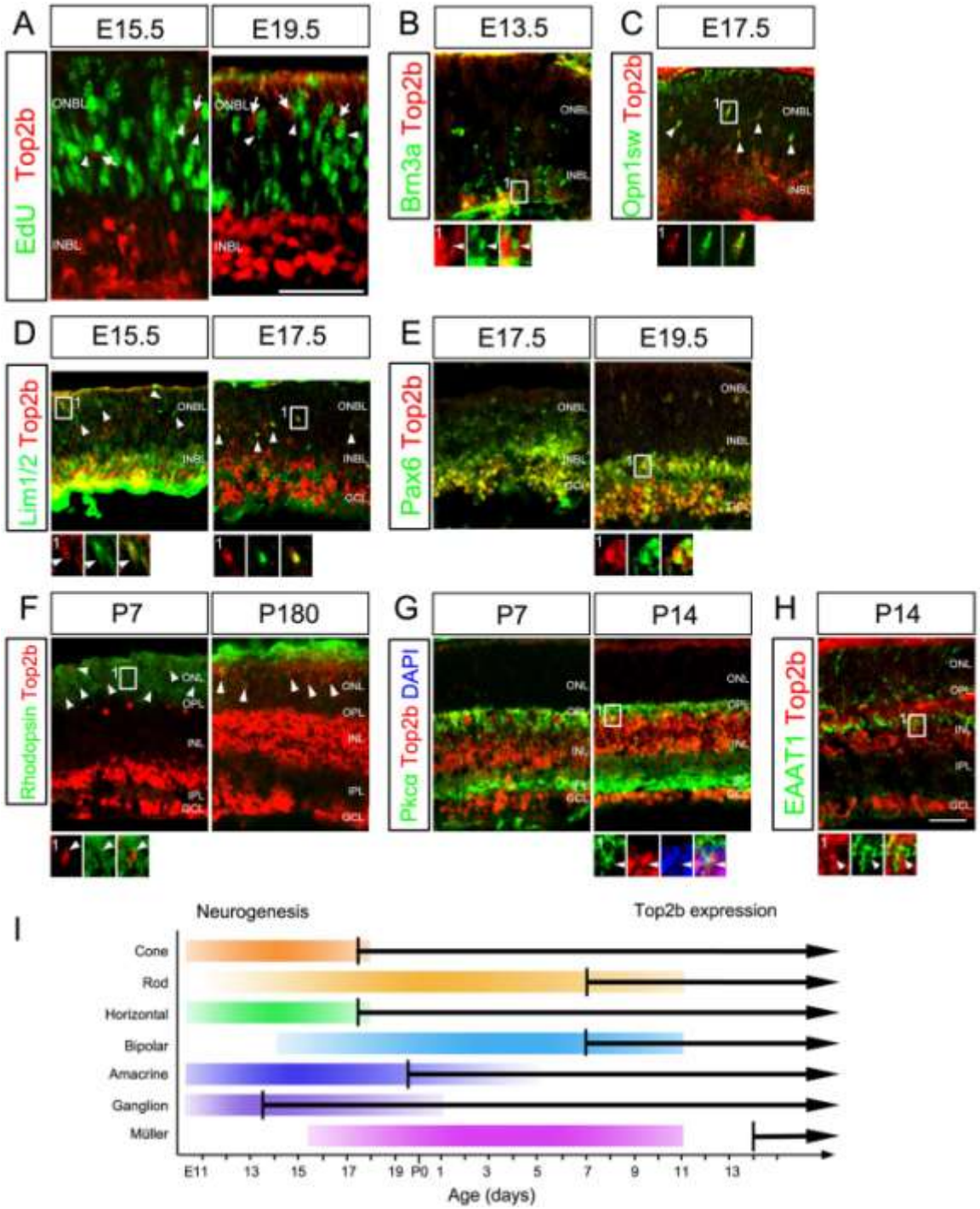

Figure II.1. Expression pattern of Top2b during mouse retinal development. (A) E15.5 and E19.5

retina sections were processed to reveal EdU *in vivo* labeling. Staining with Top2b show that the vast majority of Top2b+ cells were in the INBL while EdU+ cells were in the ONBL. No EdU+ cells (arrowheads) were co-labeled with Top2b (arrows). (B) Top2b+ cells were co-labeled with Brn3a at E13.5. (C) Top2b+ cells were co-labeled with Opn1sw at E17.5. (D) Co-staining of Lim1/2 and Top2b at E15.5 and E17.5. (E) Co-staining of Pax6 and Top2b at 17.5 and E19.5. (F) Co-staining of Rhodopsin and Top2b at P7 and P180. (G) Co-staining of Pkcα and Top2b at P7 and P14. (H) Co-staining of EAAT1 and Top2b at P14. Boxed regions are shown in a higher magnification. Arrowheads in (B-H) indicate double-labeled cells with Top2b and a retinal cell type specific marker. (I) Timeline of Top2b expression and neurogenesis in mouse retina. Color bars indicate the process of retinal development based on Young's work (Young, 1985a). Black arrows represent the starting points of Top2b expression in different retinal cell types. INBL, inner neuroblastic layer; ONBL, outer neuroblastic later; GCL, ganglion cell layer; INL, inner nuclear layer; IPL, inner plexiform layer; ONL, outer nuclear layer; OPL, outer plexiform layer. Scale bars = 50μm.

To determine whether Top2b is expressed in proliferating or postmitotic cells, we pulse-labeled proliferating retinal progenitors with the thymidine analog EdU (5-ethynyl-2'-deoxyuridine) (Salic and Mitchison, 2008) and immunostained retinal sections with Top2b antibody at embryonic day 15.5 (E15.5) and E19.5. We found that no cells were co-labeled with Top2b and EdU in the retina (**Fig. II.1A**), indicating that Top2b was not expressed in proliferating retinal progenitors.

Next, we determined the onset of Top2b expression in each specific retinal cell type by double immunostaining for Top2b and cell-specific markers, and by cell-specific laminar location in the retina. Top2b expression was not detected before or at E12.5 (data not shown). Weak Top2b staining was detected first in regions near the vitreous surface of the inner neuroblastic layer (INBL) at E13.5 (**Fig. II.1B, S1A**). Many Top2b+ cells were co-labeled with Brn3a, a differentiated ganglion cell marker (Xiang, 1998; Xiang et al., 1995) (**Fig. II.1B**). Starting from E17.5, Top2b expression became apparent in newly born Opn1sw+ cone photoreceptors (**Fig. II.1C**), Lim1/2+ horizontal cells (**Fig. II.1D**), and Pax6+ amacrine cells (**Fig. II.1E**). In postnatal stages, Top2b expression was maintained in postmitotic cells of both neuronal and glial origin, including Rhodopsin+ rod photoreceptors (**Fig. II.1F**), Pkcα+ bipolar cells (**Fig. II.1G**), and EAAT1+ Müller glia (**Fig. II.1H**), subsequent to their differentiation.

The expression pattern of Top2b in retinal cells correlated well with the period of retinal neurogenesis and overlapped with the period of retinal cell differentiation (**Fig. II.1I, S1**). These results indicate that Top2b is expressed and maintained in all differentiated and mature retinal cell types.

2) Top2b deficiency does not affect early mouse embryonic neurogenesis but causes morphological defects in the postnatal eye

The role of Top2b during embryonic retinal development was examined using the traditional constitutive Top2b knockout (KO) embryos (Yang et al., 2000). Immunostaining showed no Top2b expression in the KO retinas (**Fig. II.S2A,B**) and no discernible differences in staining with retinal ganglion cell markers Brn3 (detects Brn3a, Brn3b and Brn3c for both ganglion progenitors and differentiated ganglion cells (Xiang, 1998; Xiang et al., 1993)) and Brn3a, cone photoreceptor marker Opn1sw, retinal progenitor marker Pax6 (Marquardt et al., 2001) and early neuronal marker Tuj-1 at E13.5 and E15.5 (**Fig. II.S3**). In addition, there is no obvious difference in the number of EdU+ cells and phosphorylated-histone 3 (PH3)-labeled M-phase cells between wild-type and Top2b KO retinas (**Fig. II.S4**). These results suggest that early retinogenesis and retinal progenitor proliferation do not require Top2b.

Since both the constitutive (Yang et al., 2000) and brain-specific Top2b KO mice die shortly after birth (Lyu and Wang, 2003b), these models cannot be used to study the role of Top2b during the postnatal CNS development. To circumvent this problem, a retina-specific Top2b KO (cKO) mouse line was generated by crossing the floxed Top2b mice (Lyu and Wang, 2003) with the *Dkk3-Cre* mice (Sato et al., 2007). The Dkk3 promoter-driven expression of the Cre recombinase (Cre) takes place in retinal progenitors at E10.5, and is able to convert the *Top2b*^{flox2} allele to the *Top2b*$^{-}$ allele in retinal

progenitors and their progenies. cKO (*Dkk3-Cre;Top2b*$^{flox2/flox2}$) mice were viable and immunohistochemistry confirmed that no Top2b expression was detected in postnatal cKO retinas (**Fig. II.S2C, D**). Initial examination showed no obvious morphological defects in the eyes between cKO mice and their control littermates before postnatal day 7 (P7); however, retinal degeneration accompanied with reduced eyeball size was observed starting from P14 (**Fig. II.S5**). The openings of eyelids appeared to be narrower in cKO mice at P14 and P21 (data not shown); and closed completely in adult cKO mice (P180) (**Fig. II.S2F**). Moreover, degeneration of the discontinuous circumferential folds in the collarette of iris of the cKO mice was observed, resulting in a smoother edge of the iris and larger pupils after P0 (**Fig. II.S5E-O**). No visible iris structure can be found in adult cKO eyes (**Fig. II.S5S**). In addition, optic nerves of the cKO mice were thinner and flatter (**Fig. II.S5D, H, L, P, T**) as compared with the cylinder-like optic nerve of their control littermates. These results indicate that Top2b deficiency caused degeneration within the inner structure of the eyeballs; and prompted us to further examine the detailed structure and organization of the retina.

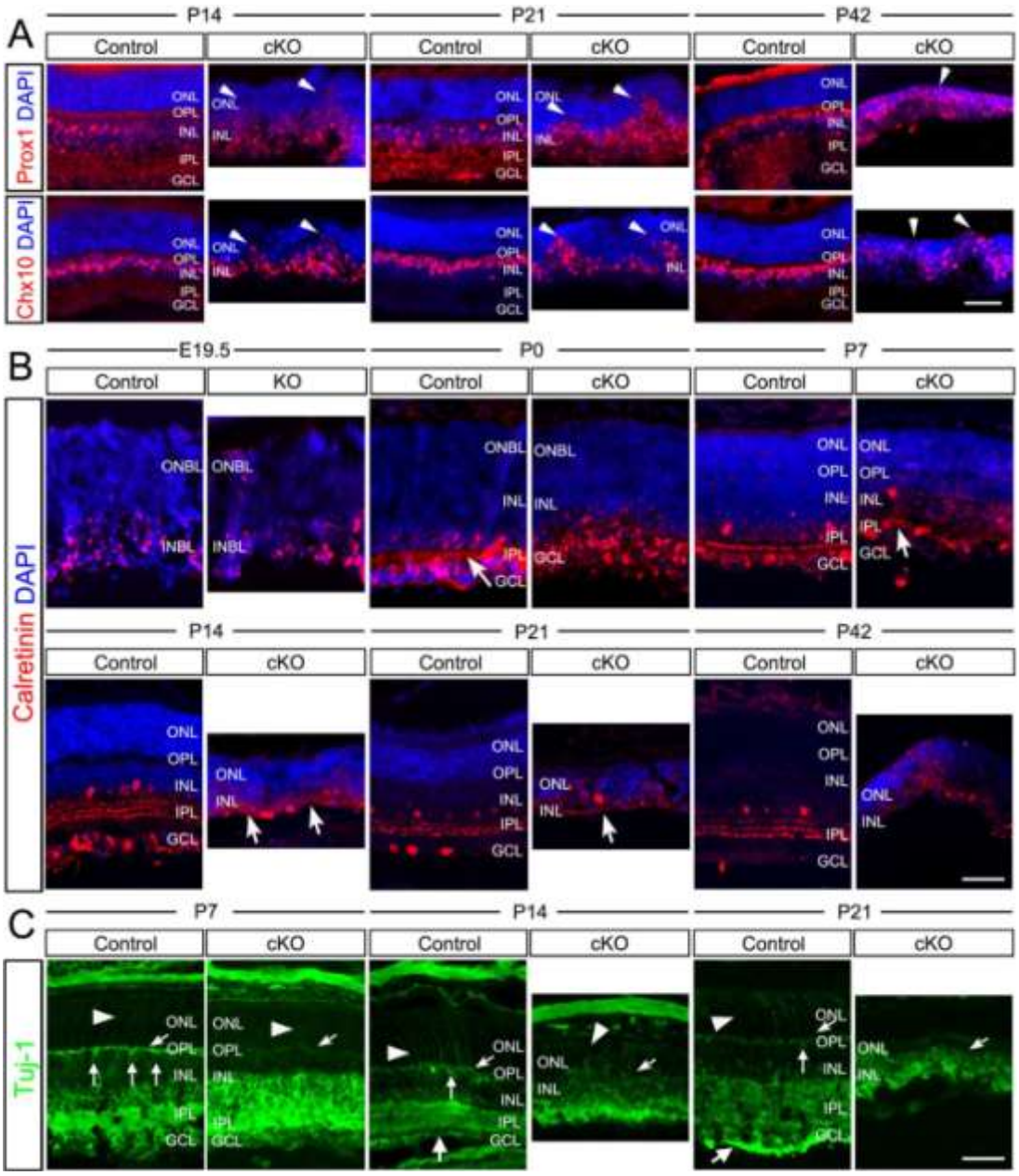

Figure II.2. Aberrant retina lamination and loss of plexiform layers caused by Top2b deletion. (A) Retina sections prepared from P14, P21 and P42 control and Top2b cKO mice were stained with DAPI and co-stained with either Prox1 or Chx10. Prox1+ and Chx10+ cells were detected in the ONL (arrowheads) in Top2b cKO retinas. (B) Co-staining of E19.5-P42 control and KO/cKO retina sections with DAPI and Calretinin, which labels neurofilaments in the IPL. In cKO retinas, only a few filament-like structures were found at P7 and P21, while in control samples the strata structure of neurofilaments appeared as early as P0 (arrows). (C) Co-staining with Tuj-1in P7, P14 and P21 control and cKO retina sections. Tuj-1 stained neurofilaments of the OPL (arrows) and processes of photoreceptors (arrowheads), which were largely missing in cKO samples. GCL, ganglion cell layer; INL, inner nuclear layer; IPL, inner plexiform layer; ONL, outer nuclear layer; OPL, outer plexiform layer. Scale bars = 50μm.

3) Top2b deletion leads to defects in retinal lamination

To determine the cause of these morphological defects observed in the postnatal cKO mice, we next examined the cKO retinas at the cellular and molecular level. Retinal sections were stained with DAPI and various cell-specific markers, e.g., Prox1, Chx10, and Calretinin for retinal cells in the INL. Compared with the controls (wild-type littermates), Prox1+ amacrine cells and Chx10+ bipolar in the cKO retinas did not retain in the INL, but protruded into the ONL (**Fig. II.2A**). This could be explained by the largely missing inner plexiform layer (IPL) and the outer plexiform layer (OPL) in the cKO retinas as revealed by the Calretinin staining (**Fig. II.2B**). Calretinin mainly stains the neurite plexuses of the IPL (formed by the processes of the amacrine cells, bipolar, and ganglion cells). In the controls, Calretinin-stained IPL was prominently present starting from P0 (**Fig. II.2B**, arrow). The matured IPL contained five strata separating from each other by three plexuses could be observed in P14, P21 and P42 (**Fig. II.2B**). However, in the cKO retinas, Calretinin staining revealed only short and disoriented neurites or processes and no plexus was visible at any postnatal stages examined (**Fig. II.2B**). These defects became progressively more severe at P14, P21 and the adult stage (P42). The disappearance of the plexiform layers, especially the OPL, was further confirmed by the staining of the type-II β tubulin using the Tuj-1 antibody (**Fig. II.2C**). In the control, both the OPL and IPL were clearly visible by P7; while in the cKO retinas, these plexiform layers were dramatically reduced by P7 and disappeared by P14 (**Fig. II.2C,** arrows). These results suggest that Top2b is required for neurite outgrowth and proper formation of retinal plexiform layers.

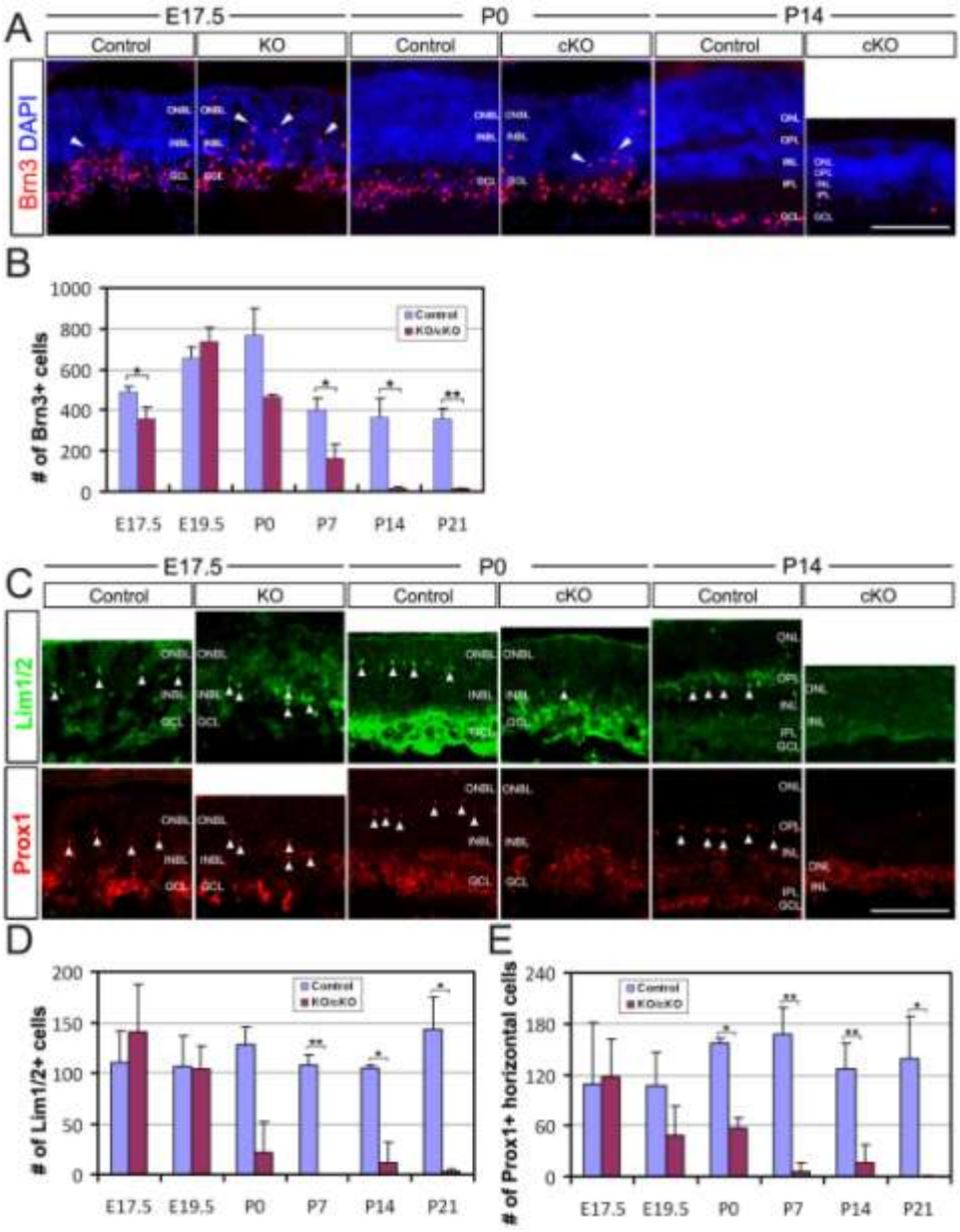

Figure II.3. Top2b deficiency leads to delayed embryonic development and decreased ganglion and horizontal cells. (A) Retina sections of E17.5 control and KO embryos and P0 and P14 control and cKO mice were co-stained with Brn3 and DAPI. Brn3+ cells were all located in the GCL in the control retinas, but they were more widely distributed in the INBL and ONBL (arrowheads) in the KO/cKO retinas. (B) Quantification of Brn3+ cells. A significant reduction in the number of Brn3+ cells in postnatal stages starting from P7 was observed. (C) Retina sections of E17.5 control and KO embryos and P0 and P14 control and cKO mice were co-stained with Lim1/2 and DAPI or Prox1 and DAPI. Lim1/2+ and Prox1+ cells horizontal cells were well-spaced and located in the horizontal cell layer (arrowheads) in the control retinas; while in the KO/cKO retinas, the majority of these cells remain in the INBL (arrowheads) at E17.5 and P0. By P14, no Lim1/2+ or Prox1+ cells were detected in cKO samples. (D) Quantification of Lim1/2+ cells cells. (E) Quantification of Prox1+ horizontal cells. Error bars are s.d. (n = 3 except n = 2 for P0). Student's t-test, * $p<0.05$, ** $p<0.01$. INBL, inner neuroblastic layer; ONBL, outer neuroblastic

layer; GCL, ganglion cell layer; INL, inner nuclear layer; IPL, inner plexiform layer; ONL, outer nuclear layer; OPL, outer plexiform layer. Scale bars = 100 μm.

4) Top2b deficiency causes delayed differentiation of ganglion, horizontal cells and affects their survival

Since the IPL is formed by the processes of INL cells (horizontal, amacrine and bipolar cells) and ganglion cells, defects in IPL could indicate that although Top2b deficiency does not affect INL and ganglion cell specification, but the final maturation and differentiation of these cell types was not accomplished. We thus further tracked the development of these retinal cells based on the expression of cell-specific differentiation markers with their laminar location and cell numbers. In KO/cKO retinas, the expression of Brn3 in ganglion cells, Lim1/2, Prox1 in horizontal and amacrine cells, and Chx10 in bipolar neurons was detected (**Fig. II.2, 3**), suggesting that specification of these retinal neuronal cell types was not affected in the absence of Top2b. However, Brn3+, Lim1/2+, and Prox1+ cells were widely dispersed in both the INBL and ONBL at E17.5 and P0 and appeared to be still undergoing the migration process in the INBL before reaching their final location in the horizontal cell layer (**Fig. II.3A, C**). These results suggest that Top2b is involved in the process of terminal maturation/differentiation of these retinal cells.

In addition, there was a dramatic decrease in the number of Brn3+ ganglion cells in the cKO retinas during postnatal retinal development starting from P7, and by P14 only a few Brn3+ were detectable in cKO retina sections (**Fig. II.3B**). This dramatic ganglion cell loss is consistent with the finding that cKO mice in late postnatal stages had thinner and flatter optic nerve (**Fig. II.S5**), which is formed by axons emanated from ganglion cells. For Lim1/2+ and Prox1+ cells, a dramatic decrease of these cells was observed in cKO retinas starting from P7 (**Fig. II.3D, E**). These results suggest that Top2b deficiency

affects terminal differentiation during embryonic retinogenesis, and retinal cell survival after birth.

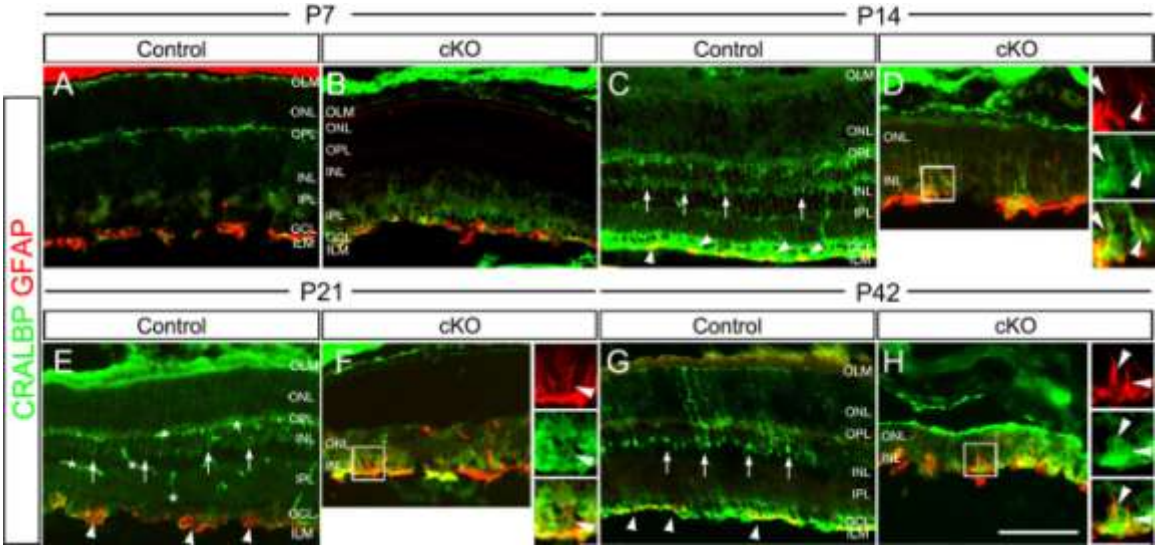

Figure II.4. Top2b deficiency causes defects in Müller glia. Co-staining of control and cKO retina sections with GFAP and CRALBP at P7 (A, B), P14 (C, D), P21 (E, F) and P42 (G, H). At P7, GFAP expression (red) was present in the endfeet of Müller glia cells in both control and cKO retinas, while CRALBP-stained neurofilaments in the OPL were seen in the control retina (green in A) but not in cKO retina (B). Up-regulation of GFAP (arrowheads) accompanied with shorter processes and disrupted lamination was seen in cKO retinas at P14 (D), P21 (F) and P42 (H). CRALBP-stained processes and cell body of Müller glia (vertical arrows) were seen in the control retinas but not in the cKO at these stages (C-H). Asterisks indicate the background blood vessels. ILM, inner limiting membrane; OLM, outer limiting membrane; GCL, ganglion cell layer; INL, inner nuclear layer; IPL, inner plexiform layer; ONL, outer nuclear layer; OPL, outer plexiform layer. Scale bar = 100μm.

5) Absence of Top2b leads to defects in Müller glia development

Müller glia play important roles in the retina by supporting and nourishing other retinal cells (Poitry et al., 2000). Thus, there may be defects in Müller glia that contribute to the observed structural defects and cell loss in the cKO retinas. To examine the role of Top2b in Müller glial development, retinal sections were stained with radial glial markers GFAP and Müller glia marker CRALBP. In both the control and cKO retinas, GFAP signal was detected in the inner half of the retina at P7, where the endfeet of Müller glia cells are located (**Fig. II.4A, B**). Starting from P14, CRALBP staining could be detected. Unlike the pattern found in control retinas in which CRALBP-stained bodies of Müller glia

were observed to reside in the INL with full length processes expanding from the inner limiting membrane (ILM) to the outer limiting membrane (OLM) from P14 to P42 (**Fig. II.4C, E, G**), there was no clear presence of Müller glia cell bodies in cKO retinas (**Fig. II.4D, F, H**). In addition, CRALBP-stained processes of Müller glia in cKO retinas were short (not expanding to the OLM) and almost no processes were detected at P21 (**Fig. II.4D, F, H**). GFAP staining in control retinas maintained in the endfeet of Müller glial throughout P14 to P42, while in cKO retinas it was stronger and more extensive (**Fig. II.4C-H**). The GFAP staining in cKO retinas was found mostly close to the ILM and extended to co-localize with the processes of CRALBP+ Müller glia (**Fig. II.4D, F, H**). Although this GFAP staining pattern is a characteristic feature of injury-induced reactive gliosis (Fisher et al., 1995; Guerin et al., 1990), the true nature of this observation requires further analysis. These results suggest that Top2b is essential for the development of Müller glia.

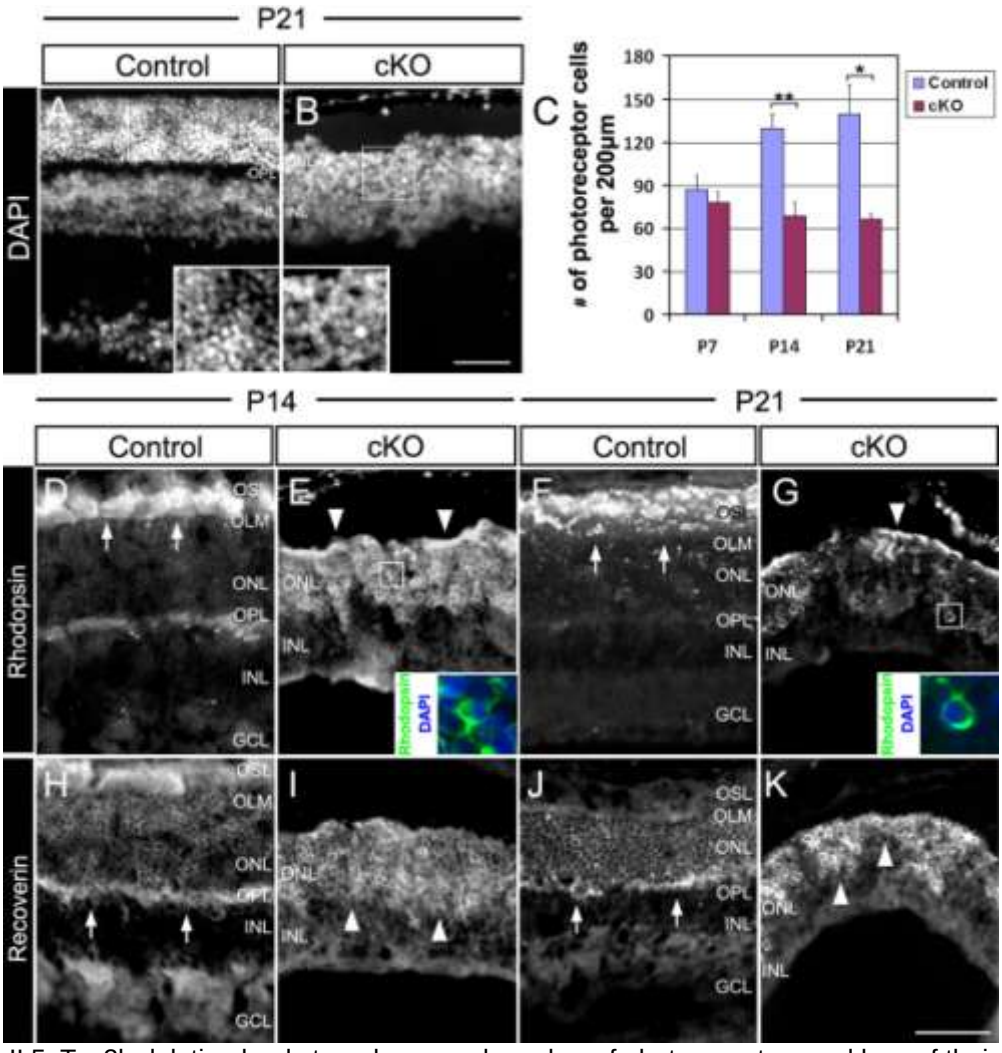

Figure II.5. Top2b deletion leads to a decreased number of photoreceptors and loss of their outer segments. (A, B) P21 retina sections of control and cKO mice were stained with DAPI. The cKO retina appeared much thinner as compare to the width of control retina. The nuclei of cells in ONL of cKO retinas were also larger than those in control retinas (enlarged). (C) Quantification of the number of ONL cells (i.e. photoreceptors) showed a dramatic decrease in cKO retinas. Error bars are s.d. (n = 3). Student's t-test: *, $p<0.05$; **, $p<0.01$. (D-G) Rhodopsin staining of P14 and P21 retina sections. Rhodopsin-stained outer segment layer (OSL) was detected in the control retinas (arrows), but not in cKO retinas (arrowheads). Instead, co-staining of Rhodopsin and DAPI (inserts in E and G show higher magnification of the boxed regions) of cKO retinas indicates the expression of Rhodopsin in the cytoplasm of ONL cells. (H-K) Recoverin staining of P14 and P21 retina sections. Recoverin stained outer plexiform layer (OPL, arrows) in the controls, but not in cKO retinas (arrowheads). GCL, ganglion cell layer; INL, inner nuclear layer; IPL, inner plexiform layer; ONL, outer nuclear layer; OPL, outer plexiform layer; OLM, outer limiting membrane; OSL, outer segment layer. Scale bars = 50µm.

6) Lack of Top2b affects the differentiation/maturation of photoreceptor cells

To further determine whether Top2b is required for photoreceptor development,

retina sections were stained with photoreceptor cell markers Rhodopsin (rod outer segment) and Recoverin (rod, cone and cone-bipolar cells). Rhodopsin+ and Recoverin+ cells were detected in both the control and cKO retina (**Fig. II.5**), indicating that the absence of Top2b did not affect photoreceptor cell fate specification. In cKO retinas however, the DAPI-stained nuclei in the ONL appear to be larger and apparently more loosely distributed (**Fig. II.5A, B**), and the number of ONL cells were significantly reduced starting from P14 (**Fig. II.5C**). In addition, rhodopsin staining revealed irregularly clustered cell bodies in the ONL, and there was no discernible outer segment layer (OSL) in the cKO retinas (**Fig. II.5E, G**). Instead of outer segments, Top2b was found in the cytoplasm of these cells in ONL of cKO retinas (**Fig. II.5E, G**, enlarged). These phenotypes are indicative of photoreceptor degeneration (Fariss et al., 1997; Louie et al., 2010). In addition, Recoverin staining revealed that both the OSL and plexiform layers were largely missing in the cKO retinas (**Fig. II.5I, K**). These results suggest that Top2b is required for the development of the OS and maintenance of photoreceptors.

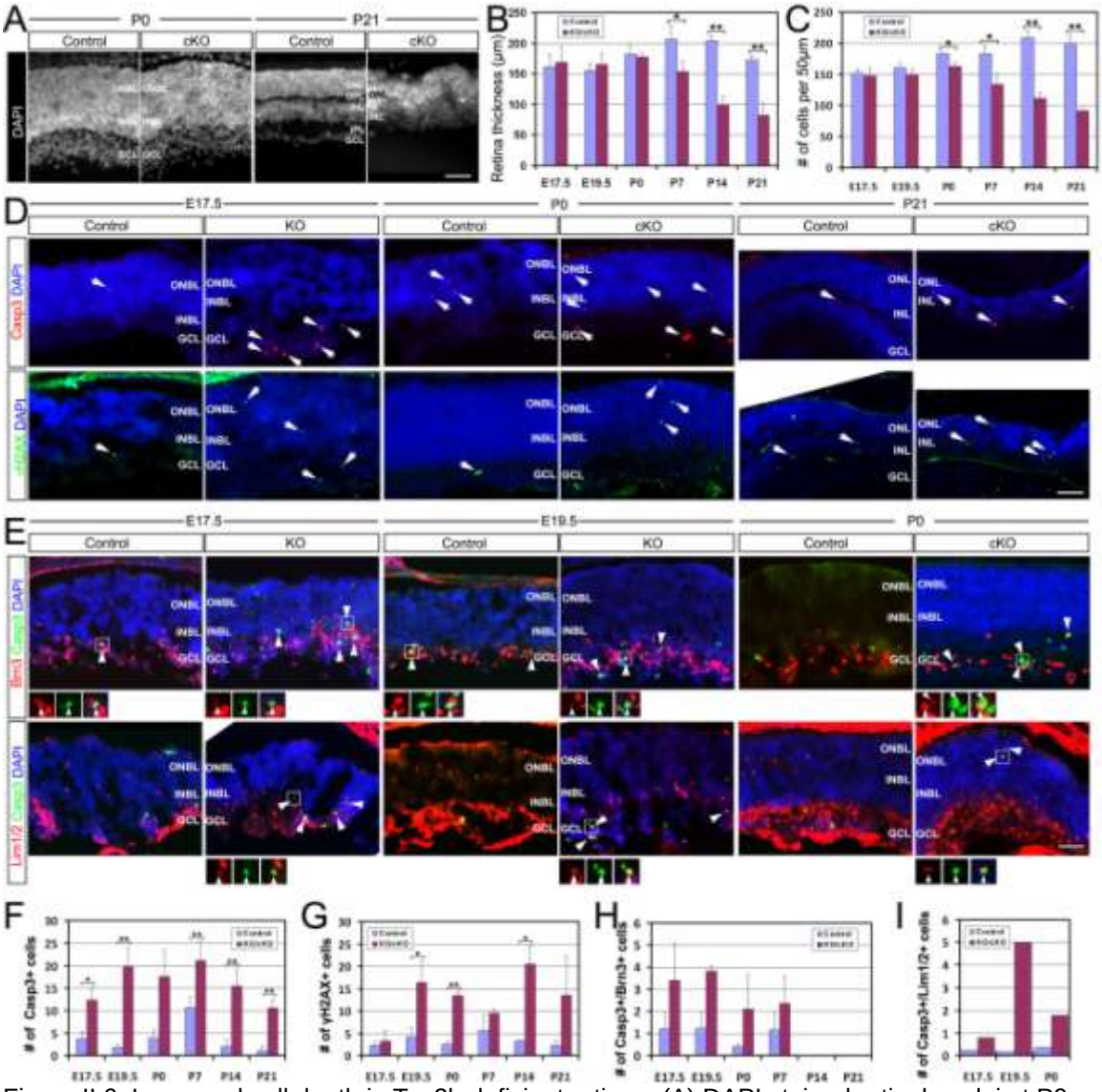

Figure II.6. Increased cell death in Top2b deficient retinas. (A) DAPI stained retinal nuclei at P0 and P21. Quantification showed a significant decrease in both retina thickness (B) and the average number of cells (C) in cKO retinas starting from P7 and P0, respectively. (D) Co-staining of retina sections with cleaved caspase 3 (Casp3) and DAPI or γ-H2AX and DAPI. There was a significant increase in Casp3+ and γ-H2AX+ cells (D, arrows, F and G). (E) Co-staining of retina sections with Casp3 and Brn3, or Casp3 and Lim1/2. There was a significant increase in Casp3+/Brn3+ and Casp3+/Lim1/2+ cells (E, arrowheads, H, I) in KO/cKO retinas. Error bars are s.d. (n=3); * $p < 0.05$; ** $p < 0.01$. INBL, inner neuroblastic layer; ONBL, outer neuroblastic layer; GCL, ganglion cell layer; INL, inner nuclear layer; ONL, outer nuclear layer. Scale bars = 50μm.

7) Top2b deletion increases retinal cell death

Examination of DAPI-stained cKO retina sections showed that there was a significant reduction in retina thickness starting from P7 (**Fig. II.6A, B**), in retinal

perimeter starting from P14 (**Fig. II.S6**), and in cell number starting from P0 (**Fig. II.6A, C**). This could be due to either a decrease in cell proliferation or an increase in cell death, or both. Since Top2b expression was absent from proliferating retinal progenitors (**Fig. II.1A**), it is unlikely that Top2b deficiency affects progenitor proliferation. Indeed. we have confirmed that Top2b deficiency did not affect cell proliferation by S-phase labeling with EdU and M-phase labeling with PH3 (**Fig. II.S4A**). There were no significant differences in the number and laminar locations of EdU+/PH3+ cells between the control and KO retinas (**Fig. II.S4B, C**); it suggests that Top2b deficiency does not affect retinal progenitor proliferation.

We next examined whether there was a difference in the cleavage orientation during cell division as it has been shown that cleavage orientation affects the cell fate decision of the daughter cells (Arai et al., 2011; Chenn and McConnell, 1995; Godinho et al., 2007), which affects the number of cells leaving cell circle. However, there were no significant differences in the number of PH3/EdU double-labeled mitotic cells lining the apical surface of the retina (**Fig. II.S4C, D**) or their mitotic cleavage orientations (**Fig. II.S4E**) between KOs and their control littermates. These findings together with the absence of Top2b expression in proliferating (EdU+) cells suggest that Top2b deficiency does not affect cell proliferation/division during retinogenesis.

Next, we examined whether Top2b deficiency causes increased retinal cell death by staining retina sections with apoptosis and DNA damage markers, cleaved caspase 3 (Casp3) and γ-H2AX, respectively. Cleavage of Casp3 is indicative of the ongoing programmed cell death known as apoptosis (Kuribayashi et al., 2006) and γ-H2AX is a surrogate marker for DNA double-strand breaks (Kinner et al., 2008; Kuo and Yang, 2008). We were not surprised to find that there was a significant increase in the number (2-6 fold) of Casp3+ and γ-H2Ax+ cells in KO/cKO retinas (**Fig. II.6D, F, G**). Double

immunostaining with Casp3 and retinal cell-specific marker Brn3 or Lim1/2 showed significantly increased cell death in the ganglion and horizontal cell population from E17.5 to P21(**Fig. II.6E, H, I**). The retinas from P42 and P180 cKO mice degenerated so severely that we were unable to find an intact section for further analysis. Together, these results suggest that Top2b deficiency causes increased retinal cell death.

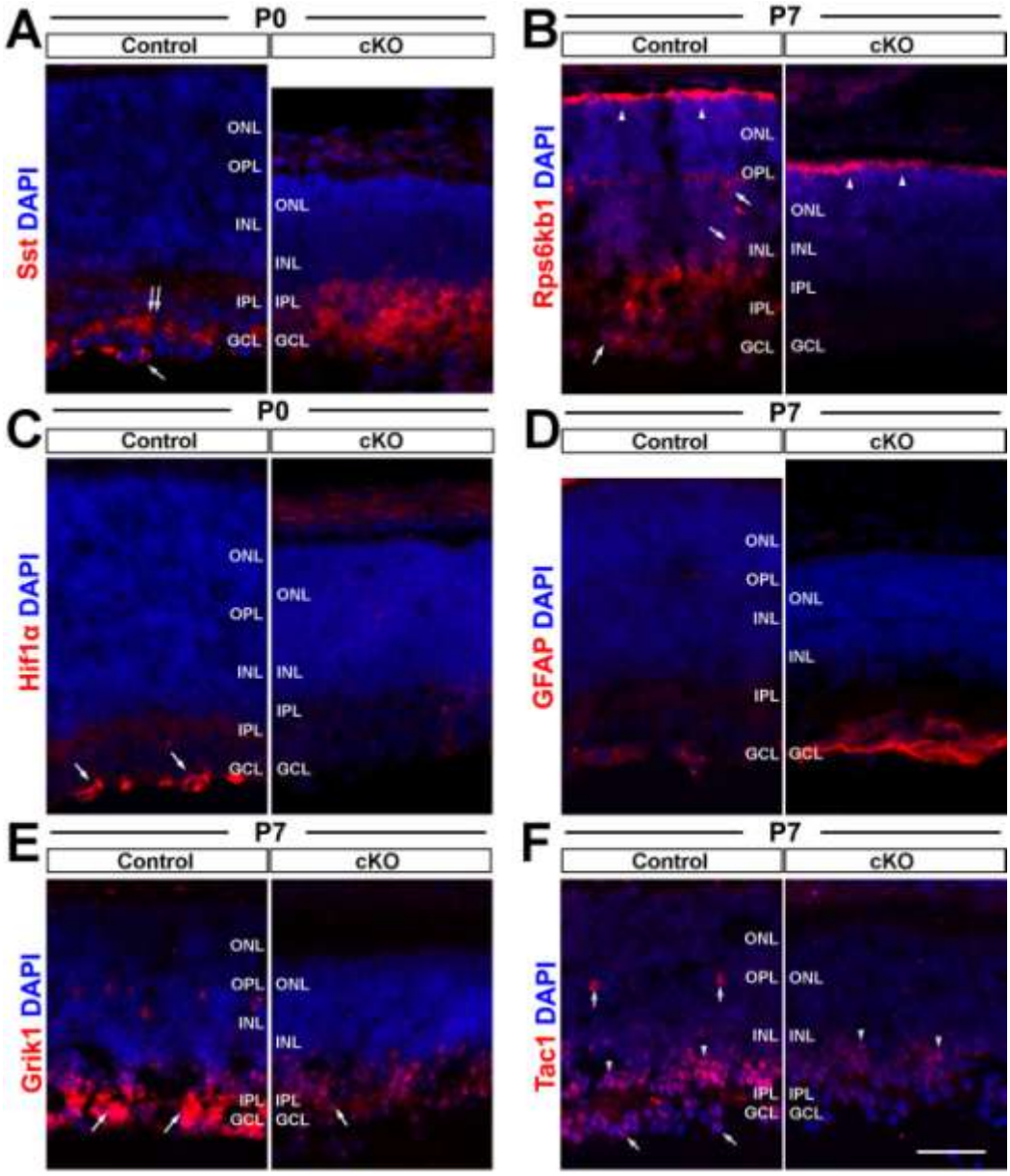

Figure II.7. Top2b deletion affects the expression of genes involved in neural cell survival and neurite growth. Control and cKO retina sections of P0 and P7 mice were stained with antibodies against six proteins with their respective mRNA differentially expressed in cKO retinas. (A) Sst

staining in cKO sample was increased but lost the specific immunoactivity in the GCL (double arrow) and ganglion cells (arrow) in the control retinas. (B) The Rps6kb1 protein was expressed in the outer segments of photoreceptors (arrowheads), ganglion cells, amacrine cells (arrows) and the IPL in the control retinas. However, its expression was only seen in the outer segments (arrowheads) in cKO retinas. (C) Hif1α was found in the cytoplasm of marginal ganglion cells in the controls (arrows), but was not detectable in the cKO samples. (D) Increased GFAP expression was found in GCL of P7 cKO retinas. (E) Grik1 was strongly stained in the IPL of the control retina, but reduced in the cKO retina (arrows). In addition, Grik1 staining in horizontal cells was missing. (F) Tac1 was found in horizontal cells (vertical arrows), amacrine cells (arrowheads) and ganglion cells (diagonal arrows) in the control retina. In the cKO retina, the signal was only found in amacrine cells with a decreased intensity. GCL, ganglion cell layer; INL, inner nuclear layer; IPL, inner plexiform layer; ONL, outer nuclear layer; OPL, outer plexiform layer. Scale bar = 50μm.

8) Top2b deletion impairs transcription of genes associated with cell survival and neurological system development

To identify genes and gene networks that are responsible for the phenotypes observed in the postnatal Top2b cKO retinas, we employed the next generation RNA sequencing (RNA-seq) analysis. Total RNA was isolated from the retinas (pool of four retinas for each sample and time point) of control and Top2b cKO mice at P0 and P6, the two critical postnatal developmental stages when major defects in cKO retinas start to appear. After sequencing, ~120 million 50 bp reads for each time point and each group were obtained and mapped to the mouse genome (MGI, as of Feb 15, 2012). Over 62,000 transcripts were identified; these include ~22,000 annotated genes (including alternative-spliced variants) which cover 76% of the whole mouse genome. Among all the annotated genes, 8.80% (1,935/22,000) for P0 and 1.25% (274/22,000) for P6 showed differential expression between the control and cKO samples (p-value ≤ 0.05, q-value ≤ 0.05). Further bioinformatic analysis revealed that these differentially expressed genes (DEGs) were associated with apoptosis, system development, cellular transportation, signal transduction at P0; and neurological system process and cytoplasm condition at P6 (**Table II.S1**). Examples include Igf1, Hras, Mapk1, HIF1α, Vegfa, Rps6bk1, Sst, Tac1, Gfap, GriK1/2, Gria4, Grm7 and Nrxn1/3, which are involve

in the mouse retinal development. The differential expression of some of these genes was confirmed by immunohistochemistry analysis (**Fig. II.7** and **Table II.S1)**.

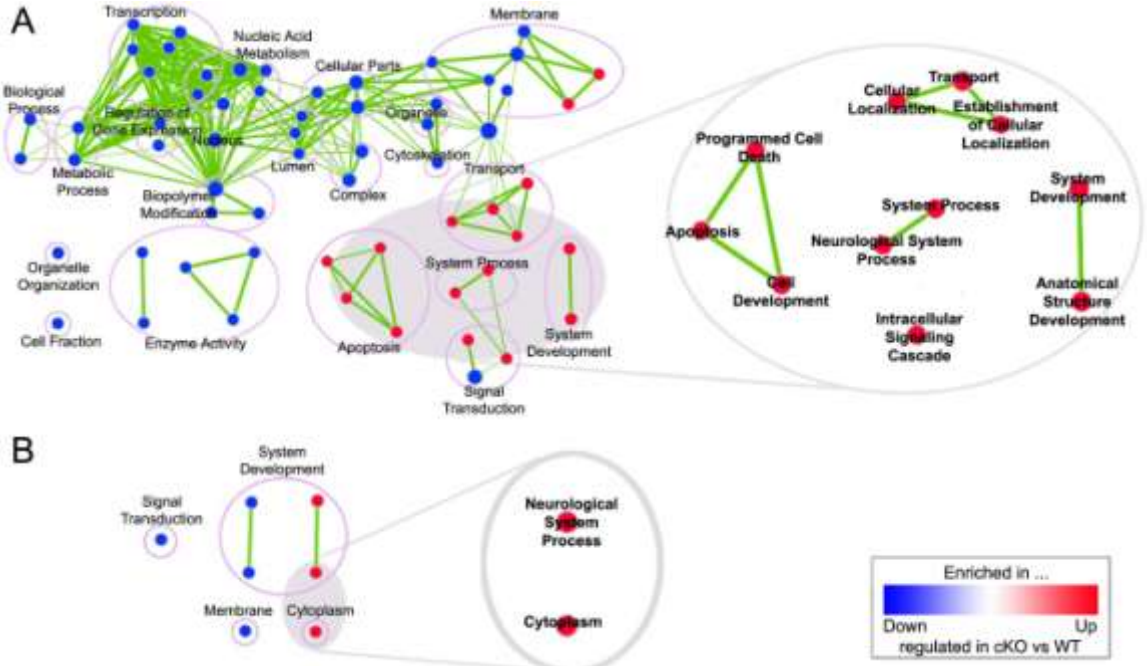

Figure II.8. Gene ontology enrichment analysis reveals Top2b function in neurite growth and maintenance/survival of retinal cells. Differentially expressed genes were analyzed for gene ontology (GO) enrichment using GSEA. The result was mapped on a network of gene-sets (nodes) connected by their similarity (edges) for P0 (A) and P6 (B) using Cytoscape (p-value ≤ 0.005, FDR q-value ≤ 1, and similarity ≤ 0.5). Nodes highly enriched with up-regulated genes in cKO samples are shown in red while those with down-regulated genes are shown in blue. Node size represents the gene-set size. Edge thickness represents the degree of overlap between two gene-sets. Nodes were grouped according to GO definition and annotated with the group names. The cluster of red nodes under restricted cutoff values (p-value ≤ 0.005, FDR q-value ≤ 0.1, and similarity ≤ 0.5) was enlarged, showing that cell death, cellular transportation and neurological system development related processes were highly enriched in cKO samples.

Further functional enrichment analysis using GSEA (Gene Set Enrichment Analysis, v2.07) (Subramanian et al., 2005) revealed that these DEGs were enriched in processes related to neural system development, apoptosis, transportation, and signal transduction (**Fig. II.8** and **Table II.S2**), confirming an important role of Top2b in retinal cell survival and maintenance.

6. Discussion

In this study, using the traditional constitutive Top2b KO and retina-specific Top2b cKO mouse models and in combination with the RNA-seq analysis, we report the functional role of Top2b in mammalian retina. We demonstrated that Top2b is required for terminal differentiation and proper laminar structure formation but not for cell fate specification during embryonic retinal development; and cell survival/maintenance in the postnatal retina. Top2b is expressed in all differentiating and mature retinal cell types; and as a DNA enzyme known to involve in transcription regulation, retinogenesis phenotypes observed in Top2b-deficient retinas are likely the consequence of altered gene expression. Our genome-wide transcriptome analysis confirmed that the differentially expressed genes are associated with neurological system development and cell survival.

Previous studies including our own have shown that Top2b deficiency does not affect cell proliferation in cultured mouse embryonic fibroblasts (Lin et al., 2013; Lyu and Wang, 2003b) and mouse embryonic stem cells (Tiwari et al., 2012). Confirming these observations, our *in vivo* data obtained from Top2b KO retinas showed no difference in the S-phase labeling with EdU, M-phase labeling with PH3, or mitotic cell cleavage orientations (**Fig. II.S4**). Together with the mutually exclusive pattern of EdU labeling and Top2b expression (**Fig. II.1A**), this study confirms that Top2b is unlikely to be involved in cell proliferation *in vivo*.

Although there were severe lamination defects and neurodegeneration in Top2b-deficient retina, all retinal cell types (i.e. ganglion, horizontal, amacrine, bipolar, rod photoreceptor, cone photoreceptor, and Müller glial cells) have emerged (**Fig. II.1B-H**, **S3**). The timing of the expression of cell-specific makers seems to follow a normal generation timeline of the corresponding retinal cell types (**Fig. II.1I**). These findings demonstrate that Top2b does not affect cell cycle withdrawal and cell fate determination

in retinal progenitors *in vivo*; and are consistent with the notion that cell fate specification is determined during the last cell cycle of neuronal progenitors before their asymmetric cell division (McConnell, 1991; McConnell and Kaznowski, 1991).

In our previous studies, the lack of Top2b was found to cause aberrant lamination in the mouse cerebral cortex, which may be resulted from the decreased Reelin expression (Lyu and Wang, 2003b). Interestingly, we found that Top2b deficiency in the retina causes a delayed differentiation phenotype in ganglion cells, horizontal cells, a lack of OS in photoreceptors, and severe defects in the plexiform layers, indicating a role of Top2b in cell differentiation, neurite outgrowth and proper retinal laminar formation. RNA-seq analysis revealed a decreased expression level of several migration guidance molecules in the cKO retinas, including Reelin. Since Reelin plays important role in guiding cell migration and positioning in laminar structures (Rice and Curran, 2001), the reduction of its expression could explain the mis-positioned horizontal and ganglion cells (**Fig. II.3**). However, although Reelin KO mice (Reeler mice) showed a disruption in synaptic circuitry formation in the IPL and decreased rod bipolar cell density, the IPL structure can still be identified even in the adult animals (Rice et al., 2001). Thus, the reduced Reelin expression itself is insufficient to cause the severe degeneration of the plexiform layers observed in Top2b cKO retinas.

Top2b deficiency not only tampers the target finding of axons (Yang et al., 2000) but also inhibits neurite growth in two levels: shorter neurite lengths and growth cone degeneration (Nur et al., 2007). In addition, Top2b has been identified as the main regulator of ganglion cell axon path finding during zebrafish retinal development by a forward genetic screen (Nevin et al., 2011b). Although the molecular mechanism underlying the role of Top2b in neurite growth remains to be determined, it is clear that the disrupted neurite growth caused by Top2b deletion can contribute to the aberrant

lamination as well as loss of synaptic connections in the IPL, OPL, and the degeneration of neurofilaments in Top2b cKO retina (**Fig. II.2, 5**).

We showed that during postnatal retinal development, Top2b is necessary for the survival of postmitotic retinal cells, including ganglion, horizontal, photoreceptor cells, Müller glia, and possibly other cell types. Lack of Top2b results in a significant increase in the number of cells that contain DNA damage and/or apoptotic signals (γ-H2AX+ and Casp3+) (**Fig. II.6**), smaller eyeballs, and the thinner optic nerves (**Fig. II.S5, S6**). The findings presented here are coherent with a critical role of Top2b in neuronal survival and maintenance *in vivo*, and with the previous report that Top2b is required for the survival of mouse embryonic stem cell-derived neurons in culture (Tiwari et al., 2012). The interpretation that Top2b plays a critical role in postmitotic retinal cells survival/maintenance may well be extrapolated to neurons located in other parts of the CNS. Interestingly, it has been reported that Top2b level decreases as neurons age (Bhanu et al., 2010) and Top2b deficiency can lead to dopaminergic neuron degeneration (Heng et al., 2012), further implicating a plausible role of Top2b in CNS degenerative diseases.

Consistent with the observed phenotypes, our RNA-seq analysis revealed that the differentially expressed genes (DEGs) in Top2b cKO retinas are associated with cell survival and neurological system development (**Fig 8, Table II.S1, S2**). For instance, Igf1 is known to be a key regulator that promotes growth and development, and can induce the differentiation of ganglion cells, rod photoreceptors and one subtype of glial cells (Fischer et al., 2010; Meyer-Franke et al., 1995; Pinzon-Guzman et al., 2011). The down-regulation of Igf1 pathway and other pathways such as Erk (Hras and Mapk1), Hif1a, Vegf, and Atk (Rps6bk1)) were known to affect cell survival (Chang et al., 2003; Dudek et al., 1997; Jin et al., 2002; Tomita et al., 2003), which may explain the dramatic

cell loss in the cKO retinas. Other DEGs such as Tac1, GriK1/2, Gria4, Grm7 and Nrxn1/3 are important neurotransmitters and receptors (Bagnoli et al., 2003; Dingledine et al., 1999; Millan et al., 2002; Uemura et al., 2010), which are involved in modulating myriad aspects of neuronal function. The up-regulation of Sst at P0 and down-regulation of Tac1 at P6 in cKO retinas can impact neuronal function and survival due to their essential role as neurotransmitters in the retinal circuits (Bagnoli et al., 2003). Sst inhibits cell proliferation (Lahlou et al., 2003) but aid neurite dendrite growth (Kungel et al., 1997). Tac1 prevents neuronal damage during development and enhances nerve growth factor-mediated neurite outgrowth (Bagnoli et al., 2003). Thus, the up-regulated Sst and down-regulated Tac1 could alter the state of retinal development in the same direction. Moreover, both factors are localized to amacrine and ganglion cells (Catalani et al., 2006; Cristiani et al., 2002; Zalutsky and Miller, 1990) where major defects were found in Top2b KO/cKO retinas.

The question of how Top2b deficiency causes differential expression of particular genes remains largely unanswered. Although we cannot rule out the possibility that the increased retinal cell death may contribute to the differential expression of specific genes, however, a series of *in vivo* and *in vitro* studies have supported the claim that Top2b is a crucial player in regulating transcription (Ju et al., 2006; King et al., 2013; Lyu et al., 2006; Lyu and Wang, 2003b; Tiwari et al., 2012; Tsutsui et al., 2001a). Top2 can modulate DNA topology and chromatin structure by performing DNA strand passage reactions. The Top2a isozyme, which is only expressed in proliferating cells, is known to orchestrate sister chromatin segregation and chromatin condensation/decondensation in association with other chromatin-modulating enzymes such as condensin (Lupo et al., 2001). The absence of Top2a and presence of Top2b in postmitotic cells undergoing terminal differentiation may imply that Top2b can regulate gene expression by controlling

local chromatin structure. Recently, the possible role of Top2b in regulating transcription near the promoter has gained further support from studies of identifying unconstrained DNA supercoiling as well as promoter melting during transcription activation (Kouzine et al., 2013a; Kouzine et al., 2013b; Naughton et al., 2013). However, the molecular mechanism that underlies Top2b function in this respect still requires further investigation.

In summary, our studies have demonstrated that Top2b plays an essential role in the survival and maintenance of postmitotic retinal cells. In the absence of Top2b, proper retinal development is affected starting at early postnatal stages. Top2b-dependent genes identified by RNA-seq are known to control neuronal survival and neurite outgrowth. Identification of genes that are directly controlled by Top2b will be the next step in unveiling the molecular mechanism of Top2b in transcription regulation.

7. Acknowledgements

We are grateful to Drs. *Takahisa Furukawa* and Hiromi Sesaki for the *Dkk3-Cre* mice and Dr. Robert S. Molday for the Rhodopsin 4D2 antibody. We also thank members of our laboratories for helpful discussions and critical reading of the manuscript. This work was supported in part by the grants from the National Institute of Health (R21EY018738 to LC and R01CA102463 to LFL) and the Busch Biomedical Research Awards (LC). LC and YLL conceived and designed the experiment; YL, HH, ET, SD and RKL performed the experiments and collected data; YL, YLL, LFL and LC analyzed the data and wrote the manuscript.

8. Supplemental Materials

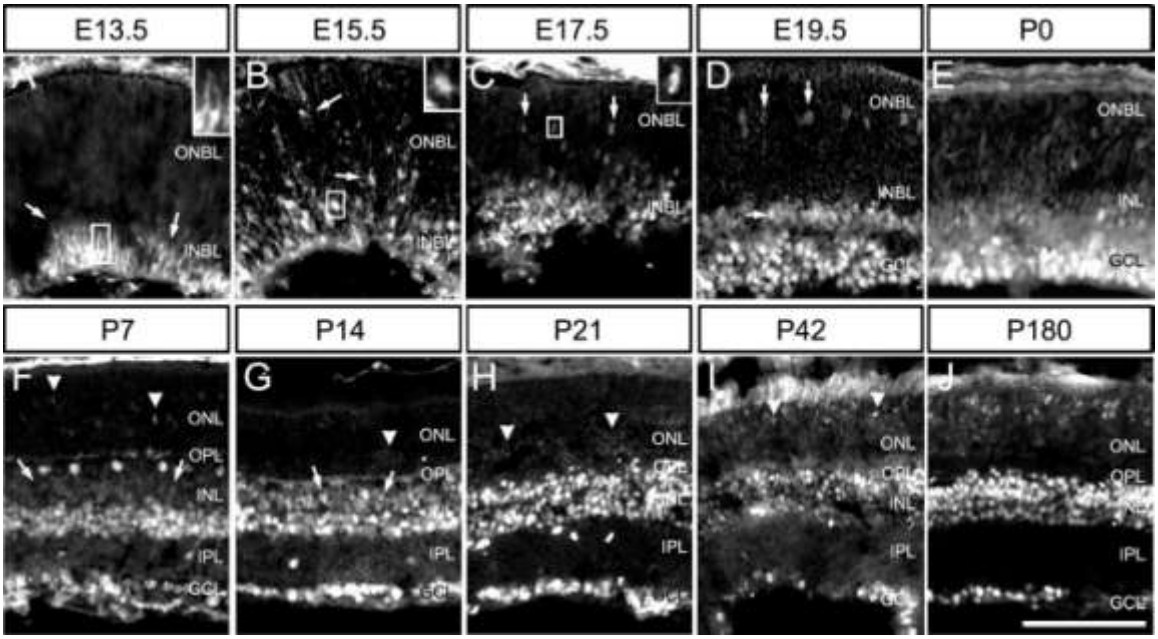

Figure II.S1. Top2b expression during mouse retinal development. Retina sections from different developmental stages were stained with the anti-Top2b antibody. Top2b expression was first detected at E13.5 in the lower portion of the INBL (A) in the cytoplasm, and then extended to the upper INBL and lower ONBL at E15.5 (B, arrows) in the nuclei. Starting from E17.5, it appeared in the horizontal cells (C-D, vertical arrows), the cells in the INL and GCL (D-J, arrows), and photoreceptor cells (F-J, arrowheads). Top2b expression is maintained in the adult retina at P180 (J). Cellular identities of Top2b+ cells were determined by their position and double staining with cell-specific markers (see Fig.1). Boxed region is shown in a higher magnification. INBL, inner neuroblastic layer; ONBL, outer neuroblastic later; GCL, ganglion cell layer; INL, inner nuclear layer; IPL, inner plexiform layer; ONL, outer nuclear layer; OPL, outer plexiform layer. Scale bar = 100 μm.

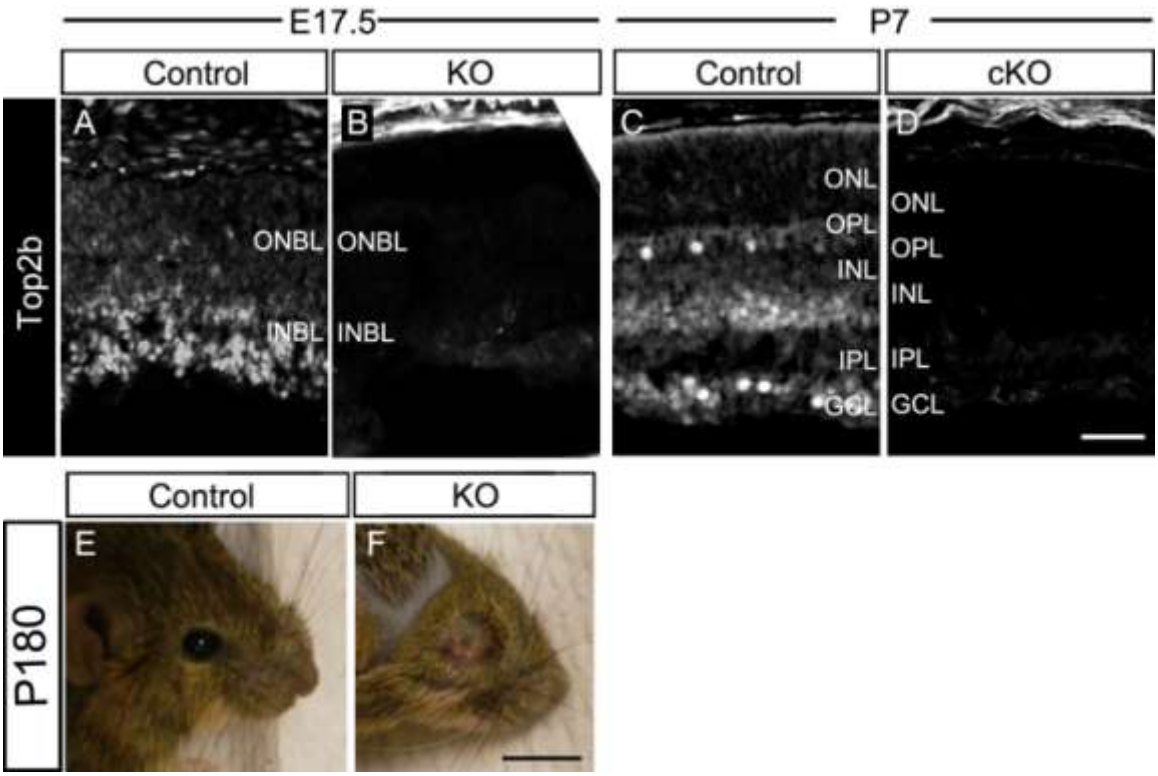

Figure II.S2. Eye degeneration in Top2b deficient mice. (A-D) Top2b expression was detected in retinas of control littermates, but not in retinas of Top2b-deficient E17.5 KO or P7 cKO littermates. (E-F) Severe eye degeneration was observed in adult retina-specific Top2b KO (cKO) mice. Scale bar in A-D = 50 μm; in E-F = 1 cm.

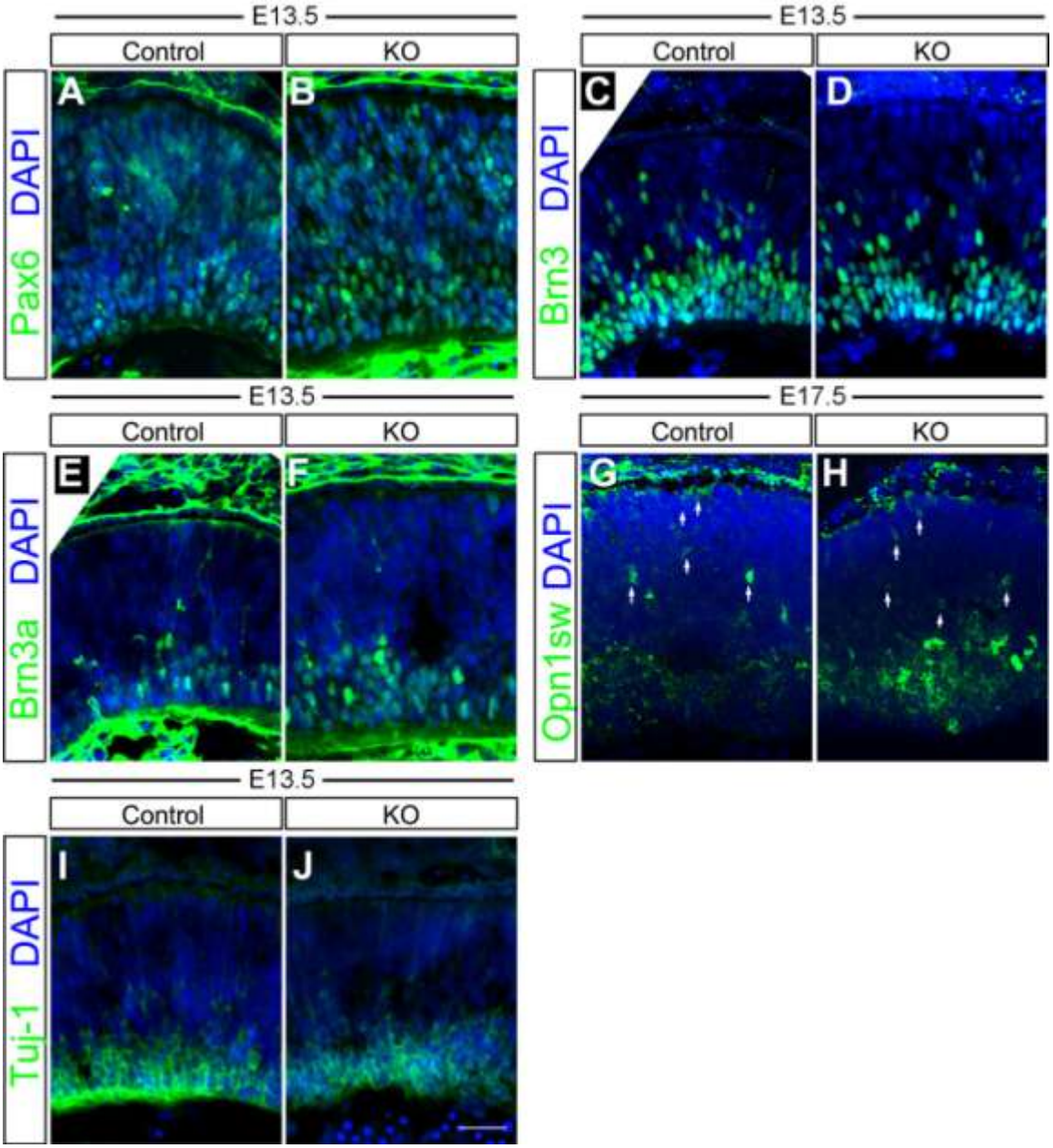

Figure II.S3. Top2b deficiency does not affect early retinogenesis. At E13.5, no obvious difference in immunostaining was detected with retinal progenitor marker Pax6 (A-B), ganglion cell marker Brn3 (C-D) and Brn3a (E-F), cone photoreceptor marker Opn1sw (at E17.5) (G-H, arrows), and early neuronal marker Tuj-1 (I-J). Scale bar = 50μm.

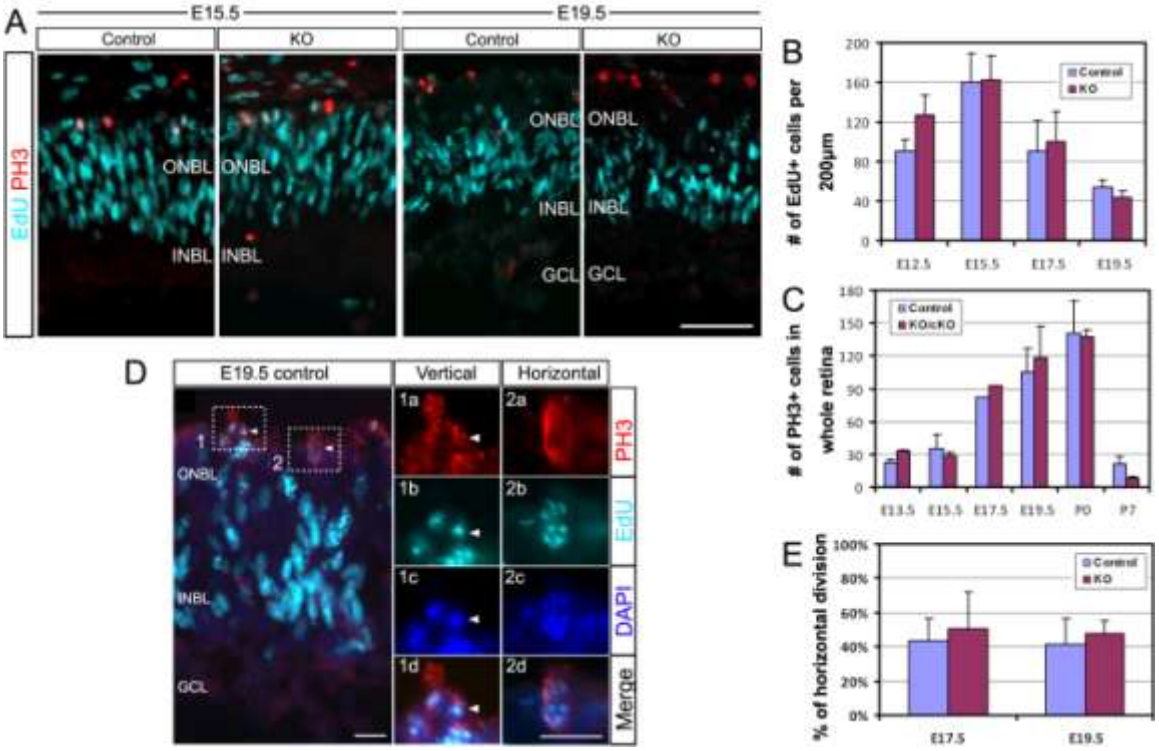

Figure II.S4. Top2b deletion does not affect embryonic retinal cell proliferation. The thymidine analog EdU was injected into pregnant female mice 2 hr before sacrifice and dissection. Retina sections were then prepared and EdU incorporation was detected using the Click-iT Edu Alexa Fluor 647 Imaging kit. (A) Cell proliferation in embryonic retina was examined by EdU labeling (S-phase cells, cyan) and phosphorylated-histone 3 (PH3) staining (M-phase cells, red). (B-C) Quantification showed no significant change in the number of EdU+ or PH3+ cells between the control and Top2b-deficient (KO) retinas. (D) Mitotic cleavage orientation of cell divisions was examined by analyzing $EdU^{+}/PH3^{+}$ cells. (E) No significant difference in the mitotic cleavage plane was observed. Error bars represent s.d. (n = 3). INBL, inner neuroblastic layer; ONBL, outer neuroblastic later; GCL, ganglion cell layer. Scale bars = 50μm.

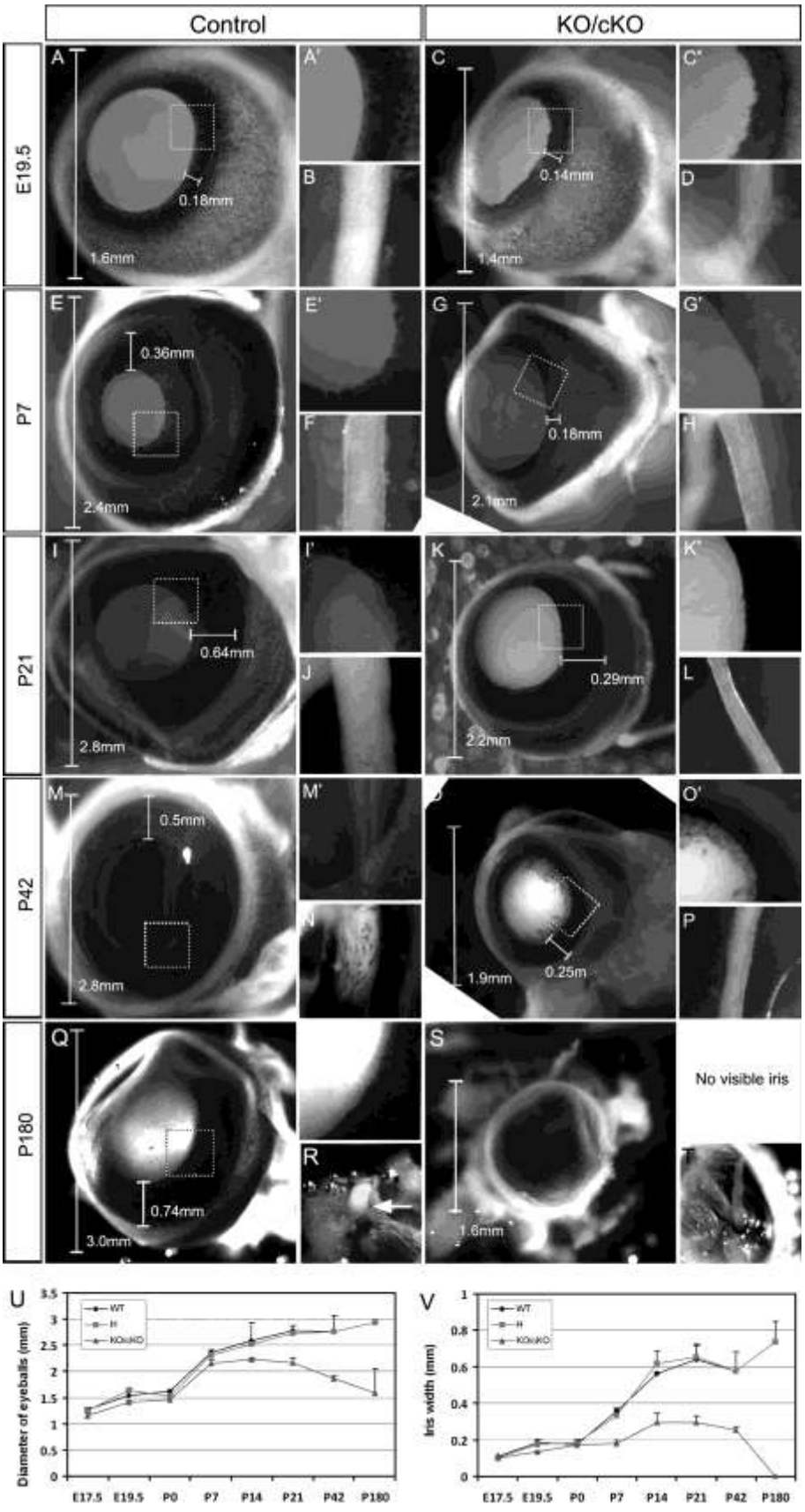
Control
KO/cKO
E19.5
P7
P21
P42
P180
A
A'
B
C
C'
D
E
E'
F
G
G'
H
I
I'
J
K
K'
L
M
M'
N
O
O'
P
Q
R
S
T
0.18mm
1.6mm
0.14mm
1.4mm
0.36mm
2.4mm
0.18mm
2.1mm
0.64mm
2.8mm
0.29mm
2.2mm
0.5mm
2.8mm
1.9mm
0.25m
0.74mm
3.0mm
1.6mm
No visible iris
U
Diameter of eyeballs (mm)
WT
H
KO/cKO
E17.5 E19.5 P0 P7 P14 P21 P42 P180
V
Iris width (mm)
WT
H
KO/cKO
E17.5 E19.5 P0 P7 P14 P21 P42 P180

Figure II.S5. Top2b deficiency causes morphological changes in the eye. Eyes were isolated from E17.5 and E19.5 wild type (WT, *Top2b*$^{+/+}$), heterozygotes (H, *Top2b*$^{+/-}$) and KO (*Top2b*$^{-/-}$) embryos; as well as from control (*Top2b*$^{flox2/flox2}$, labeled as WT; H, *DKK3-Cre:Top2b*$^{+/flox2}$) and cKO (*DKK3-Cre:Top2b*$^{flox2/flox2}$) postnatal pups. Diameter of the eye ball and thickness of the iris were measured. (A, C, E, G, I, K, M, O, Q, S) Smaller eyeball, larger pupil and reduced iris thickness were observed in Top2b-deficient eyes. (A', C', E', G', I', K', M', O', Q', S') Defective iris collarette structure was found in Top2b-deficient eyes. (B, D, F, H, J, L, N, P, R, T) Thinner and flatter optic nerve was observed in Top2b-deficient eyes. (U) Quantification of the diameter of eyeballs. (V) Quantification of the iris width. Error bars represent s.d. (n=3, except n=2 for P0 and P42).

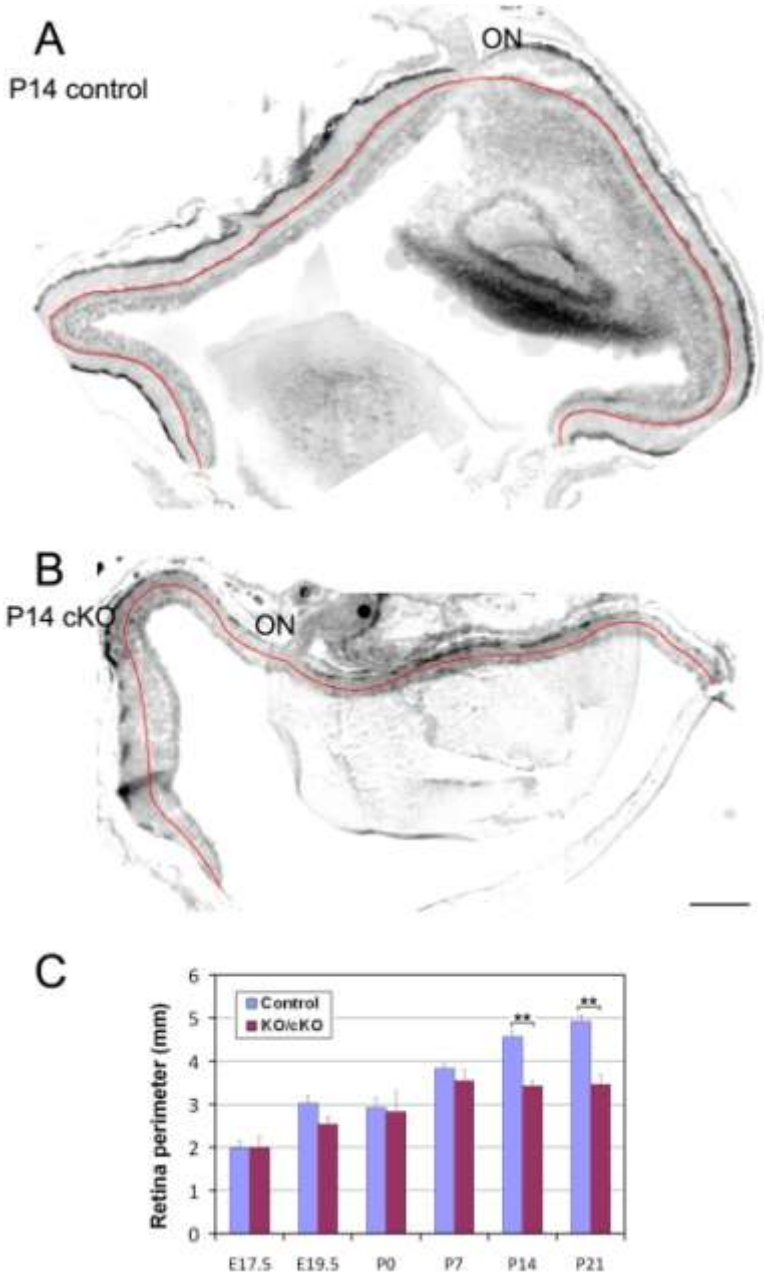

Figure II.S6. Reduced perimeter in Top2b-deficient retinas. (A-B) Retina perimeter was determined by measuring the length of the midline (red line) in sections through the central retina where optic nerve (ON) locates. (C) Quantification showed that retina perimeter was significantly reduced starting at P14 in the Top2b-deficient retinas. Error bars represent s.d. (n = 3). T-test: ** $p<0.01$. Scale bar = 200μm.

Stage	Factor	RNA-seq analysis		Related function	References
		Log(fold change)	p-value		
P0	Sst *	7.8	3.4E-7	Growth hormone inhibitor; Neurotransmitter; Aid dendrite growth	(Bagnoli et al., 2003; Kungel et al., 1997; Lahlou et al., 2003)
	Igf1	-1.8 E+308	5.8E-12	Mediating cell growth and develop; inducing the differentiation of ganglion cells, rod photoreceptor and one subtype of glial cells	(Fischer et al., 2010; Meyer-Franke et al., 1995; Pinzon-Guzman et al., 2011)
	Hras	-1.9	5.7E-4	Member of Erk pathway which regulates cell proliferation, differentiation and prevention of apoptosis; member of Igf1 pathway	(Chang et al., 2003)
	Mapk1	-1.2	6.4E-6	Member of Erk pathway which regulates cell proliferation, differentiation and prevention of apoptosis; member of Igf1 pathway	(Chang et al., 2003)
	HIF1α *	-0.77	5.9E-5	Hif1a pathway; protective function of neurons; member of Igf1 pathway	(Tomita et al., 2003)
	Vegfa	-0.99	1.3E-3	Member of Vegf pathway which is critical for retinal blood supply; stimulating neurogenesis; member of Igf1 pathway	(Jin et al., 2002; Robinson et al., 2001)
	Rps6bk1 *	-1.6	1.3E-4	Member of Akt pathway; regulating cell growth; member of Igf1 pathway	(Dudek et al., 1997; Harada et al., 2001)
P6	Gfap *	2.2	5.8E-11	Promoting the radial glial cells to re-enter cell cycle	(Francke et al., 2001; Guerin et al., 1990)
	Tac1 *	-2.7	5.2E-5	Neurotransmitter; preventing neuronal damage during development and enhancing nerve growth factor-mediated neurite outgrowth	(Bagnoli et al., 2003)
	Grik1*/2	-2.0/-1.7	3.0E-14/1.4E-11	Neurotransmitter receptors	(Dingledine et al., 1999)
	Gria4	-1.3	2.57E-12	Neurotransmitter receptors	(Dingledine et al., 1999)
	Grm7	-1.2	1.2E-4	Neurotransmitter receptors	(Millan et al., 2002)
	Nrxn1/3	-1.2/-2.1	2.0E-6/0	Neurotransmitter receptors; synapse formation	(Uemura et al., 2010)
* indicates the expression of the gene was confirmed with immunohistochemistry analysis (see Fig. 7).					

Table S1. A partial list of differentially expressed genes identified by RNA-seq analysis

Stage	Gene sets	Genes
P0	Apoptosis/Programmed cell death	Cdkn1a, Asns, Gadd45a, Dad1, Psen2, Dap3, Pde1b, Dedd, Traf7, Mapk1, Glo1, Raf1, Prkce, Sst, Dap, Cryaa, Apaf1, Tspo, Grin1, Hif1a, VEGFA, Rps6kb1, Atp2c1, Nr3c1, Hras, Gnao1, Gm4617/Ptma, Xrcc6, Srpine2, Ptgd3, Apaf1, Mapk14, Drd2, Igf1, Cdkn1a, Vegfb, Smn1/2, Etv6, Srpk2, P4hb, Creb1
	Cell development	Tspo, Apaf1, Trappc4, Dap, Sst, Nptn, Cryaa, Racgap1, Nlgn1, Raf1, Glo1, Prkce, Mapk1, Asns, Gadd45a, Dad1, Cdkn1a, Nrd1, , Traf7, Dedd, Pde1b, Smarca1, Ubb, Thy1, Dap3, Psen2
	Cellular localization	Cdc23, Nup160, Cadps, Pex19, Arfgef2, Kpna4, Kif5a, Vps4b, Atp2c1, Smg7, Pdia3, Syt1, Flna, Nlgn1, Cspg5, Cryaa, Tspo
	Transport	Kcnmb2, Tspo, Slc16a8, Abcg2, Cryaa, Ghrh, Cspg5, Slc11a2, Nlgn1, Flna, Syt1, Pdia3, Smg7, Atp2c1, Necap2, Snap25, Atp11b, Ptgds, Lrp3, Abcd2, Vps4b, Slc25a11, Kif5a, Arfgef2, Kpna4, Nup160, Cadps, Pex19
	Establishment of Cellular localization	Cdc23, Nup160, Cadps, Pex19, Arfgef2, Kpna4, Kif5a, Vps4b, Atp2c1, Smg7, Pdia3, Syt1, Flna, Nlgn1, Cspg5, Cryaa, Tspo
	System Process	Pde6b, Emd, Chrna5, Sst, Cort, Kcnmb2, Drd2, Cryaa, Nptn, Eml2, Atxn7, Gucy1b3, Flii, Kif5a, Kcnip1, nao1, Syt1, Ubb, Nr2e3, Nlgn1, Crx, Mapk1
	Neurological system process	Pde6b, Chrna5, Sst, Cort, Kcnmb2, Drd2, Cryaa, Nptn, Eml2, Nlgn1, Crx, Nr2e3, Atxn7, Syt1, Ubb, Kcnip1, Kif5a, Mapk1
	System Development	Lig1, Dpysl3, Ndufv2, Fabp7, Tpd52, Prps1, Crx, Atp2c1, Adam22, Thy1, Smarca1, Ubb, Ptprz1, Igf1, Nrd1, B3gnt5, Flna, Nlgn1, Racgap1, Emd, Trappc4, Pbx4, Apaf1, Matk, Cspg5, Prdx1, Drd2, Tle1, Nptn, Apba2
	Anatomical structure development	Flna, Nlgn1, Tpd52, Fabp7, Ndufv2, Lig1, Dpysl3, Crx, Prps1, Smarca1, Vcl, Ptprz1, Ubb, Thy1, Atp2c1, Adam22, Igf1, Nrd1, B3gnt5, Apba2, Emd, Racgap1, Trappc4, Prdx1, Pbx4, Apaf1, Kcnmb2, Drd2, Tle1, Cspg5, Dkk3, Matk, Nptn
P6	Neurological system process	Grm7, Syt1, Vsx1, Cartpt, Grik2, Iqcb1, Opn1sw, Grik1, Coch, Nlgn1, Pdc, Cryba1, Rcvrn, Cryba4, Crygd, Cryaa, Crybb3, Cryga, Abca4, Cbln1, Crybb1, Reln, Nrxn1, Gria4, Tac1, GFAP, Qki
	Cytoplasm	Cops5, Chuk, Ergic3, Hspb1, Nos3, Cryaa, Utp11l, Nrsn1, Vdac3, Cct6a, Ubl5, Exoc4, Top2b, Hspe1, Ndufb6, Glo1, Bzw1, Atp5a1, Nefl

Table S2. Differentially expressed genes are involved in neural cell survival and neural system development (see Fig. 8)

Chapter III

Transcriptional Regulatory Network for Retinal Development

1. Prologue

Retina, similar to the other parts of the CNS, has a complicated layered structure which requires mediated gene expression during development (Hu et al., 2010; Kumar, 2009). Many studies have been carried out focusing on the transcriptional regulatory network for specific retinal cell lineage, e.g., the photoreceptor cells (Brzezinski and Reh, 2015; Corbo et al., 2010; Hsiau et al., 2007; Swaroop et al., 2010) and bipolar cells (Kim et al., 2008). Recent genome-wide gene expression profiling and gene-protein interaction profiling have provide insights in massive identification of novel *cis*- and *trans*-elements involved in specific cell types on determined stage (Brooks et al., 2011; Yin et al., 2014). Databases such as Ensembl (http://www.ensembl.org), Assembly (NCBI, http://www.ncbi.nlm.nih.gov/assembly) and JASPAR (http://jaspar.binf.ku.dk/) were built collecting the daily-increasing information of a variety of genes and their regulatory companions

In this study, the main hypothesis is that there exists a general network involving several critical retinal-specific genes. Such network governs the specification of retinal progenitors and distinguishes them from other neural stem cells. To test the hypothesis, I tempted to use a novel computational method to analyze the retina-specific enhancers, TFs, TF binding sites (TFBSs) and expression of the TF-flanking gene. In details, sequence elements with retinal tissue-specific enhancer activity were Identified from Ensembl database. They were analyzed by TFBS-predicting programs. Common TFBSs for a group of enhancers were identified, which would allow the binding of master TFs. The resulting TFs were then reviewed by comparison to literatures and existing

databases. As a result, a transcription regulatory network centered on Pou3f2, Crx, Hes1, Meis1, Pbx2, Tcf3 and the eight enhancers was built. It is shown to be involved in the determination of the retinal progenitor cells and all seven types of retinal cells.

The remainder of this chapter is reproduced verbatim from a published manuscript in Biology Open (Li et al., 2011) with minor modifications.

---

2. Abstract

The process of cell-fate determination and differentiation in vertebrate retina during embryonic development is well organized through complicated interactions with transcription factors. Previous studies report on genetic function and networks of the development of certain specific cell lineages, e.g., the photoreceptors. However, transcription factor regulatory networks that contribute to the entire tissue are still elusive. Here, we attempt to provide a new computational method for the study of DNA-protein interactions and the construction of tissue-specific transcription factor regulatory networks for the development of retina cell types. The novelty of our study was based on the functional tissue-specific regulatory sequence elements. Using the mouse retina as a model, we searched for experimentally verified *cis*-regulatory elements, e.g., promoters and enhancers, which were shown to function specifically in neural retina. Potential binding sites of *trans*-acting factors on these enhancers were predicted using sequence analysis tools. Common *trans*-acting factors among these *cis*-regulatory elements were then selected to construct transcription factor regulatory networks. The resulting common *trans*-acting factors and networks showed importance for embryonic retinal cell-fate determination and differentiation. Furthermore, potentially novel functions, interactions, and pathways of these protein factors were predicted. This computational analysis based on the retina-specific DNA regulatory elements together with experimental studies can be used to predict the *trans*-acting factors and transcriptional regulatory networks for mouse embryonic retinal development. Our results confirmed experimentally verified factors and known regulatory networks in retinal development. This novel method generates important hypotheses for retinal development, but also can be readily applied to studies of other developmental systems.

3. Introduction

The formation of the neatly layered retina during embryonic development is dictated by a series of complicated transcription factor interactions. Retina-specific expression of these transcription factors is an essential step in establishing retinal progenitor cells (RPCs) from embryonic stem cells. The transcriptional control of gene expression is largely mediated by the combinatorial interactions between *cis*-regulatory DNA elements and *trans*-acting transcription factors, which cooperate/interact with each other to form a transcription factor regulatory network during this developmental process. Such regulatory networks are essential in regulating tissue/cell-specific gene expression, e.g., in cell fate determination and differentiation during embryonic retinal development (Hu et al., 2010; Kumar, 2009; Swaroop et al., 2010). Many genes, involved in transcriptional networks for the specification of a certain retinal cell lineage, have already been identified and characterized (Corbo et al., 2010; Kim et al., 2008b; Tang et al., 2010). The transcriptional regulatory networks for specific retinal cell lineages, e.g., the photoreceptors (Corbo et al., 2010; Hsiau et al., 2007) and bipolar neurons (Kim et al., 2008b), were established in recent years. However, the transcriptional regulatory network that governs the entire neural retinal development is still elusive.

Identifying tissue/cell-specific *cis*-regulatory elements, *trans*-acting factor binding sites (TFBSs), and their binding transcription factors (TFs) represent key steps towards understanding tissue/cell-specific gene expression and further successful reconstruction of transcriptional regulatory networks. These steps also present major challenges in both fields of experimental biology and computational biology.

Currently, the prevailing method of studying TFBSs and transcriptional regulatory networks is to determine the function of tissue-specific trans-acting factors based on data from genome-wide gene expression profiling and chromatin immunoprecipitation

(ChIP). ChIP is often used to investigate protein-DNA interactions in a cell. Coupled with massive parallel sequencing, ChIP-seq is capable of mapping the genome-wide protein-DNA interaction at a finer resolution (Valouev et al., 2008) to identify candidate enhancer sequences (Visel et al., 2009). Thus, a regulatory cascade can be recognized via consequential analysis of the factors involved.

Here, we present a new method for the computational analysis of TFBSs and transcriptional regulatory networks utilizing genome-wide sequencing, expression, and enhancer data. In contrast to the traditional method, which mainly focuses on factor expression analysis, we emphasize the sequence elements with tissue-specific enhancer activity. Our hypothesis is that enhancers, non-coding sequences that direct gene expression in a cell-/tissue-specific manner, contain common TFBSs that allow the key protein factors (important for the development of that cell/tissue type) to bind. Experimentally verified tissue-specific enhancer elements selected from enhancer databases were carefully screened for common trans-acting factor binding sites to predict potential sequence-factor interacting networks. DNA-binding protein factors that associate with multiple enhancers can be analyzed using experimental methods.

As proof-of-principle, simple transcriptional regulatory networks of embryonic retinal development were assembled based on common/key factors and their interacting genes, as determined by literature search. These resulting networks provide a general view of embryonic retinal development and a new hypothesis for further experimentation.

4. Methods and Results

In this study, we aimed to develop a method for the identification of regulatory networks for cell/tissue-specific gene expression. To test our hypothesis of the existence of common TFBSs on the enhancers of cell/tissue type specific genes, we employ the mouse developing retina as a model system. Enhancers that direct retina-specific gene expression were selected and their sequences were thoroughly screened for common TFBSs and *trans*-acting factors (protein factors) using open-access software such as TESS, JASPA, MatInspector, and MEME, etc. For common TFBS selection, we developed a Matlab program. These common protein factors were further studied for their expression profiles. Thereafter, we were able to construct transcriptional regulatory networks based on the known function of the enhancer-binding *trans*-acting factors using a network construction tool, BioTapestry (Longabaugh et al., 2009).

1) Retina-specific enhancers

To determine the transcriptional regulatory networks that govern retinal development, we identified and selected enhancer elements that direct gene expression in the retina by searching the VISTA Enhancer Browser. The VISTA Enhancer Browser is a central resource for experimentally validated human and mouse non-coding DNA fragments with enhancer activity as assessed in transgenic mice. Most of these non-coding elements were selected for testing based on their extreme conservation in other vertebrates or epigenomic evidence (ChIP-Seq) of putative enhancer marks. The results of this *in vivo* enhancer screen are provided through this publicly available website (Frazer et al., 2004). Of the 1503 non-coding DNA elements from human and mouse genomes that were tested for their ability to direct gene expression on embryonic day 11.5 (E11.5) using a reporter assay in transgenic mouse, a total of 47 elements were

shown to possess enhancer activity in the retina (as of February 10, 2011). Of the 47 elements, 25 show enhancer activities in both the retina and other tissues, e.g., heart, limb, brain and spinal cord, etc. These 25 elements were separated for further analysis as we focused on retina-specific sequence elements. In addition, among the 22 remaining elements, 17 elements were active enhancers in the retina in at least half of the tested transgenic embryos (Supporting data 1). To further increase the possibility of identifying the key enhancer elements that are critical for retinal development, we applied more stringent selection criteria based on the following two properties: 1) the reporter expression is restricted in the retina and not in any other regions of the CNS; 2) there is expression of at least one of the flanking genes in the retina at E11.5 (or Theiler Stage 18-21). The second category was applied because a majority of known enhancers were found in the immediate up- or downstream region of their target genes, and thus the regulatory activities of enhancers were considered to be most likely associated with their flanking genes. Any enhancer elements that did not fit into at least one of the two categories were thus eliminated (details in Supporting data 5). Based on the above criteria, 8 enhancer elements were identified (**Table III.1**).

Group	Enhancer ID	Length (bp)	Reporter expression pattern derived from enhancer activity	Annotation of reporter expression	Flanking genes of enhancers and their endogenous expression in mouse embryos	
					Upstream	Downstream
1	**hs27**	1113	eye(4/6), limb(4/6)	Retina + non-CNS	**Irx5: E11-19 retina**	**Irx6: E11-19 retina**
	hs258	1487	eye(3/5), limb,	Retina + non-CNS	Ccdc39: E14.5	**Fxr1: E12-14, E19 retina**
	hs546	1753	eye(7/7), limb, nose	Retina + non-CNS	**Nr2f1: E11-19 in retina**	Arrdc3: E14-19
	hs1170	1288	eye(8/8)	Retina	**Nr2f1: E11-19 in retina**	Arrdc3: E14-19
2	**hs932**	775	eye(6/9), limb, nose, branchial arch	Retina + non-CNS	AA408296: unknown	Irf6: not in retina
	mm165	926	eye(4/5), heart	Retina + non-CNS	Lao1: unknown	Slc2a1: not in retina

3	**hs1122**	1218	eye(6/7)	Retina+ Spinal cord	**Ascl1: E11-19 in retina (MGI)**	Pah: not in retina
	mm269	760	eye(5/5), heart, other	Retina+ Spinal cord	**Zfand5** (intragenic): **E11-13**/E13-19 in retina	

Table III.1. A list of eight retina-specific enhancers. The 8 retina-specific enhancers from the VISTA Enhancer Browser are listed above. They are grouped into 3 sub-groups according to the reporter expression in mouse embryos derived from these enhancers and the expression pattern of their flanking genes. The enhancer IDs, their expression pattern and the flanking gene names were retrieved directly from VISTA Enhancer Browser, with an expression pattern described as 'tissue type (positive sample number/total sample number)'. Flanking genes with expression in the retina are shown in **bold**.

2) *Trans*-acting factor binding sites on retina-specific enhancers

The binding of trans-acting factors (e.g., transcription factors) to non-coding regulatory DNA (e.g., promoters, enhancers, etc.) is an essential process in the control of gene expression. This protein-DNA interaction helps recruit the DNA polymerase complex and co-activators to form the transcription machinery. The binding of these protein factors can also act as repressors to prevent transcription. Identification of a TFBS in the enhancer and promoter for a gene may indicate the possibility that the corresponding factors play a role in the regulation of that gene. Importantly, the ability of an enhancer to direct cell/tissue-specific gene expression is achieved via the binding of tissue-specific *trans*-acting protein factors. To determine what protein factors regulate retina-specific gene expression, it is important to determine what TFBSs are located on the retina-specific enhancers. We thus searched DNA sequences of the 8 retina-specific enhancer elements for their known TFBSs using TESS (Schug, 2002), JASPA (Portales-Casamar et al., 2010; Sandelin et al., 2004) and MatInspector (Cartharius et al., 2005). For example, TESS (Transcription Element Search System - http://www.cbil.upenn.edu/cgi-bin/tess) is a web tool for predicting TFBSs in DNA sequences. It can identify TFBSs using site or consensus strings and positional weight matrices mainly from the TRANSFAC (Knuppel et al., 1994). TRANSFAC contains data on transcription factors, their experimentally-proven binding sites, and regulated genes.

Its broad compilation of binding sites allows the derivation of positional weight matrices (Knuppel et al., 1994). The following search parameters were set when searching TESS: a minimum string length of 6, a maximum allowable string mismatch of 10%, a minimum log-likelihood ratio score of 12, and organism selection of *Mus musculus* (the house mouse). Our search results show that there are approximately 150 TFBSs for each of the 8 enhancer sequences (Supporting data 2). Similar results were reported by JASPA and MatInspector. The corresponding protein factors of these TFBSs were considered to be capable of binding with the 8 retina-specific enhancers, and thus they are important in activating/suppressing gene expression in the retina.

3) A motif containing Pou3f2 binding sites

Since all 8 enhancers possess the ability to direct retina-specific gene expression, there may be key TFBSs shared amongst these retina-specific sequence elements. To test this hypothesis, we sorted and screened the TFBSs of each of the 8 enhancers to identify common ones using a Matlab program that we developed for this study (Supporting data 6). This MatLab program for common TFBS selection was designed to compare the TFBSs on each of the retina-specific enhancer elements predicted by TESS. TFBSs for two or three different enhancers can be sequentially compared. A “model” character was used as the comparison category instead of the binding site name in both TESS and our MatLab program. As defined in TESS, a model is “the site string or weight matrix used to pick this site” (Schug, 2002), and thus describes the nature of a binding site. One factor may have multiple models, and one model may be shared by multiple factors. The model character is the only necessary parameter to characterize the transcription factors depending on their binding site property.

With this sorting/searching program, we identified a TFBS for Pou3f2 (also known

as Brn2) that was present in all 8 retina-specific enhancers (**Fig. III. 1A**). Previous studies have demonstrated that the Pou3f2 transcription factor plays an important role in the development of neural progenitor cells (Catena et al., 2004; Kim et al., 2008b; McEvilly et al., 2002; Sugitani et al., 2002). Furthermore, the literature reports that this motif was first discovered as a *cis*-element in the Chx10 enhancer, which can drive reporter expression in intermediate and late RPCs (Rowan and Cepko, 2005). In this study, Pou3f2 was also shown to affect bipolar interneuron fate determination through interactions with Chx10 and Nestin.

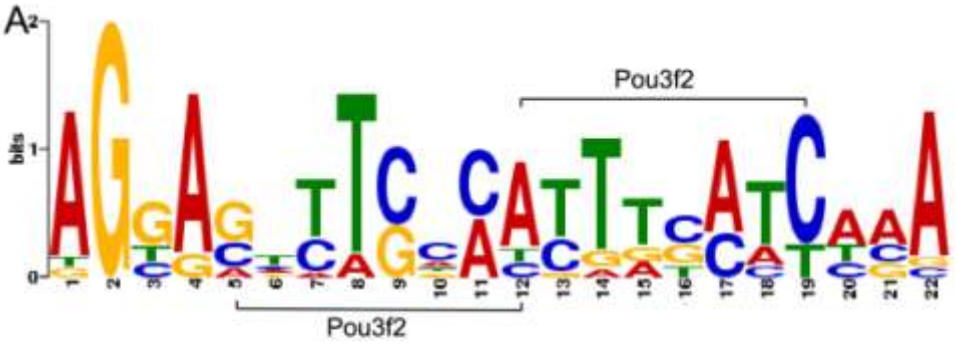

B

Name	Strand	Start	p-value	Sites
cis-element_of_r_CyclinD1	+	0	5.31e-10	AGGACTTTGCAACTTCAACAAA
cis-element_of_m_CyclinD1	+	0	5.31e-10	AGGACTTTGCAACTTCAACAAA
cis-element_of_h_CyclinD1	+	0	5.31e-10	AGGACTTTGCAACTTCAACAAA
cis-element_of_h_Chx10	+	0	6.16e-09	AGGAGATTCCCCTTTTATCCAA
cis-element_of_m_Chx10	+	0	9.18e-09	AGGAGATTCCCTTTTTATCCAA
mm269.chr19:21,348,574-21,349,333	+	295	1.10e-07	GACAGGCTGA AGCGCCCTCCCATGTGATCTAA GCTTCAGAGA
hs546.chr13:78,463,126-78,464,675	+	567	2.55e-07	CCTTCTCCCC AGCAGAATGCAATTACCTCTAA AGCCCGTGGT
hs1122.chr10:86,963,003-86,964,413	-	1377	2.78e-07	ACAGAAGAGC AGGAGCCTCACATTGGCTCTGG CTCTGCAGCT
hs932.chr1:194,967,242-194,967,917	-	343	4.61e-07	TGGAAGCCCT GGGAGTTTCGCTCTGGCTCAGA GCAGACATGC
hs258.chr2:33,781,318-33,782,778	+	517	7.37e-07	GAGAGATAGG AGGACTTTCTAATTTGCTTTCC CTCTATTTTA
hs1170.chr13:78,817,206-78,818,434	+	709	1.23e-06	ATAAACCAAG TGTAGGCTGGCATTGTATCAAA CTGGCTTTAT
hs27.chr8:94,973,252-94,974,310	+	916	1.61e-06	GGAGAAGGGG AGGGGGCTGCCAGGTGCCCAGA GGCCCTTGTG
cis-element_of_h_Pax6	+	0	2.68e-06	AGTAATTACAAATTACATTACA
cis-element_of_q_Pax6	+	0	2.68e-06	AGTAATTACAAATTACATTACA
mm165.chr4:110,691,756-110,692,681	-	304	3.02e-06	GGGGGAGGGT AGCAGCCTCTCCCATCACCCCA GGCTTAGTGA

Figure III.1. A 22 bp motif is present in all 8 retina-specific enhancers and *cis*-elements of retinal progenitor gene Chx10, CyclinD1 and Pax6. Sequence alignment was performed using MEME and the output shows a motif exists among all above 15 sequences (p-value < 3e-6). (A) a SeqLog presentation of the 22bp motif. Dual binding sites of Pou3f2 were located next to each other forms Pou3f2 binding site repeats. (B) sequence alignment reveals the 22bp motif among the 8 enhancers and *cis*-elements of RPC-specific genes (e.g., Chx10, CyclinD1 and Pax6) (Rowan and Cepko, 2005). Abbreviation: R, rat; m, mouse; h, human; q, quail. RPC, retinal progenitor cell.

We thus speculate that this Pou3f2 binding site may exist in regulatory sequences among genes important for the development of neural retinal progenitor cells (RPCs). Therefore, the *cis*-elements of Chx10, Cyclin D1, Pax6, Rax, and Six3 were examined because these genes are known for their role in regulating RPC development and retinal cell differentiation (Conte et al., 2010; Martinez-de Luna et al., 2010; Oliver et al., 1995; Rowan and Cepko, 2005; Sicinski et al., 1995). Confirming our prediction, Pou3f2 binding sites were also present in the *cis*-elements of Chx10, Cylin D1, and Pax6 genes (sequences can be found in Supporting data 4). Next, sequence alignment analysis was performed to identify a common motif for Pou3f2 binding sites using MEME (Multiple Em for Motif Elicitation, http://meme.sdsc.edu/meme4_4_0/cgi-bin/meme.cgi) (Bailey and Elkan, 1994). It is commonly believed that there are dependencies among different positions in a motif. MEME may ignore such kind of dependency. Sequence alignment reveals a 22 bp motif containing two Pou3f2 binding sites among all 8 enhancer elements (with a stringent E-value of 7.2e-20 and p-value < 3.02e-6) and also in the *cis*-elements of RPC-specific genes, e.g., Chx10, CyclinD1, and Pax6, from multiple vertebrate species (**Fig. III. 1B**). In addition, a line of evidence indicates that Pou3f2 binds to the Rax enhancer to regulate the expression of Rax in RPCs (Martinez-de Luna et al., 2010). Such prevalent existence of repeated Pou3f2 binding sites among retina-specific enhancer elements and cis-elements of RPC-specific genes suggests that Pou3f2 is a key regulatory factor in the embryonic retinal development.

4) Key *trans*-acting factors involved in transcriptional regulatory networks of retinal development

It is unlikely that only one factor (i.e., Pou3f2) is involved in regulating retina-specific gene expression. *Trans*-acting factors often do not function alone but rather in a

cooperative manner. To identify other key protein factors for retina-specific gene expression, we applied the following assumptions to the enhancer elements and their binding *trans*-acting factors:

a. Key TFBSs should be common to all or a subset of retina-specific enhancer elements;
b. The flanking genes of these enhancer elements should be expressed in the retina during early retinal development, because an enhancer often regulates the expression of its flanking gene(s);
c. The binding factors should have a known function in retinal development, or
d. If the binding factors have an unknown function in retinal development, they should be at least expressed in the retina during retinal development. In this case, the expression of the factor provides novel hypothesis for their function in retinal development, which needs to be tested by functional studies.

Based on the above assumptions, the information on the expression of the flanking genes of enhancer elements in the developing retina is necessary for the TFBS analysis. Five databases of gene expression (see **Table III.2**) were searched. The information on the expression of these flanking genes were retrieved from these databases (**Table III.1, 4** and supporting data 3). The factors that do not express in the retina during embryonic retinal development, e.g., around E11.5 (when enhancer elements were active), were set aside for further analysis of retinal transcriptional regulatory networks. We then searched common TFBSs among subsets of the 8 retina-specific enhancers. The TFBSs common to individual different sub-groups were combined. In addition to Pou3f2, five other factors (i.e., Crx, Hes1, Meis1, Pbx2, and Tcf3) were identified (**Table III.3**). Four of the 6 factors have known functions in retinal development, which is consistent with our hypothesis. The last two factors do not have known functions in the retina. However, the prediction of

their binding with groups of enhancers suggests they play a role during retinogenesis. As the binding sites of these 6 factors were shared among a subset of retina-specific enhancer elements, these 6 binding *trans*-acting factors were predicted as the key factors that participate in regulating retina-specific gene expression during embryonic development.

Database	Source	Reference
Gene expression database (emage) of Edinburg Mouse Atlas Project (EMAP, v5.0_3.3)	http://www.emouseatlas.org/emage/	(Richardson et al., 2010)
Gene Expression Database in Mouse Genome Informatics (MGI, version 4.4)	http://www.informatics.jax.org	(Finger et al., 2011)
Eurexpress	http://www.eurexpress.org	(Diez-Roux et al., 2011)
VisiGene Image Browser	http://genome.ucsc.edu/cgi-bin/hgVisiGene	(Kent et al., 2002)
Genome-scale mouse brain transcription factor expression analysis	Supporting data 4 and 6	(Gray et al., 2004)

Table III.2. A list of gene expression databases used in this study.

Factor	Binding site	Known function	Expression pattern	Presence in enhancer element
Pou3f2	ATTTGCAT	Induce Bipolar cells	E10.5-14.5 in retina; diencephalon, future midbrain, future SC, rhombencephalon	All 8 elements
Crx	tgaggGGATCAAcagact	Induce Photoreceptors	E11-adult in retina	hs27, hs258, hs546, hs1170
Hes1	CTTGTG	Repress Amacrine, Horizontal, and Ganglion cells; Induce Photoreceptors	E11-13 in retina, thalamus, hypothalamus, striatum, olfactory epithelial	hs27, hs258, hs1170
Meis1	CTGTCActaagatgaca	retinal cell fate determination	E10.5-14.5 in retina, lens vesicle, diencephalon, future sc, hindbrain	hs27, hs258, hs546, hs1170, hs932, mm165
Pbx-2	cacctgagagTGACAGaaggaaggcagggag	No function known in retina	E10.5-14.5 in retina, thalamus, midbrain, hindbrain, sc, ear	hs27, hs258, hs546, hs1170, hs932, mm165
Tcf3	ccaccagCACCTGtc	No function known in retina	E13.5 in retina (MGI)	hs27, hs258, hs546, hs1170

Table III.3. A list of binding factors that show their temporal and spatial co-localization of

expression with each group of enhancers. For each factor, elements shown in the last column indicate the enhancer elements which share a potential common binding with it. The 'Expression pattern' column shows available evidence of the co-localization with enhancers. Corresponding databases are noted because different databases recorded different expression pattern for the corresponding factor. The general function of each factor is also included for future reference. Abbreviation: RPC, retinal progenitor cell; B, bipolar cell; A, amacrine cell; H, horizontal cell; G, ganglion cell; PR, photoreceptor cell.

Gene	Function (related to retina development) and reference
Ascl1	With Mash3, regulate the neuron/glia fate determination (Hatakeyama et al., 2001); with Mahs3 and Chx10, specify Biopolar cell identity (Satow et al., 2001).
Irx5	Off circuit subsets of bipolar interneuron (Cheng et al., 2005; Cohen et al., 2000; Kerschensteiner et al., 2008).
Irx6	No known clear function in retina. But It expresses in the in the area lining the lumen of the otic vesicle including the region giving rise to ganglion complex of CN VII/VIII at E11.5 through E16.5 and overlaps with Mash1 (Cohen et al., 2000; Mummenhoff et al., 2001)
Fxr1	Retina pigmentation(de Diego Otero et al., 2000); other function not known.
Nr2f1	Amacrine development, may involve in cone differentiation; express in a unique gradient in retina along D/V axis (Inoue et al., 2010).
Zfand5	No known function in retina.

Table III.4. A list of flanking genes with their function and references

Interestingly, three common TFBSs (i.e., Pou3f2, Crx, and Meis1) were present among enhancer elements: hs27, hs258, and hs1170 (see Tables 1, 3). Sequence alignment of the three enhancer elements and *cis*-elements of RPC-specific genes (e.g., Chx10, Cyclin D1, and Pax6) revealed another 22 bp motif (**Fig. III. 2**). Crx binding sites were present on enhancer elements hs546 and hs1170, while Hes1 binding sites were present on enhancer element hs546. Since these two enhancer elements (hs1170 and hs546) were both located in the non-coding region between Nr2f1 and Arrdc3, and since Arrdc3 was not active at E11.5 in the retina, the binding of Crx and Hes1 may participate in regulating the expression of Nr2f1. This result is supported by the finding that both Crx (Peng et al., 2005) and Nr2f1 (Inoue et al., 2010; Satoh et al., 2009) play a role in inducing photoreceptor cell fate, though at different stages. In addition, Crx has been shown to be expressed in bipolar cells, paired with Otx2 and Pou3f2, in binding with a 164bp Chx10 enhancer (Kim et al., 2008a). Hes1 has been shown to be active during

early eye formation. By suppressing Math5, Hes1 was shown to be involved in the development of cone photoreceptors, amacrine, horizontal and ganglion cells from the RPCs (Le et al., 2006; Lee et al., 2005).

Meis1 together with Meis2, as members of the TALE-homeodomain protein Homothorax (Hth) related protein family, were known to be expressed in the RPCs of mouse and chick (Heine et al., 2008). Meis1 was expressed in RPCs throughout the entire neurogenesis period, and Meis2 was expressed more specifically in RPCs before the initiation of retina differentiation. Together, they function to maintain the RPCs in a rapid proliferating state and control the expression of other ocular genes, e.g., Pax6, CyclinD1, Six3 and Chx10 (Bessa et al., 2008; Heine et al., 2008). Since Meis1 binding sites are present in a subset of retina-specific enhancers, Meis1 may function as an RPC-specific factor. Since the onset of mouse retina neurogenesis is approximately at E10.5 when the ganglion cells first appear (Leo M. Chalupa, 2008). By E11.5, RPCs of all six cell types are highly active. Therefore, binding of Meis1 with enhancers might influence the cell fate of these RPCs.

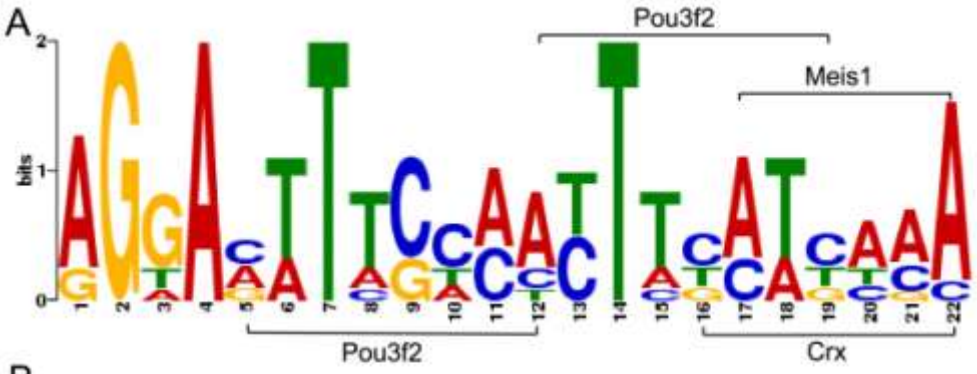

Figure III.2. A 22 bp motif presents in a subset of enhancer elements and *cis*-elements of RPC-specific genes, (e.g., Chx10, Cyclin D1, Pax6). (A) Sequence alignment was performed using MEME among enhance elements (hs258, hs546, and hs1170) and *cis*-elements of genes Chx10, Cyclin D1, Pax6. A. a SeqLog presentation of the 22bp motif . (B) This 22 bp motif contains binding sites for 3 factors: Pou3f2, Meis1 and Crx. Abbreviation: R, rat; m, mouse; h, human; q, quail.

The presence of common Pbx2 binding sites may indicate a novel functional role of Pbx2 in RPCs, since the function of Pbx2 in retinal development has not been documented. Previous studies have shown that Pbx2 was shown to be expressed in the zebrafish retina and tectum (French et al., 2007), together with Pbx1 and Meis1, down-regulated in their expression caused by the deficiency of Prep, the prolyl endopeptidase (Deflorian et al., 2004; Ferretti et al., 2006). Pbx and Meis proteins are major DNA-binding partners that form abundant complexes (Chang et al., 1997). Thus, there is a possibility that Pbx2 may function in the development of RPCs via the interaction with Meis1 and also regulate other RPC-specific genes (e.g., Irx5, Nr2f1, etc) through enhancer binding (**Table III.1**).

Tcf3 is not yet known to have a function in embryonic retinal development. However,

since Tcf3 has common binding sites among the retina-specific enhancer elements. Although it was expressed in the retina during embryogenesis, its specific function in retinal development needs to be confirmed.

5) Generation of transcription regulatory network for early retinal development

Based on the available expression data from VISTA Enhancer Browser and gene expression databases (**Table III.2**), it is known that these 8 enhancer elements and their common binding trans-acting factors are active during embryonic development in the retina. Among the 8 retina-specific enhancer elements, we have identified 6 common trans-acting factors. These 6 predicted factors are experimentally verified key protein factors known to be involved in regulating gene expression and cell differentiation of progenitor cells during embryonic retinal development (**Table III.3**).

Retina-specific gene expression is most likely determined by two kinds of interactions: (1) the enhancers with their binding protein factors, and (2) the protein factors with their interacting partners. The information about these interactions together was used to generate the transcriptional regulatory networks important for retinal development. Therefore, transcriptional regulatory networks of embryonic retina were predicted based on these 6 common/key trans-acting factors (**Table III.3**) and their known interacting partners (**Table III.5**).

To construct retinal transcriptional regulatory networks, a java-based software program named BioTapestry (Longabaugh et al., 2009) (http://www.biotapestry.org/, version 5.0.2) was used to organize the factors and their known interacting partners. BioTapestry is a network facilitating software program designed for dealing with systems that exhibit increasingly complex over time, such as genetic regulatory networks. Its unique annotation system allows the illustration of enhancer-regulated gene expression

and connection between factors. Experimental evidence can also be added to network elements after the network was built, as a proof of particular interactions. We only used the presenting function of BioTapestry here to show the networks of retinal development during early neurogenesis. For better illustration, the network was mapped according to the 3-layer structure of the mouse retina.

Based on the published information on the interacting factors of these 6 *trans-acting factors* and their known functions in retinal cell development, we were able to build transcriptional regulatory networks for all six major retinal cell types (**Fig. III.3**). In RPCs, Meis1 is regulated by Prep1 since it has been shown that insufficient Prep1 expression leads to a decrease in Meis1 expression (Deflorian et al., 2004). Meis1 itself can regulate or interact with 4 other factors (e.g., Pax6, CyclinD1, Six3 and Chx10) important to retinal cell differentiation (Bessa et al., 2008; Heine et al., 2008). Crx, interacting with other factors (e.g, Otx2, Nrl and Nr2e3) plays an important role in both cone and rod photoreceptor cell fate determination (Peng et al., 2005). Crx can also influence Chx10 and Irx5 expression to affect the bipolar cell formation (Cheng et al., 2005; Kerschensteiner et al., 2008; Kim et al., 2008a), which is similar to the function of Pou3f2 (Kim et al., 2008a; Rowan and Cepko, 2005) and Otx2 (Kim et al., 2008a). Another important factor is Hes1. Hes1 functions in maintaining RPC proliferation (Wall et al., 2009) and regulating Math5, a critical factor for the generation of amacrine, horizontal, and ganglion cells (Lee et al., 2005). In addition, Hes1 is regulated by Hes6 (Bae et al., 2000). The Nr2f1 gene expresses in the retina in a gradient along the dorsal-ventral axis and has been found to influence the development of amacrine cells. At the same time it can affect cone and rod photoreceptors differentiation (Inoue et al., 2010). The references of all genes/factors in the networks are listed in **Table III.5**.

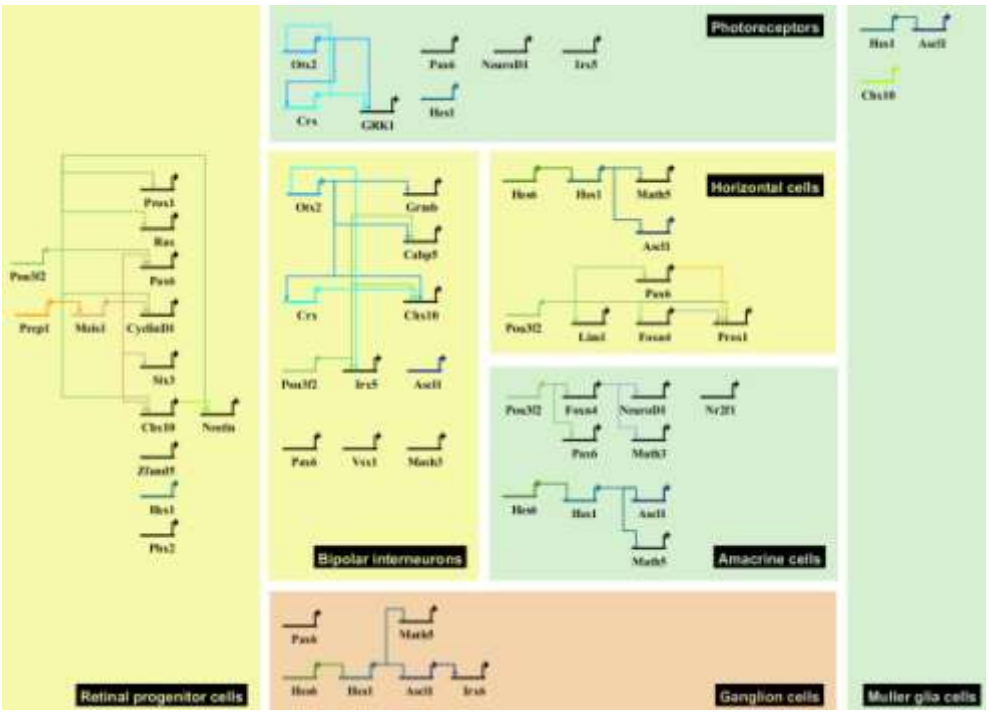

Figure III.3. Examples of transcriptional regulatory networks of embryonic retinal development. Genes and factors are connected with arrows or bars to indicate the promoting and suppressing relationship, respectively.

Factor name	Reference cited
Cabp5	(Kim et al., 2008a)
Chx10	(Hatakeyama et al., 2001)
CyclinD1	(Bessa et al., 2008; Heine et al., 2008)
Foxn4	(Shengguo Li, 2004)
Grk1	(Young and Young, 2007)
Grmb	(Kim et al., 2008a)
Hes6	(Bae et al., 2000)
Mash3	(Hatakeyama et al., 2001; Satow et al., 2001)
Math5	(Lee et al., 2005)
Nestin	(Rowan and Cepko, 2005)
NeuroD1	(Conte et al., 2010)
Nr2f1	(Inoue et al., 2010; Satoh et al., 2009)
Otx2	(Kim et al., 2008a; Young and Young, 2007)
Pax6	(Ferretti et al., 2006; Lee et al., 2005; Oliver et al., 1995)
Prep1	(Deflorian et al., 2004; Ferretti et al., 2006)
Rax	(Heine et al., 2008; Martinez-de Luna et al., 2010)
Six3	(Oliver et al., 1995)
Six6	(Conte et al., 2010)

Table III.5. A list of protein factors that interact with the 6 key *trans*-acting factors in a network model

In summary, the computational method we developed in this study can be summarized as following. First, experimentally verified enhancer elements can be

selected from enhancer databases, e.g., the Vista Enhancer Browser, based on tissue/cell-specific expression patterns derived from the enhancer element and its flanking gene (**Fig. III.4A-B**). These tissue-specific enhancer elements can be located in the non-coding regions in inter- or intra- genetic sequences. Then, the *trans*-acting factor binding sites (TFBS) of all tissue-specific enhancer elements can be predicted using TFBS search tools such as TESS and MatInspector. Common binding sites shared by all tissue-specific enhancer elements or subsets of elements are later determined as shown in (**Fig. III.4C**). Those common factors can be further analyzed according to their expression pattern. Only the ones with spatio-temporal expression patterns can be selected as key factors for construction of tissue-specific transcriptional regulatory network. In addition, factors that interact with these key factors can also be found from the literature. Finally, these enhancers, genes, factors and interactions can be pieced together to build the network (**Fig. III.4D**).

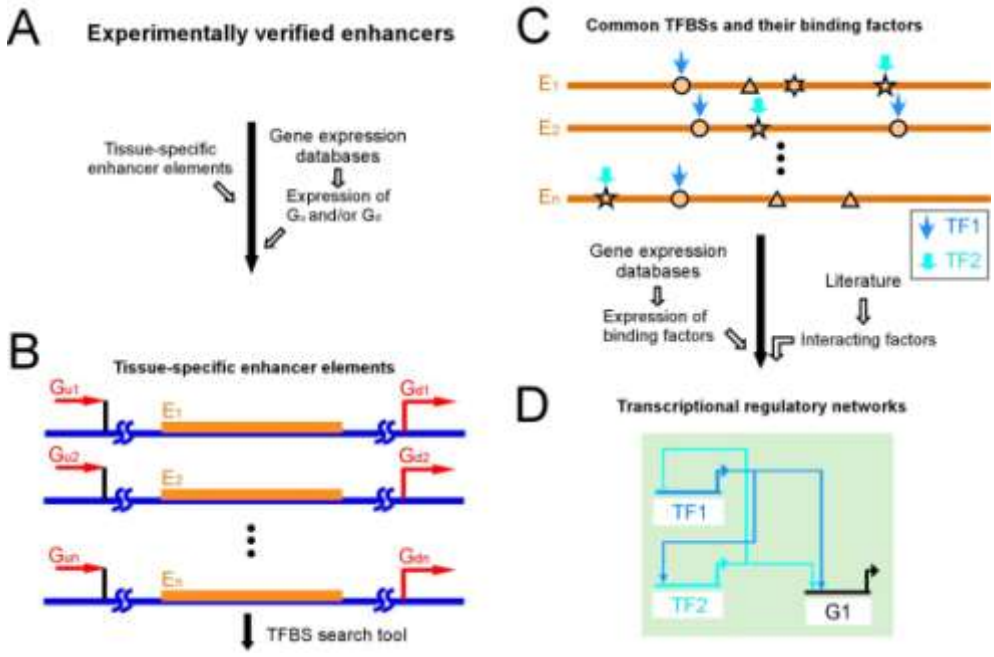

Figure III.4. Computational analysis of TFBSs and transcriptional regulatory networks for tissue/cell-specific gene expression.

A. Selection of experimentally verified enhancer elements from enhancer databases. B. Depiction of enhancer elements and their flanking genes. Orange boxes represent tissue-specific enhancer elements. Red bars represent transcript start sites of downstream flanking genes. Black bars represent the end of the last exon of upstream flanking genes. Enhancer elements in the intronic region of a gene were not illustrated. C. Comparison of the *trans*-acting factor binding sites (TFBSs). Two examples of common TFBS-TF pairs are illustrated by pairs of circle/azure arrows and pentagon/cyan arrows. Other polygons on the enhancer elements (orange bars) represent binding sites that are not common to all members. D. A simple example of a tissue-specific transcriptional regulatory network generated with two key factors (TF1 and TF2) and their interacting genes (G). The thick horizontal lines on top of factor and gene names (TF1, TF2 and G1) represent the *cis*-regulatory region of the corresponding genes. Arrows and bars terminating on this line illustrate the input from other factors, promoters or repressors, respectively. The arrow derived from the thick line represents the regulatory outputs. Abbreviation: E, enhancer element; G, gene; Gd, downstream gene; Gu, upstream gene; TF, *trans*-acting (e.g., transcription) factor; TFBS, transcription factor binding site.

5. Conclusion and Discussion

In this study we have explored a new way of using existing TFBS-finding methods to predict trans-acting factors and networks that regulate tissue-specific gene expression (**Fig. III. 4**). As a proof-of-principle study, using this method, we have identified experimentally verified transcription factors (Pou3f2, Crx, Meis1, and Hes1) and their transcriptional regulatory networks that are known to be important for embryonic retinal development. This not only provides a general idea about the development of the RPCs and retinal cell differentiation, but also validates the effectiveness of our newly developed method. Furthermore, we predicted that two other factors (Pbx2 and Tcf3, expressed in retina) may have a novel functional role in embryonic retinal development, which generates new hypotheses for future experimentation, i.e., to test the involvement of the two factors, i.e., Pbx2 and Tcf3, in the development of RPCs. This method is based on the assumption that non-coding DNA sequences contain signals regulating tissue-specific gene expression. The feasibility of this method relies on the existing data of experimentally verified tissue-specific enhancers (Visel et al., 2007) and available information of tissue-specific gene expression (Finger et al., 2011; Richardson et al., 2010). The identification of retina-specific trans-acting factors and networks indicates that our method is useful for the analysis of TFBSs and transcriptional regulatory networks. Since our method utilizes the existing/known information about tissue-specific enhancer elements and gene expression, we will not be able to identify novel factors that are involved in the transcriptional regulatory networks. In order to reconstruct a more sophisticated network in future studies, we will need to include all of the retina-specific enhancer elements. Finally, this method can be applied to the analysis of TFBSs and transcriptional regulatory networks in other tissue types.

6. Acknowledgements

This work is supported in part by grants (EY018738 and EY019094) from the National Institute of Health, the New Jersey Commission on Spinal Cord Research (10A-003-SCR1 and 08-3074-SCR-E-0), and Busch Biomedical Research Awards (6-49121). The authors thank the Cai lab members for helpful discussions and for proof-reading the manuscript.

7. Supplemental Materials

enhancer	pattern	flanking genes (mouse only)	remark
hs27	eye(4/6), limb(4/6)	Irx5-Irx6	
hs59	eye(8/8), branchial arch, nose	Rpgrip1l(intragenic)	slightly in SC
hs129	eye(2/4)	Klhl1-Dach1	1/2 in fore brain
hs131	eye(3/4)	Dach1-2410129H14Rik	appear in SC when staining is very strong
hs141	eye(2/2), dorsal root ganglion	Dach1-2410129H14Rik	2/2 in SC
hs258	eye(3/5), limb,	Ccdc39-Fxr1	
hs381	eye(5/6)	C80913(intragenic)	very weak in SC(1/5)
hs461	eye(9/9)	Tbx20-Herpud2	weak in SC compare in eye(3/9)
hs546	eye(7/7), limb, nose	Nr2f1-Arrdc3	
hs932	eye(6/9, around eye), limb, nose, branchial arch	AA408296-Irf6	
hs1122	eye(6/7)	Ascl1(mASH-1)-Pah	weak in SC, but also weak in eye
hs1170	eye(8/8)	Nr2f1-Arrdc3	
hs1351	eye(9/9)	Ahi1-Myb	1/9 in SC
mm9	eye(3/4)	Irf2(intragenic)	weak
mm134	eye(5/10), heart	Dusp10(intragenic)	weak in SC
mm165	eye(4/5), heart	Lao1 - Slc2a1	
mm269	eye(5/5), heart, other	Zfand5(intragenic)	other tissue

Supporting data 1. The 17 eye-specific enhancers. Genes in red have expression at E11.5.

Supporting data 2. TFBSs predicted by TESS analysis.

Please find the Supporting data 2 in the link below:

https://onedrive.live.com/redir?resid=E6631B5EC3CCCA10!244&authkey=!AFSSYPouhYXO7aA&ithint=file%2czip

Supporting data 3. The common TFs shared by groups of enhancers.

Please find the Supporting data 3 in the link below:

https://onedrive.live.com/redir?resid=E6631B5EC3CCCA10!244&authkey=!AFSSYPouhYXO7aA&ithint=file%2czip

Enhancer	Sequence
qPax6	AGTAATTACAAATTACATTACA
hPax6	AGTAATTACAAATTACATTACA
hPax6	CTTAATTATGCTTTTAATTAAA
qPax6	CTTAATTATGCTTTTAATTAAA
hPax6	CGCAACTACCGCCTCTAAAAAA
hCyclinD1	AGGACTTTGCAACTTCAACAAA
mCyclinD1	AGGACTTTGCAACTTCAACAAA
rCyclinD1	AGGACTTTGCAACTTCAACAAA
hChx10	AGGAGATTCCCCTTTTATCCAA
mChx10	AGGAGATTCCCTTTTTATCCAA
mChx10	AGCGATTAGGAATTCCAAAAAG
hChx10	AGCGATTAGGAATTCCAAAAAG
mCyclinD1	AGCGATTTGCATATCTACGAAG

Supporting data 4. Enhancer sequences for the retina-specific genes. Abbreviation: r, rat; m, mouse; h, human; q, quail.

No.	Enhancer	Length (bp)	Expression pattern	Flanking genes*	Flanking gene expression pattern (upstream; downstream)
9	**hs59**	1241	eye(8/8), branchial arch, nose	Rpgrip1l(intragenic)	not express duringTS18~28 in retina
10	**hs129**	521	eye(2/4)	Klhl1-Dach1	not express duringTS18~28 in retina
11	**hs131**	2606	eye(3/4)	Dach1-2410129H14Rik	not express duringTS18~28 in retina
12	**hs141**	1971	eye(2/2), dorsal root ganglion	Dach1-2410129H14Rik	not express duringTS18~28 in retina
13	**hs381**	890	eye(5/6)	C80913(intragenic)	not express duringTS18~28 in retina
14	**hs461**	1419	eye(9/9)	Tbx20-Herpud2	not express duringTS18~28 in retina
15	**hs1351**	2355	eye(9/9)	Ahi1-Myb	not express duringTS18~28 in retina
16	**mm9**	1676	eye(3/4, weak)	Irf2(intragenic)	not express duringTS18~28 in retina
17	**mm134**	1493	eye(5/10), heart	Dusp10(intragenic)	not express duringTS18~28 in retina

Supporting data 5. The 10 enhancer elements excluded from study.

Supporting data 6. The script of the Matlab program used for comparing TFBSs.

```
%  Read  from  TESS  result  file  and  compare  the  predicted  binding
sites/factors (hits). Limited to 3 hits per run.
tn = 3; % amount of DNA sequences in this  TESS result
models = [1 2 3]; % the Hits want to compare

[FileName,PathName] = uigetfile('*.xls','Select the xls-file.');
%[typ, desc] = xlsfinfo(FileName);

% import data
for i = 1:tn
    [       data(i).num,        data(i).txt,        data(i).raw]       =
xlsread(FileName,(1+2*i));
end

% compare
Model_0 = data(1,models(1)).txt(2:end,2);
Model_1 = data(1,models(2)).txt(2:end,2);
m = size(Model_0);
res = zeros(m,1);
for i = 1:m
    cmp = strncmp(Model_0(i),Model_1,6);
    row = find(cmp ~= 0);
    res(i,1) = size(row,1); % compare result = how many times the model
'Model_0(1)' appears in the result of other enhancer
    %data(1).res(i,2) = i;  % and record the position of this model
end
[sres,index] = sort(res,'descend');
%A = [sres,index];

% sorting, get rid of the ones not appear in Hit2
row = find(sres ~= 0);
mf = size(row,1);
Model_s = Model_0(1:mf); % sorted model array
for i = 1:mf
    Model_s(i) = Model_0(index(i));
end
index = index(1:mf);

% continue comparing with the Hit3
Model_2 = data(1,models(3)).txt(2:end,2);
[m,n] = size(Model_s);
res = zeros(m,2);
res(:,2) = index;
for i = 1:mf
    cmp = strncmp(Model_s(i),Model_2,6);
    row = find(cmp ~= 0);
    res(i,1) = size(row,1); % compare result = how many times the model
'Model_0(1)' appears in the result of other enhancer
        %data(1).res(i,2) = i;  % and record the position of this model
end
[sres,index2] = sort(res,'descend');
for i = 1:mf
    sres(i,2) = index(index2(i)); % keep the index number from Hit1
end
```

```
% sorting, getting rid of zeros
row = find(sres(:,1) ~= 0);
mf = size(row,1);
A = sres(1:mf,:);
Model_s = Model_s(1:mf); % sorted model array
factor = data(1,models(1)).txt(2:end,1);
TF = factor(1:mf);
for i = 1:mf
    Model_s(i) = Model_0(sres(i,2));
    TF(i) = factor(sres(i,2));
end
data(1).sort = {A,Model_s,TF};

% print to .xls file
nf = numel(FileName)-4;
filename = blanks(nf+9);
filename(1:nf) = FileName(1:nf); filename(nf+1:nf+9) = '_commonTF';
xlswrite([PathName filename '.xls'],data(1).sort{1,2});
xlswrite([PathName filename '.xls'],A,'B1:C200');
xlswrite([PathName filename '.xls'],TF,'D1:D200');
%xlswrite('test1.xls',data(1).sort{1,2});
%xlswrite('test1.xls',A,'B1:C200');
```

Chapter IV

Nkx6.1 Regulates Notch1 Expression during Interneuron Development

1. Prologue

It has been of public interest to invest the Notch1 pathway, since it is critical for many major developmental and pathological events in the CNS and non-CNS tissues. During the development of CNS, Notch1 is involved in the maintenance of NSCs, specification of glial cell type, acceleration of apoptotic cell death and axonal guidance of post-mitotic neurons (Alexson et al., 2006; Grandbarbe et al., 2003; Kawaguchi et al., 2008; Mason et al., 2006; Pierfelice et al., 2011; Redmond et al., 2000; Yang et al., 2006b). In the spinal cord, besides the function mentioned above, Notch1 is also part of the interneuron regulatory network. It is important for the fate determination of general dorsal interneurons and V2b interneurons (Del Barrio et al., 2007; Iulianella et al., 2009; Peng et al., 2007). Upon all these studies, questions were raised as how is Notch1 itself regulated on the transcription level? What is the *cis*-element that silences/enhances Notch1 expression? What are its upstream regulators? This chapter is an attempt to address these questions.

In the previous chapter, a new method combining enhancer analysis, TFBS prediction and Motif finding was presented. This method is capable of generating the transcriptional regulatory network that governs the temporal-spatial-specific cellular events. In this chapter, similar computational method was used to predict the TFs that interacts with a previously identified CNS-specific *cis*-element of Notch1 (Notch1CR2, or CR2). CR2 is a 399bp sequence in the second intron of Notch1 gene. It is involved in the development of GABAergic interneurons in brain (Tzatzalos et al., 2012). To answer the question of how Notch1 is regulated by CR2, a transgenic mouse line with CR2-GFP

inserted into the genome was used for study of the specificity of CR2 in spinal cord. Electrophoretic mobility shift assay (EMSA) and reporter assay on sub-regions of CR2 was used to identify the minimum function sequence. The consequential sequence was then analyzed by site-direct mutagenesis in a chick model, in which Nkx6.1 and Gsx1 were found to be required for CR2 function. Afterwards, Nkx6.1 was found to be able to regulate Notch1 transcription by qPCR combining with the gene knock-down assay and overexpression assay.

In summary, results in this study show that Nkx6.1 is able to regulate Notch1 gene expression via interaction with CR2. A simple network involved in ventral interneuron development was proposed. It is constructed with Nkx6.1, Notch1, Notch1 downstream genes and several other interneuron-related genes. These findings provide the link between Notch1 and the genes that are critical for interneuron development. They also shed new insight into Notch1 regulation during of the spinal cord development.

The remainder of this chapter is reproduced verbatim from a manuscript that has been submitted for publication.

---

2. Abstract

Notch1 signaling is central to the maintenance of neural stem cell identity and the determination of neural cell fate, yet the transcriptional regulation of Notch1 itself remains poorly understood. Here, we show that a cis-element (CR2, an evolutionarily conserved non-coding fragment in the second intron of Notch1 gene) regulates Notch1 expression in neural stem/progenitor cells of the developing spinal cord. In CR2-GFP transgenic mice, CR2 activity is prominent in the developmental stages from embryonic day 9.5 to postnatal day 7, mainly in the interneuron progenitors and absent in the motor neuron progenitors. CR2 activity persists in a subset of ependymal cells in the adult spinal cord, suggesting CR2 is active in both embryonic and adult neural stem/progenitor cells. We further show that the expression of Notch1 and genes in the Notch1 signaling pathway is regulated by the interaction of Nkx6.1 with a core 139bp fragment within CR2. Notch1 and its target genes were significantly down-regulated by either the deletion of Nkx6.1 binding site or the knockdown of Nkx6.1 expression, and upregulated by the overexpression of Nkx6.1. Together, our findings reveal a novel mechanism of Notch1 regulation by Nkx6.1 and its interaction with CR2 in neural stem/progenitor cells during spinal cord development.

3. Introduction

Notch1 is a member of the Notch protein family which encodes a single-pass trans-membrane receptor. Notch1 signaling plays a critical role in the development of the central nervous system (CNS) by inhibiting neuronal progenitor differentiation, maintaining radial glia identity, specifying glial cell type, promoting apoptotic cell death and regulating axonal guidance of post-mitotic neurons (Alexson et al., 2006; Grandbarbe et al., 2003; Kawaguchi et al., 2008; Mason et al., 2006; Pierfelice et al., 2011; Redmond et al., 2000; Yang et al., 2006). In the spinal cord, Notch1 is involved in the fate determination of dorsal interneurons and V2b interneurons (Del Barrio et al., 2007; Iulianella et al., 2009; Peng et al., 2007). Notch1 deficiency results in an accelerated premature neuronal differentiation in the ventral spinal cord and a gradual depletion of the ventral central canal (Yang et al., 2006). Despite the importance of Notch1 pathway, however, the regulation of Notch1 transcription is not well understood.

Transcription regulation plays an essential role in cell fate determination. Transcription factors function by binding to gene regulatory DNA elements, e.g., promoters, enhancers. Often these *cis*-elements are evolutionarily conserved (Pennacchio et al., 2006; Poulin et al., 2005). We have previously identified such an evolutionarily conserved *cis*-element in the second intron of Notch1 gene (Notch1CR2, or CR2, a 399 bp non-coding DNA fragment). CR2 regulates gene expression in neural stem/progenitor cells and was predominantly active in the GABAergic interneuron progenitors in the ganglionic eminence during neocortical development (Tzatzalos et al., 2012).

In the spinal cord, in addition to Notch1, the ventral interneuron fate is also determined by Nkx6.1, Nkx2.2 and several other ventral-specific transcription factors (Alaynick et al., 2011). Nkx6.1, in particular, is critical for the fate determination of

progenitor cells in ventral interneuron layer 2 and 3 (V2, V3) (Sander et al., 2000). Nkx6.1 deletion leads to the loss of V2 and motoneuron markers such as Lhx3, Isl1/2 and Hb9 (Sander et al., 2000), while over-expression of Nkx6.1 leads to an increase of V2, MN markers and decrease of V1 marker Dbx2 (Briscoe et al., 2000).

In this study, we investigated the gene regulatory activity of CR2 in the developing mouse and chick spinal cord. We show that a 139bp fragment within CR2 containing binding sites for transcription factor Nkx6.1 is essential for its gene regulatory activity in neural stem/progenitor cells. Deletion of the core sequence of Nkx6.1 binding sites or knockdown of Nkx6.1 expression diminishes CR2 activity and reduces the expression of Notch1 and genes of Notch1 signaling pathway. Meanwhile, overexpression of Nkx6.1 dramatically elevated the Notch1 expression. Furthermore, in CR2-GFP transgenic mice, CR2 is predominantly active in neural stem/progenitor cells fated to become interneurons, but not motor neurons. CR2 activity also persists in adult neural stem/progenitor cells of the spinal cord. These results suggest that Notch1 expression and Notch1 signaling in interneuron progenitors of the developing spinal cord are modulated by Nkx6.1. Therefore, our study provides a novel mechanism of Notch1 gene regulation in neural stem/progenitor cells by CR2-Nkx6.1 interaction during the development of the spinal cord.

4. Experimental Methods

Mouse strains and tissue preparation

All animal work was conducted following the regulation of the Institutional Animal Care and Use Committee (IACUC) at Rutgers University. The CR2-GFP transgenic mouse (*Mus musculus*) strain was generated as previously described (Tzatzalos et al., 2012) and maintained in our lab. Embryonic and neonatal spinal cords were obtained from the transgenic animals via microsurgical dissection. They were washed in 1x PBS and fixed with 4% (w/v) paraformaldehyde overnight. Fixed tissues were washed again and then cryopreserved in 30% (w/v) sucrose overnight. Afterwards, the spinal cord tissue was embedded in cryo-preserving media (Tissue Tek® OCT compound) and kept frozen at -80ºC.

Immunohistochemistry

Frozen spinal cord tissue was sectioned transversely (10-12 µm in thickness) using a cryostat (ThermoScientific) and air dried. Sections were blocked and permeablized for 1 hr in blocking buffer containing 10% donkey serum, 0.1% TritonX, and 0.1% Tween® 20 at room temperature. Afterwards, they were incubated with primary antibodies overnight at 4ºC. Following three 10-min washes in PBS, sections were incubated in the blocking buffer containing corresponding fluorophore-conjugated secondary antibodies for 1 hr at room temperature. Slides were then washed for three times with PBS (10-min each), and mounted with mounting media (Vector Laboratories) in the presence or absence of DAPI (to label the nuclei). The following primary antibodies were used: Notch1 (1:100, 6014-R), Gata2 (1:200, sc-9008x) and Chx10 (1:300, sc-21692) from Santa Cruz Biotechnology, Inc.; En1 (1:1000, 4G11-c), Evx1 (1:10, 99.1-3A2), Isl1 (1:100,

39.4D5), Nkx2.2 (1:10, 74.5A5), Pax7 (1:25) and Pax6 (1:15) from Developmental Studies Hybridoma Bank (DSHB); Brn3a (1:100, MAB1585), NeuN (1:1000, MAB377) and Sox2 (1:500, MAB4343) from Millipore; anti-GFP (1:1000, AB5450) from Abcam; anti-GFP (1:500, a11122) from Invitrogen; S100b (1:1000, S2532) from Sigma; Pax2 (1:250, 71-6000) from Zymed; Olig2 (1:10000, gift from Dr. Charles Stiles at Harvard University). The staining with anti-Olig2 antibody requires pre-heating of slides with 1 mM Tris-EDTA buffer (PH 8.5) at 96oC for 10-min to retrieve the antigen. Images were captured using a Zeiss Axio Imager M1 fluorescence microscope and visualized with AxioVision 4.8.

Cell counting and Statistical analysis

Cell counting was performed manually on T8~T10 spinal cord sections basing on the DAPI stained nuclei. For each cellular marker, 3~5 sections from at least 3 animals at each time point were counted. Since GFP protein is expressed in the cytoplasm while Notch1 staining is located on the surface of cells, DAPI nuclei staining confirmed the double labeling of GFP and Notch1. Quantitative data were presented as mean ± standard deviation. Significance (p-value) was determined by Student's t-test.

Plasmid construction for cis-element activity assay and site-directed mutagenesis assay

Plasmid reporter constructs were designed to reveal the gene regulation activity of CR sub-regions and mutated CR2.a sequences in chick embryos. Designed sub-regions (Fig. IV.7, Table IV.S2) and mutated CR2.a sequences (Fig. IV.8, Table IV.S4) were subcloned into an expression vector which contains a minimal β-globin promoter (βGP) and a GFP reporter gene. Clones were confirmed by PCR and sequencing. A

transfection control construct with a constitutively active CAG promoter and a DsRed reporter was also generated.

In ovo electroporation

SPF fertilized eggs were purchased (Sunrise Farms, Inc., New York) and incubated at 37^{o}C with 60% humidity. The developmental stages of the chicks were determined according to stages established by Hamilton and Hamburger (Hamburger and Hamilton, 1951). In ovo electroporation was performed on E2 chick embryos (HH11-12) following the protocol (Nakamura and Funahashi, 2001) with modifications. Mixed DNA for CR2 sub-regions and mutated CR2.a sequences contains ~2.5 µg/µl experimental plasmid, ~0.2 µg/µl transfection control plasmid and 0.025% Fast Green dye. Mixed DNA for shRNA assay contains ~2.5 µg/µl experimental shRNA plasmid, ~2.5 µg/µl CR2.a-GFP plasmid and 0.025% Fast Green dye. Mixed DNA for overexpression assay contains ~2.5 µg/µl factor expressing plasmid, ~2.5 µg/µl CR2.a-GFP plasmid and 0.025% Fast Green dye. Injection of the mixed DNA was performed to the middle region of chick neural tube (region with somites), following by electroporation of five 12V pulses. Eggs were harvested at E5 and embryos were examined under a fluorescent whole mount microscope (Leica, MZ16FA). The chick embryo tissues were then washed in 1x PBS and fixed with 4% (w/v) paraformaldehyde for 1hr. Processes following fixation are the same as preparing mouse spinal cord tissue.

Electrophoretic mobility shift assay (EMSA)

ESMA was performed with the designed double strand probes (**Fig. IV.6**) and

nuclear extract from E15.5 mouse spinal cord. Single strand probes were first synthesized by IDT (Piscataway, NJ). They are biotinylated using the Biotin 3´ End DNA Labeling Kit (Thermo Fisher Scientific Inc, IL) and annealed at room temperature for one hour. Biotin labeled double strand probes were stored at -20^{o}C for no longer than 1 week. Unlabeled single stranded probes were also annealed at room temperature for one hour and used as competitors. The ratio of labeled probes and unlabeled probes was 1: 50. EMSA is performed using the LightShift Chemiluminescent EMSA Kit (Thermo Fisher Scientific Inc, IL) following the manufactory's instruction. Reaction mixtures were then loaded onto 8% non-denaturing polyacrylamide gel and run at 100V for 120-150 min at 4°C.

Quantitative RT-PCR

Total RNA was extracted from mouse spinal cord tissues at E15.5, P0 and P14 using Tri Reagent Solution (Ambion). First strand cDNA library was constructed by reverse transcription with qScript cDNA SuperMix (Quanta Biosciences) and used as the template. qRT-PCR was performed on a Roche 480 LightCycler using SYBR Green FastMix (Applied Biosystems) following manufactory's instruction using primers designed for GFP, Notch1, GAPDH and other genes (Table IV.S6).

Similarly, qRT-PCR analysis was performed with chick spinal cord samples. E5 chick embryos were transfected with the shRNA-based Nkx6.1 gene knockdown construct (with RFP as a reporter), the scr-shRNA construct, and the Nkx6.1 overexpression construct (see below for details) using in ovo electroporation technique. Electroporation results in RFP+ cells in half of the spinal cord. On E6, the RFP+ half of the spinal cord tissues were harvested for total RNA extraction. cDNA library was

constructed as described above and used as template to generate a 20-cycle PCR product for the following q-PCR. Primers designed for all target genes are shown in Table IV.S6.

For all qRT-PCR, results were reported as relative threshold cycles (ΔCt). It is calculated by normalizing the threshold cycles based on the GAPDH expression. Each data points contains at least 3 samples with 3 replicates.

RNAi-mediated gene knockdown assay

For RNA interference assay, two 23~29-mer shRNA hairpins were designed based on chick mRNA for each of the Gsx1, Nkx6.1 and Phox2b genes. They were subcloned into a shRNA expressing vector (Origene TR30014) which contains a RFP reporter. Clones were confirmed by PCR and sequencing. A negative control construct with scrambled-shRNA (Origene TR30015) was used. Normal in ovo electroporation procedure described above is performed to transfect cells in chick neural tube.

Nkx6.1 overexpression assay

A Nkx6.1 overexpression construct (Tet-O-FUW-Nkx6.1) (Rowe et al., 2007) was obtained from Addgene (plasmid #45846). It was injected into chick neural tube on various stages followed by *in ovo* electroporation as described above. DNA mixture contains ~2.5 μg/μl Tet-O-FUW-Nkx6.1, ~0.2 μg/μl CAG-DsRed and 0.025% fast green dye. Immunohistochemistry and qPCR analysis were used to confirm the successful overexpression of Nkx6.1.

5. Results

1) CR2 activity is in neural stem/progenitor cells and diminishes at the end of spinal cord neurogenesis

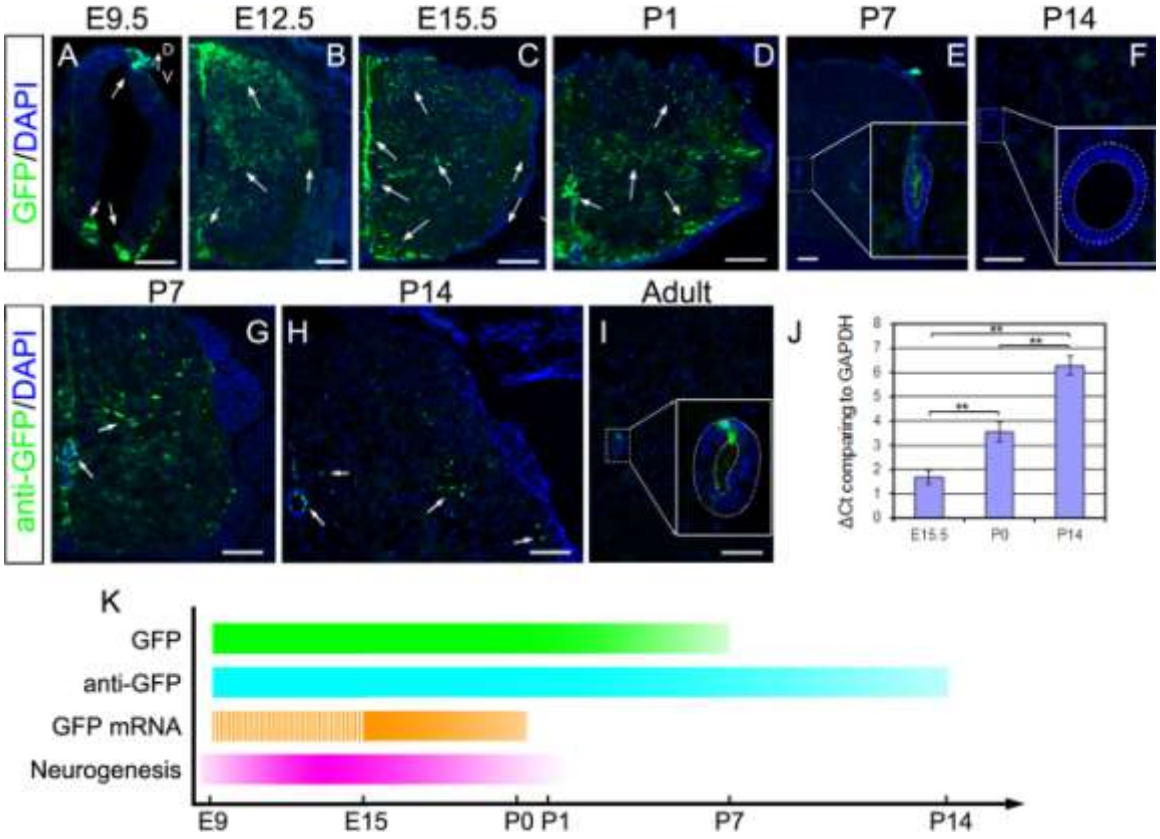

Figure IV.1. CR2 activity is parallel to neurogenesis in the developing spinal cord. GFP expression was examined in cross sections of transgenic spinal cord at various developmental stages, e.g., E9.5 (A), E12.5 (B), E15.5 (C), P1 (D), P7 (E, G), P14 (F, H), and adult (I). At E9.5, the majority of GFP+ cells were located in dorsal and ventral portion of the developing spinal cord. From E12.5 to P1, GFP+ cells were widely distributed first in dorsal regions, then throughout the developing spinal cord. At P7 and P14, GFP+ cells can only be observed in the ependymal cells (enlarged). After P7, low level of GFP can be detected by immunofluorescence staining with anti-GFP antibody (G, H). In adult, GFP+ cells can only be detected in ependymal cells surrounding the central canal (dotted circles in I, also see Fig. IV.S4). Arrows indicate regions where GFP+ cells located. The levels of GFP mRNA were determined by qRT-PCR and decreased from E15.5 to P14 (J). Timeline of GFP mRNA and protein expression is depicted along with neurogenesis in the mouse spinal cord (Wang and Bordey, 2008) (K). Scale bars = 100μm. * p-value < 0.1, ** p-value < 0.05; n ≥ 3.

The spatiotemporal activity of CR2 during spinal cord development was determined by examining GFP expression patterns at various embryonic and postnatal stages in the

CR2-GFP transgenic mouse (Tzatzalos et al., 2012). GFP expression was first observed near the roof plate (RP) and the floor plate (FP) at embryonic day 9.5 (E9.5) (**Fig. IV.1A**). At E12.5, the GFP+ cells were widely distributed throughout the dorsal half of the spinal cord (**Fig. IV.1B**). The GFP+ cells expanded to the entire spinal cord (**Fig. IV.1C,D**) from E15.5 to postnatal day 1 (P1). By P7, the number of GFP+ cells was dramatically decreased; only a few ependymal cells near the central canal maintained a low level of GFP (**Fig. IV.1E**). No GFP+ cells were directly observed by P14 and later stages (**Fig. IV.1F**). However, with anti-GFP antibody staining, we were able to detect some GFP+ cells at P7 (**Fig. IV.1E,G; Fig. IV.S1G, H**) and a few GFP+ cells outside ependymal cell layer at P14 (**Fig. IV.1H**). In the adult, GFP+ cells were only visible in the ependymal region with anti-GFP antibody staining (**Fig. IV.1I)**. No obvious difference was observed in GFP+ cell distributions at E12.5 and E15.5 between samples with or without anti-GFP retrieval (**Fig. IV.S1A,B**). qPCR analysis showed that GFP mRNA level was decreased dramatically at P0 by comparison to the level at E15.5 and was even lower at P14 (**Fig. IV.1J**). Thus, CR2 activity was prominent during embryonic stages and dramatically decreased by P0 (**Fig. IV.1K**), which is also the end of embryonic neurogenesis in mouse spinal cord (Wang and Bordey, 2008).

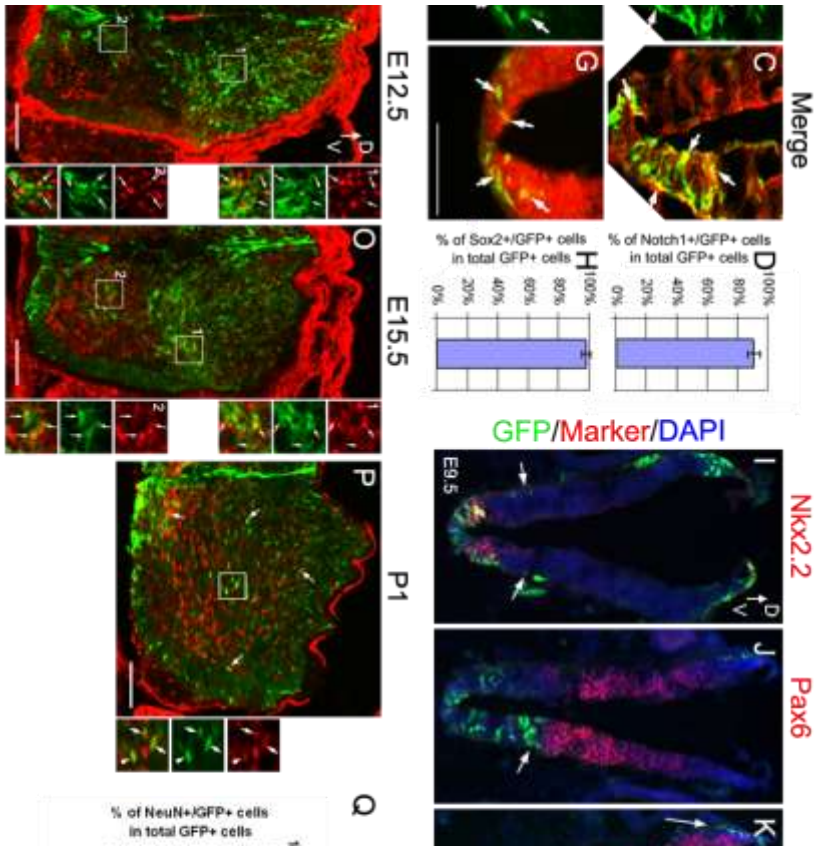

Figure IV.2. CR2 activity is prominent in neural progenitors during early embryonic spinal cord development. The identity of the CR2-GFP+ cells in transgenic spinal cord was examined using double immunofluorescence staining. GFP+ cells were first stained with Notch1 (A-C) and neural stem cell marker Sox2 (E-G). Histograms show the quantification of the co-labeled GFP+ cells (D, H). Staining with the domain specific markers Nkx2.2 (I), Pax6 (J) and Pax7 (K) showed that GFP+ cells were localized to the dorsal progenitor layer 1-3 (dP1-3), motor neuron progenitor layer (pMN), and ventral progenitor layer 3 (pV3). (L) Schematic drawing depicts the distribution of GFP+ cells in the E9.5 spinal cord. Further staining with post-mitotic neuronal marker NeuN (M-P) suggests that the majority of GFP+ cells became neurons. (Q) Quantification shows that the percentage of NeuN+/GFP+ cells increased from E9.5 to E15.5 and remained over 70% at P1. Arrows indicate the co-labeled cells. Scale bars = 100 μm. T-test * p-value < 0.05, ** p-value < 0.01; n ≥ 3.

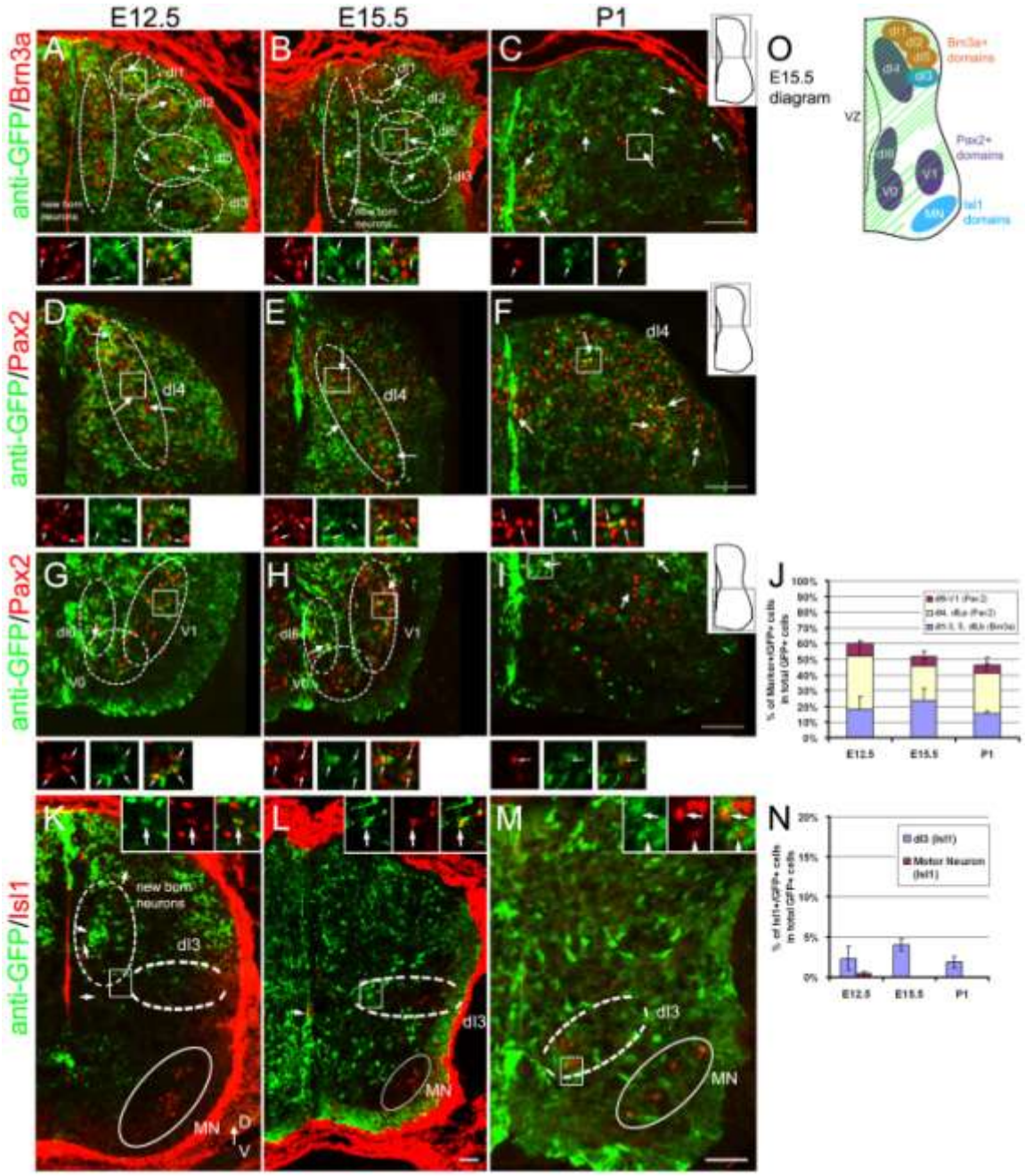

Figure IV.3. CR2 activity is preferentially in interneuron progenitor domains but not motor neuron domain. Cross sections of transgenic spinal cord at E12.5, E15.5 and P1 were stained with domain-specific markers Brn3a (A-C), Pax2 (D-I) (interneuron) and Isl1 (K-M) (interneuron and motor neuron). Co-labeled GFP+ cells (arrows) were found in all Brn3a+ domains, e.g., the region adjacent to the ventricular zone and the dorsal interneuron layers 1-3 and 5 (dI1-3, dI5) (dashed oval circles in A-C) and the ventral interneuron layer 0 (V0) (not shown). Co-labeled GFP+ cells were also found in all Pax2+ domains including the dorsal interneuron layer 4, 6 (dI4, dI6), the ventral interneuron layer 0-1 (V0-1) (dashed circles/ovals in D-I) and Isl1+ dI3 domain (dashed ovals in K-M). However no Isl1+/GFP+ cells were found in the motor neuron domain (MN) (solid ovals in K-M). Boxed regions are shown in higher magnification with arrows indicating co-labeled

cells. . (L, N) Histogram shows the quantification of Brn3a+/GFP+, Pax2+/GFP+ and Isl1+/GFP+ cells. Less than 0.5% co-labeled cells were found in MN layer at E12.5 and 0% at E15.5 and P1. (O) Schematic of the distribution of Brn3a+ (orange, V0 not shown), Pax2+ (purple) and Isl1+ (blue) cells at E15.5. Green shade indicates the expression pattern of GFP. Scale bars = 100 μm; n ≥ 3.

2) CR2 activity is restricted to specific neural progenitor domains

Since cis-elements and enhancers regulate gene expression in a spatiotemporal manner, we thus determined the specificity of CR2 regulatory function by examining the CR2-GFP+ cells in the transgenic mice via immunostaining with cell specific markers. At E9.5, the vast majority of GFP+ cells were co-labeled with neural stem cell markers Sox2 (97.8±3.2%; n=3) and Notch1 (90.1±4.3%; n=3) (**Fig. IV.2A-H**), confirming expression of CR2-GFP in these neural stem cells. GFP+ cells mainly resided in the two regions near the RP and FP. Using the progenitor domain specific markers Pax7 (dorsal progenitor layer 1-6 (dP1-6)), Pax6 (dP4-6 and the ventral progenitor layer 0-2 (pV0-2)) (Tanabe and Jessell, 1996) and Nkx2.2 (pV3) (Liem et al., 2000), we observed GFP expression in the dP1-3, pV3 and both dorsal and ventral region of the spinal cord (**Fig. IV.2I-K**). GFP expression was also observed in the motor neuron progenitor layer (pMN) next to Pax6+ domains (**Fig. IV.2J**, arrows). However, in later developmental stages (e.g., E15.5 and P1 (**Fig. IV.3K-M**)), no GFP+ cells were detected in the more mature motor neuron domain, indicating these GFP+ cells were not motor neuron progenitors.

At later developmental stages, GFP+ cells were co-stained with NeuN (a postmitotic neuron marker) (**Fig. IV.2M-P**), Brn3a and Pax2 (domain specific interneuron markers) and Isl1 (a marker for dorsal layer 3 interneurons (dI3) and motor neurons) (**Fig. IV.3**). We observed an increasing percentage of GFP+ cells labeled with NeuN from 25.6±12.4% at E9.5 to 81.3±11.7% at E15.5 and 73.7±8.1% at P1 (**Fig. IV.2Q**). We also determined interneuron domain-specific GFP expression. At E12.5, E15.5 and P1, 18.4±7.8%,

23.6±7.7% and 15.2±1.7% of GFP+ cells were labeled with Brn3a in the dI1-3 and dI5 domain (**Fig. IV.3A-C**); 33.8±9.2%, 22.13±4.7% and 26.1±10.2% of GFP+ cells were labeled with Pax2 in the dI4 domain (**Fig. IV.3D-F)**; 7.8±1.8%, 6.1±3.4% and 4.7±1.3% of GFP+ cells were labeled with Pax2 in the dI6 and V0-1 domains (**Fig. IV.3G-I**), respectively. Since the Pax2 staining of dI6 and V0-1 interneurons are clustered and cannot distinguished, additional staining with V0 cell marker Evx1, V1 cell maker En1, and V2a cell marker Chx10, V2b cell marker Gata2 were performed. The results showed that only a very small percentage of GFP+ cells reside in these ventral domains (**Fig. IV.S2**). Meanwhile, immunostaining with Isl1 showed co-localization with GFP+ cells in dI3 but not in the differentiated motor neurons at E15.5 and later stages (**Fig. IV.5**). Thus, the majority of the GFP+ cells reside in the Brn3+ and Pax2+ dorsal interneuron domains and not in mature motor neurons of the developing spinal cord.

A few of GFP+ cells were also found co-stained with the glial/astrocyte markers S100b and GFAP, and oligodendrocyte marker Olig2 (**Fig. IV.S3**). The percentage of S100b+/GFP+, or GFAP+/GFP+ co-labeled cells was very small (**Fig. IV.S3C, F**). Furthermore, no Olig2+/GFP+ cells were found outside the VZ (**Fig. IV.S3G-I**), indicating that CR2 may not be active in developing oligodendrocytes.

3) CR2 activity persists in the adult neural stem cells

Ependymal cells are known to be adult NSPCs, which remain quiescent in normal conditions and proliferate rapidly after injury (Horky et al., 2006; Johansson et al., 1999; Meletis et al., 2008; Sabelstrom et al., 2013). To determine the CR2 activity in the adult, we examined the GFP expression in the adult spinal cord. A few GFP+ cells were detected in the ependymal cells lining the central canal (**Fig. IV.1I**). Double

immunofluorescent staining shows that these GFP+ cells were co-labeled with stem cell markers in the spinal cord, e.g., Sox9 , S100b? and GFAP (Barnabe-Heider et al., 2010; Meletis et al., 2008) (**Fig. IV.S3**). Thus , the expression of GFP in ependymal cells indicates that CR2 is involved in gene regulation of adult neural stem cells. This is also consistent with Notch1 function in the adult CNS (Imayoshi et al., 2010; Zhao et al., 2009).

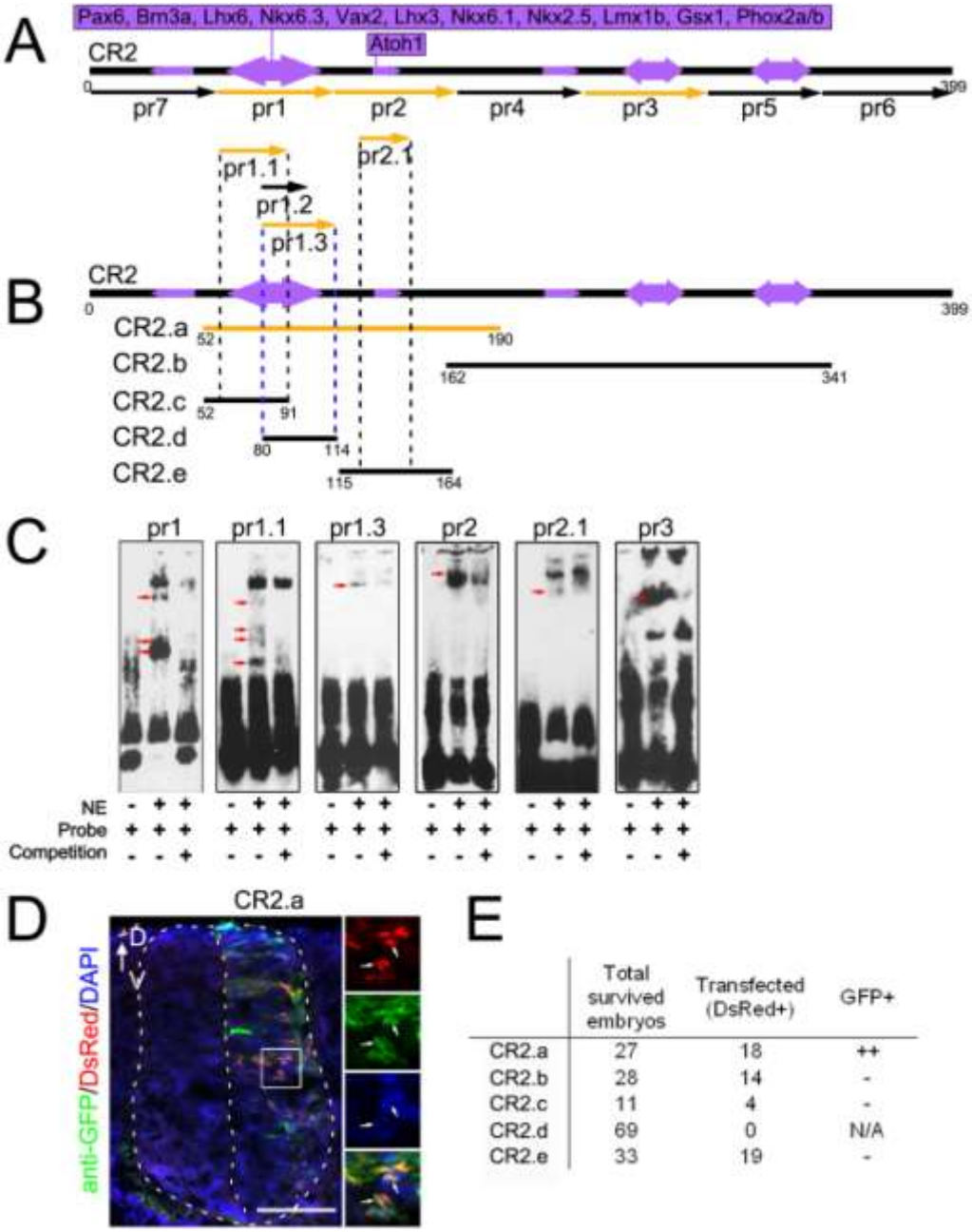

	Total survived embryos	Transfected (DsRed+)	GFP+
CR2.a	27	18	++
CR2.b	28	14	-
CR2.c	11	4	-
CR2.d	69	0	N/A
CR2.e	33	19	-

Figure IV.4. A 139bp subregion of CR2 is required for its gene regulatory activity. Subregions of CR2 were tested individually by EMSA and reporter assay with *in ovo* electroporation for their role in gene regulation. A total of eleven EMSA probes (A, pr1-7, pr1.1-1.3, pr2.1) and five CR2 subregions (B, CR2.a-2.e) were designed based on the location of transcription factor binding sites (purple arrows) on CR2 (black bar). CR2.c, CR2.d and CR2.e contains the sequences of pr1.1, pr1.3 and pr2.1, respectively (dotted line). Probes and sub-regions that showed positive results were colored in yellow. The factors having binding sites in these regions are listed in the boxes. (C) Multiple bands (red arrows) were detected in EMSA using E15.5 mouse spinal cord nuclear extracts with pr1, pr1.1, pr1.3, pr2, pr2.1 and pr3. (D) A cross section of E5 chick spinal cord shows that only CR2.a-GFP construct resulted in GFP expression by reporter assay with *in ovo* electroporation at E3. CAG-DsRed construct was used as a transfection control. Arrows

indicate CR2.a-GFP+ cells. (E) A table summarizes the results of all the tested subregions of CR2. Scale bar = 50 μm.

4) A fragment of 139bp is required for CR2 activity

To determine the minimum sequence and protein factors required for CR2 activity in the developing spinal cord, we analyzed protein binding and gene regulatory activities within subregions of CR2. Using MatInspector (Genomatix, Germany), we identified a total of 173 potential transcription factor binding sites (TFBSs) on the 399bp CR2, among which 126 were unique (**Table IV.S7**). We analyzed all 173 TFBSs and their corresponding transcription factors by literature searches and found that 20 of these transcription factors are expressed in the developing spinal cord during mid-late embryonic stages (E10-E20) (**Fig. IV.S6**). We thus focused on these 20 factors in further analysis. In particular, 7 of the 20 TFBSs are 100% conserved between mouse and chick (**Fig. IV.S5,** red), suggesting that these 7 factors may have critical function in the spinal cord (Pennacchio et al., 2006; Poulin et al., 2005).

To determine the minimum CR2 subregions, we performed electrophoretic mobility shift assays (EMSA) using nuclear protein extracts from E15.5 mouse spinal cord. A total of 7 probes were designed based on the TFBS analysis (pr1-7, **Fig. IV.4A, Table IV.1**). Sequence specific binding activity was detected with pr1-3 (**Fig. IV.4C**). Since pr1 contains a cluster of 12 TFBSs and showed multiple bands in EMSA, it was further dissected into pr1.1, pr1.2 and pr1.3 (**Fig. IV.4A**). Protein binding activities were detected with pr1.1 and pr1.3 (**Fig. IV.4C**). Multiple bands were observed with pr1.1, suggesting that multiple proteins interact with pr1.1. Thereafter, subregions of CR2 with positive binding in EMSA (CR2.a-e, **Fig. IV.4A, Table IV.2**) were selected for a GFP reporter assay to determine their gene regulatory activity in developing chick spinal cord.

The reporter plasmid DNA mixture containing one of the subregions (CR2.x-GFP) and a positive control (CAG-DsRed) was injected and electroporated to transfect the developing neural tube of E2 chick embryos. Results show that only CR2.a was able to drive GFP expression in E5 chick spinal cord (**Fig. IV.4D**, **Fig. IV.S7B**). No GFP expression was detected in the samples transfected with constructs containing CR2.b or subregions of CR2.a (CR2.c, CR2.e) (**Fig. IV.S7B**). In addition, no reporter expression (neither GFP nor DsRed) was observed in the transfected chick embryos (n=69) with CR2.d construct. This suggests that CR2.d may interfere with the proper gene expression since 55% of chick embryos transfected with constructs containing other subregions have the control DsRed expression (**Fig. IV.4E**). Thus, CR2.a is determined as the minimum required sequence and its interaction with multiple TFBSs is required in CR2 activation.

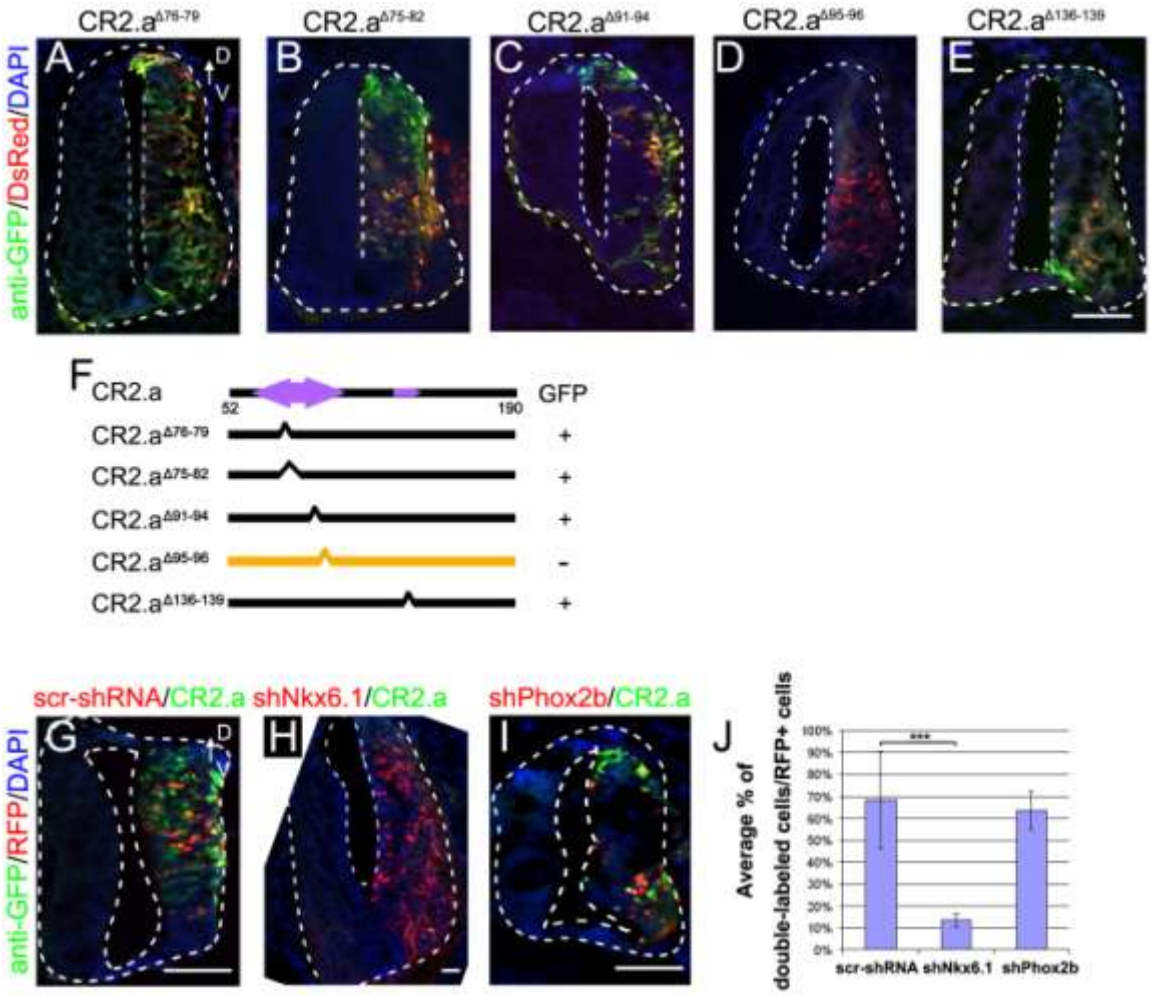

Figure IV.5. Nkx6.1 is required for CR2.a activity. Site-direct mutagenesis and shRNA assays were performed in chick developing spinal cord to determine the functional role of factor binding sites. (A-F) Five mutated reporter constructs (with human beta-globin basic promoter and GFP reporter) were generated with 2~8 bp deletion in the core region of factor binding sites on CR2.a (F). Each of the five constructs was tested its ability to drive GFP expression in chick embryos electroporated at E2 and harvested at E5 (A-E). CAG-DsRed construct was used as the transfection control. GFP expression was not observed in the sample electroporated with CR2.a$^{\Delta 95\text{-}96}$ (D), which is the core region of the binding sites of Gsx1, Nkx6.1 and Phox2b (Table IV.S4). Gene knockdown analysis was performed using shRNA constructs targeting the above three factors and coupled with a reporter RFP. Each knockdown construct was electroporated into E2 chick neural tube together with CR2.a-GFP (H-J), respectively. A scramble shRNA sequence (scr-shRNA) was used a negative control (G). Chick embryos were harvested at E4-5. (K) The percentage of GFP+/RFP+ cells was determined by cell counting and dramatic decrease of GFP+ cells were found in samples with shNkx6.1. V, ventral; D, dorsal. Scale bars = 50 μm. T-test * p-value < 0.05, ** p-value < 0.01, *** p-value < 0.005; n = 3.

5) Nkx6.1 regulates CR2 activity

To identify the specific factors which interact with CR2.a, we performed site-directed

mutagenesis on CR2.a. Based on the predicted core matrix of TFBSs, 2-8 bps in the CR2.a sequence were deleted to eliminate each specific protein factor binding site (**Fig. IV.5, Table IV.S4, S5**). The resultant five mutated sequences were checked with TFANSFAC (Wingender et al., 2000) to avoid generation of new TFBSs. Then the sequences were tested with the reporter assays in the chick neural tube at E2 together with a control CAG-DsRed construct, respectively (**Fig. IV.5A-E**). GFP expression was eliminated in the samples electroporated with CR2.a$^{\Delta 95\text{-}96}$ construct (**Fig. IV.5D**), comparing to the ones electroporated with CR2.a (**Fig. IV.4D**) or other mutated sequences (**Fig. IV.5A-C, E**). This indicates that the 2bp located at 95th-96th in CR2 are essential for its enhancer activity. The deletion of the 2 bps in CR2.a disrupts the core binding sites for Gsx1, Nkx6.1, Phox2a and Phox2b. Analysis of the ChIP-seq results (Mazzoni et al., 2013) revealed that Phox2a does not bind to CR2 region. Since the NCBI no longer provides the information on chick Gsx1 mRNA sequence, we thus further analyzed the remaining two factors Nkx6.1 and Phox2b for their ability to activate CR2.a using shRNA-based gene knockdown assay. The knockdown shRNA constructs for these two factors (shNkx6.1 and shPhox2b with RFP as reporter) were electroporated individually in the chick neural tube together with CR2.a-GFP at E2. The expression of GFP in the RFP+ cells was examined at E5 to determine the effect of the factor knockdown on CR2.a activation. Results show that knockdown of Nkx6.1dramatically decreased the number of GFP+/RFP+ cells, while knockdown of Phox2b has no effect on GFP expression (**Fig. IV.5G-K**). These results suggest that Nkx6.1 interacts with CR2 and is required for its gene regulatory activity.

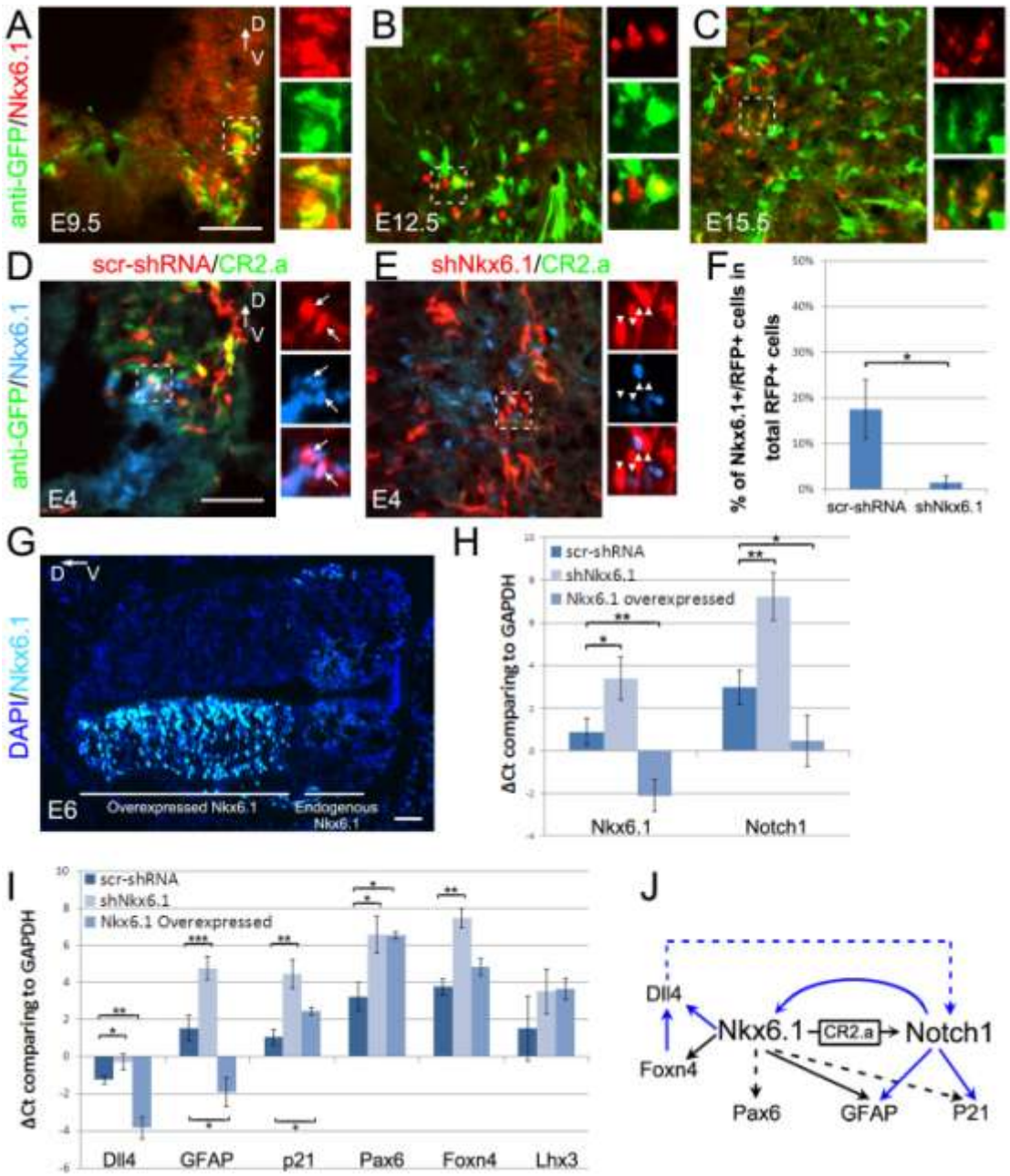

Figure IV.6. Nkx6.1 regulates Notch1 expression during early spinal cord development. (A-C) Co-staining of Nkx6.1 and CR2.a-GFP in developing mouse spinal cord. (D-F) Nkx6.1 expression was knocked down in developing chick spinal cord using a shNkx6.1 construct. The reduction of Nkx6.1 expression caused a decrease of the number of CR2.a-GFP+ cells (D, E). RFP was used as a reporter in both scrambled-RNA negative control (scr-shRNA) and shNkx6.1. (G) Expression of Nkx6.1 in dorsal spinal cord as a result of introduction of the Nkx6.1 overexpression construct. (H) qRT-PCR analysis shows larger ΔCt (threshold cycle number) for Notch1 in samples lack of Nkx6.1, indicating reduced transcription level; while smaller ΔCt for Notch1 was observed in samples with Nkx6.1 overexpression. (I) Change of the transcription level of some related genes was also observed using qRT-PCR analysis. (K) A simplified gene regulatory network of Nkx6.1 and Notch1 for V2 interneuron development. Black arrows represent data presented in this study. Blue arrows represent data from publications. Dotted lines indicates potential regulatory

connection while solid lines indicate experimental testified connection. Scale bars = 50 μm. T-test * p-value < 0.05, ** p-value < 0.01, *** p-value < 0.005; n = 3.

6) Nkx6.1 regulates expression of Notch1 and neurogenesis-related genes

We next examined the interaction between Nkx6.1 and CR2.a and the expression of Notch1 and other neurogenesis-related genes. Immunostaining showed that GFP+ cells were co-labeled with Nkx6.1 in E9.5~E15.5 spinal cord of the transgenic mice (**Fig. IV.6A-C**), supporting its role in regulating domain specific gene expression. A significantly decreased expression of Notch1 and its downstream genes (e.g., GFAP and p21) was observed along with Nkx6.1 knockdown (**Fig. IV.6**) and a reduction of the number of CR2.a-GFP+ cells (**Fig. IV.5G, Fig. IV.6D-E**). Quantitative RT-PCR revealed a significant reduction in the expression of Nkx6.1 and Notch1 (**Fig. IV.6H**, showing relative threshold cycle number (ΔCt)). Transcription level of Notch1 was less than 1/16 of the control samples, while the level of Nkx6.1 is about 1/4. Such exponential decrease of Notch1 transcription level indicates that Nkx6.1 is required for proper enhancer activity during Notch1 expression. In addition, The transcription level of Notch1 downstream genes (e.g., GFAP and p21) and Notch1 associated gene (e.g., Dll4) was also found decreased in transfected cells (RFP+) with Nkx6.1 knockdown (**Fig. IV.6**). We also found decrease of the expression of some of the interneuron-related genes (e.g., Pax6 and Foxn4) while some other (e.g., Lhx3) was not affected (**Fig. IV.6I**).

Conversely, we also performed gain-of-function assay via Nkx6.1 overexpression using plasmid Tet-O-FUW-Nkx6.1 (Rowe et al., 2007) (**Fig. IV.6G**). Analysis of transfected cells with qPCR show that with an 8-fold increase in Nkx6.1 expression, we observed a 4-fold increase in Notch1expression (**Fig. IV.6H**), suggesting that Nkx6.1 overexpression enhances Notch1 expression during spinal cord development. In

addition, an increase of transcription level in GFAP and Dll4 was observed while p21 and Pax6 was found decreased. No significant change in Foxn4 or Lhx3 was found (**Fig. IV.6I**).

6. Discussion

Our study in both chick and mouse determines the spatiotemporal gene regulatory activity of CR2, an enhancer in the second intron of Notch1 gene, in the neural stem/progenitor cells during the development of the spinal cord, and reveals a novel mechanism underlying Notch1 transcription regulation by the interaction of Nkx6.1 with CR2.

1) Nkx6.1 regulates Notch1 expression and both are involved in a regulatory network controlling V2 interneuron cell fate

Nkx6.1 has been known to define the cell fate in the V2-3 interneuron and motor neuron progenitor domains (Liem et al., 2000; Sander et al., 2000), while Notch1 also plays a critical role in the V2 interneuron and motor neuron development (Del Barrio et al., 2007; Peng et al., 2007; Yang et al., 2006). Common effects were reported in the Notch1 and Nkx6.1 knockout animals, e.g., an increase of V1 and V0 interneurons, and a decrease of V2 interneurons and motor neurons (Sander et al., 2000; Yang et al., 2006). These findings establish a gene network including Notch1 and Nkx6.1 in the development of the ventral spinal cord where our finding that Nkx6.1 directly regulates Notch1 expression in the developing spinal cord provides a missing link between the two molecules. Previous studies also showed that there is a reduction of Nkx6.1 in Notch1 conditional knockout animals (Yang et al., 2006), suggesting Notch1 is involved in manipulation of Nkx6.1 expression. Thus, our study uncovers a feedback mechanism of Notch1 and Nkx6.1 expression in neural stem/progenitors. In addition, we observed that the transcription level of Notch1 downstream genes (e.g., GFAP and p21) are affected in the cells with Nkx6.1 knockdown or overexpression, together with Dll4, Foxn4 and Pax6

(**Fig. IV.8**). Foxn4 and Pax6 are interneuron progenitor markers and both involved in the determination of V2 interneurons (Alaynick et al., 2011; Jessell, 2000). Dll4 is a marker for V2a interneuron, which expression is parallel to the V2b interneuron and is promoted by Notch1 (Alaynick et al., 2011; Del Barrio et al., 2007). Dll4 itself is directly regulated by Foxn4 (Misra et al., 2014). The changes of their transcription levels with the manipulation of Nkx6.1 expression suggest that these molecules are involved in a gene regulatory network that controls the V2 interneuron cell fate. Although the expression levels of p21, Foxn4 and Pax6 were not increased when Nkx6.1 is overexpressed, suggesting uncovered mechanism in the network such as compensation effect caused by high level of Nkx6.1. The finding that Lhx3, a gene plays a role in V2a interneurons (Alaynick et al., 2011), did not change its transcription level with the manipulation of Nkx6.1 expression may indicate that it is not a part of this Nkx6.1-Notch1 regulatory network (**Fig. IV.8**).

2) CR2 activity is modulated by its interaction with Nkx6.1

Our result showed that a 139 bp region (CR2.a) is sufficient to drive GFP expression in chick embryo (**Fig. IV.6**). Although a smaller piece of CR2 (CR2.1) functions as an enhancer in the developing brain (Tzatzalos et al., 2012), it lacks the ability to drive GFP expression in the spinal cord indicating that a different mechanism may be involved in the developing brain and spinal cord. CR2 may interact with a different set of nuclear factors in different parts of the CNS its enhancer activity. In supporting this idea, our studies with site-directed mutagenesis and shRNA gene knockdown analysis confirm that Nkx6.1 binds with CR2 and this interaction is required for its gene regulatory activity in the spinal cord (**Fig. IV.7**), while Gsx1 is required for CR2 activity in the brain

(Tzatzalos et al., 2012). In fact, Gsx1 and Nkx6.1 factors both function within distinct domains, i.e., Gsx1 in the dorsal and Nkx6.1 in the ventral domains, of the spinal cord (Mizuguchi et al., 2006; Sander et al., 2000; Valerius et al., 1995). This suggests that Gsx1 and Nkx6.1 interact with CR2 in a domain specific manner (**Fig. IV.8** and **Table IV.S3**). However, it is possible that the binding of Gsx1 with CR2 is a critical step in activating CR2 activity during dorsal spinal cord neurogenesis. Since sequence information on chick Gsx1 transcripts is no longer available at the NCBI nucleotide database, the functional role of Gsx1 in regulating CR2 and subsequent Notch1 signaling in the developing dorsal spinal cord remains to be determined.

3) CR2 activity is prominent in interneuron progenitors and persists in adult neural stem cells

Cell development in the mouse spinal cord is controlled in a progenitor domain-specific manner. These domains are defined by the gradient expression of distinct factors, e.g., Nkx2.2/2.9/6.1/6.2, Pax3/6/7 (Jessell, 2000; Tanabe and Jessell, 1996). Notch1, a molecule critical for maintaining stem cell identity, is expressed throughout the ventricular zone of the developing spinal cord and is involved in fate determination of both dorsal and ventral interneurons (Mizuguchi et al., 2006; Okigawa et al., 2014; Tanabe and Jessell, 1996; Yang et al., 2006). The spatiotemporal activity of CR2 in transgenic mouse supports its role in Notch1 regulation in a domain specific manner for the spinal cord development (**Fig. IV.1**).

CR2 activity was determined by tracking GFP expression. GFP protein has a relatively long half-life of ~26 hrs (Corish and Tyler-Smith, 1999). The GFP signal is visible for ~7 days after its production (Tzatzalos et al., 2012) and the residue of GFP

protein in cells can be detected for ~14 days (expression level reduce to <1%;,calculation was based on half-life of 26 hrs) (**Fig. IV.1**). Since GFP in the transgenic mice was directly observed from E9.5 to P7 (**Fig. IV.1A-F**) and GFP signal can be retrieved at P14 by immunofluorescence staining (**Fig. IV.1H**), we estimate that GFP protein was produced from E9.5 to P0. This is consistent with the result from GFP mRNA analysis (**Fig. IV.1J**). Thus, we conclude that the duration of CR2 activity is from E9.5 to P0, which is corresponds to the period of neurogenesis in the mouse spinal cord (Jessell, 2000; Wang and Bordey, 2008).

Interestingly, we also observed a low level of GFP expression in the ependymal cells in adult transgenic animals with anti-GFP antibody staining (**Fig. IV.1I**). Ependymal cells are known to be adult neural stem cells, which remain quiescent in normal conditions and proliferate rapidly after injury (Horky et al., 2006; Johansson et al., 1999; Meletis et al., 2008; Sabelstrom et al., 2013). These GFP+ cells co-labeled with Sox9 and GFAP (**Fig. IV.S3**), indicating that CR2 activity persists in a subset of adult neural stem cells in the spinal cord. Since adult neural stem cells like ependymal cells are crucial for neural regeneration after CNS diseases or injuries (Barnabe-Heider et al., 2010; Meletis et al., 2008), the CR2-GFP+ cells may serve as an endogenous cell source for post-injury neural repair. Studies have shown that an up-regulation of Notch1 and Nkx6.1 after spinal cord injury (GSE5296, GEO database, NCBI), suggesting auto-activation of a neural regeneration mechanism including both molecules. Thus, we will continue our study with the endogenous activation of Notch1 and Nkx6.1 with injury models, in hope of aiding the treatment on patients with trauma in CNS.

In summary, we characterize the activity of the Notch1 enhancer CR2 and identify the key regulators Nkx6.1 during spinal cord development. CR2 is active preferentially in

a subset of interneuron progenitors, and a low level of CR2 activity is maintained in the adult ependymal cells, which may serve as adult neural stem cells. Furthermore, deletion of Nkx6.1 binding sites or knockdown of Nkx6.1 reduced CR2-GFP expression while manipulation of Nkx6.1 expression affects Notch1 expression. Thus, our study provides new insights into the regulatory mechanism of Notch1 gene expression in the interneuron progenitor domains of the developing spinal cord. Our findings also support a potential role of CR2 in adult neural stem cells, which may provide useful information for studies of adult neurogenesis in animals under the conditions of disease or injury.

7. Acknowledgements

We thank Dr. Connie Cepko (Harvard Medical School) for the reporter construct of plasmid DNA pCAG-GFP, and Dr. Charles Stiles (Harvard Medical School) for Olig2 antibody. We also thank Dr. Bonnie Firestein (Rutgers University) and Dr. Mladen-Roko Rasin (Rutgers-Robert Wood Johnson Medical School) for constructive advices, and all members of the Cai lab for helpful discussion and proof-reading. This work was supported in part by the grants from the National Institute of Health (EY018738) and the New Jersey Commission on Spinal Cord Research (08-3074-SCR-E0; 10-3091-SCR-E-0; CSCR12FEL001). The authors declare that there is no conflict of interests.

8. Supplemental Materials

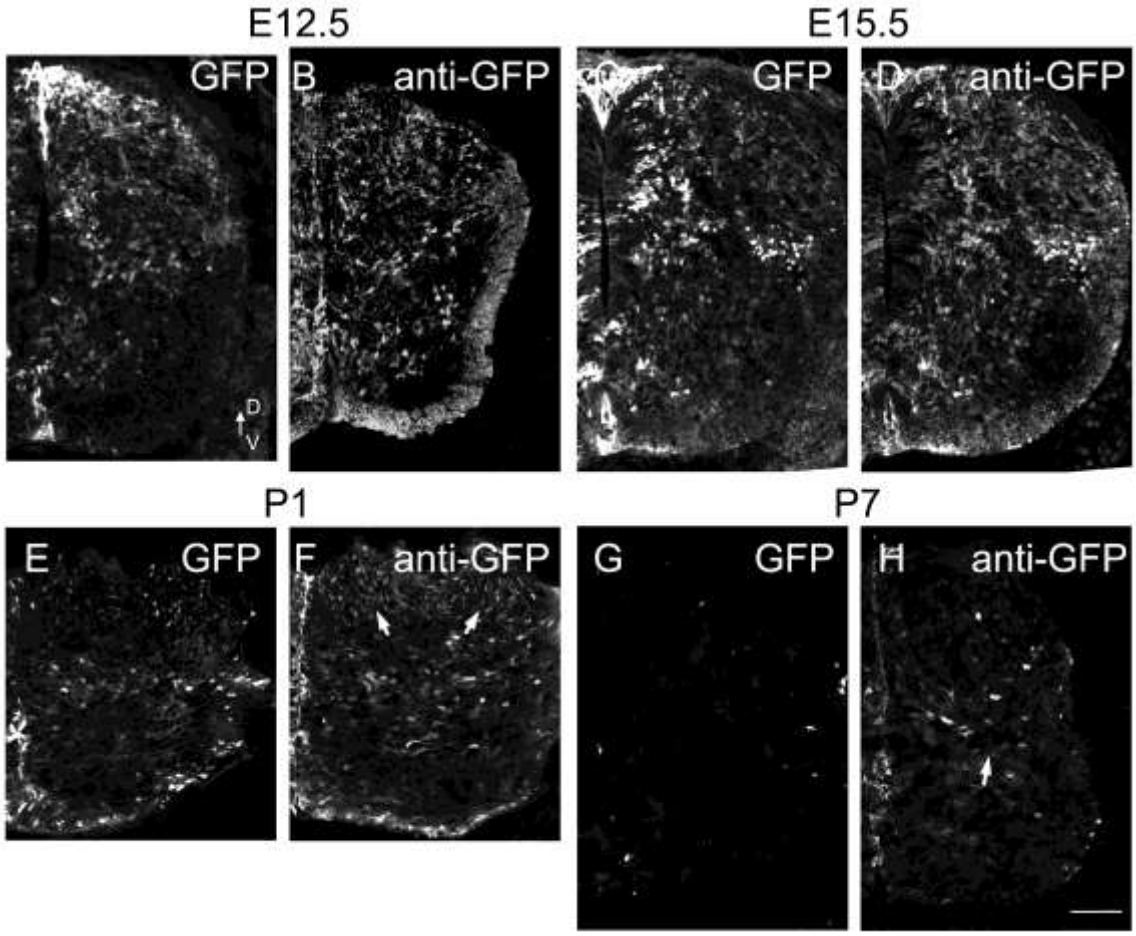

Figure IV.S1. Comparison of GFP expression in the transgenic mice with or without antibody retrieval. GFP expression in transgenic spinal cord at various developmental stages, e.g., E12.5 (A-B), E15.5 (C-D), P1 (E-F), and P7 (G-H) were examined by direct observation of GFP fluorescence (A, C, E, G) and with anti-GFP antibody staining (B, D, F, H). In all four stages, antibody staining either enhanced the GFP signal or revealed more cells have or had GFP expression. Arrows indicate cells only visualized in samples with anti-GFP staining. Scale bars = 100 μm.

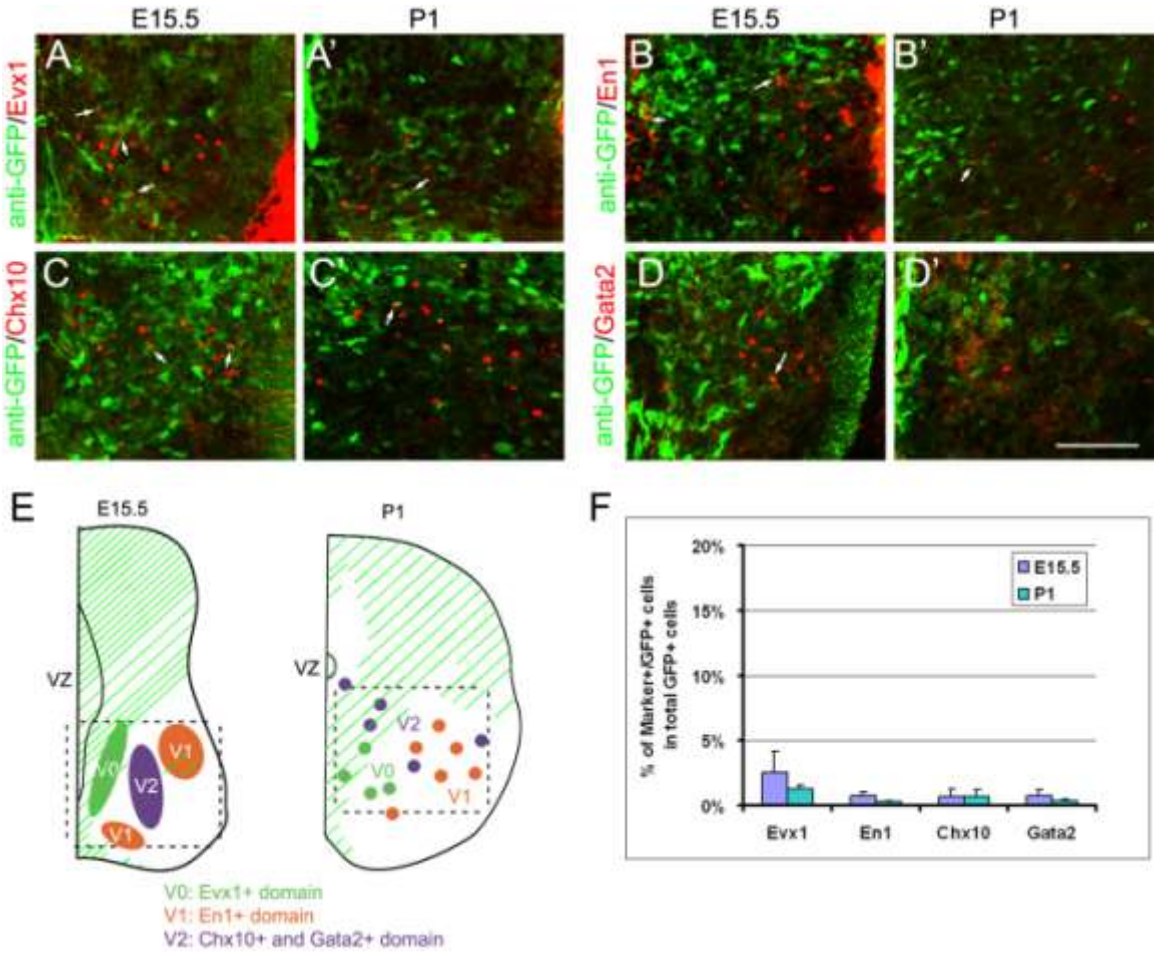

Figure IV.S2. A small portion of CR2-GFP+ cells are located in the V0-2 domains of the developing spinal cord. Cross sections of transgenic spinal cord at E15.5 and P1 were immunostained with domain specific markers Evx1, En1, Chx10 and Gata2 (A-D). The expression pattern of the four markers is shown in schematic diagrams (E, the dotted rectangle areas are shown in (A-D)). A histogram of the marker+/GFP+ cells shows that about 3% of GFP+ cells locate in V0 at E15.5 and about 1% at P1, and less than 1% of GFP+ cells locate in V1 or V2 at E15.5 and P1 (F). Scale bar = 100 μm.

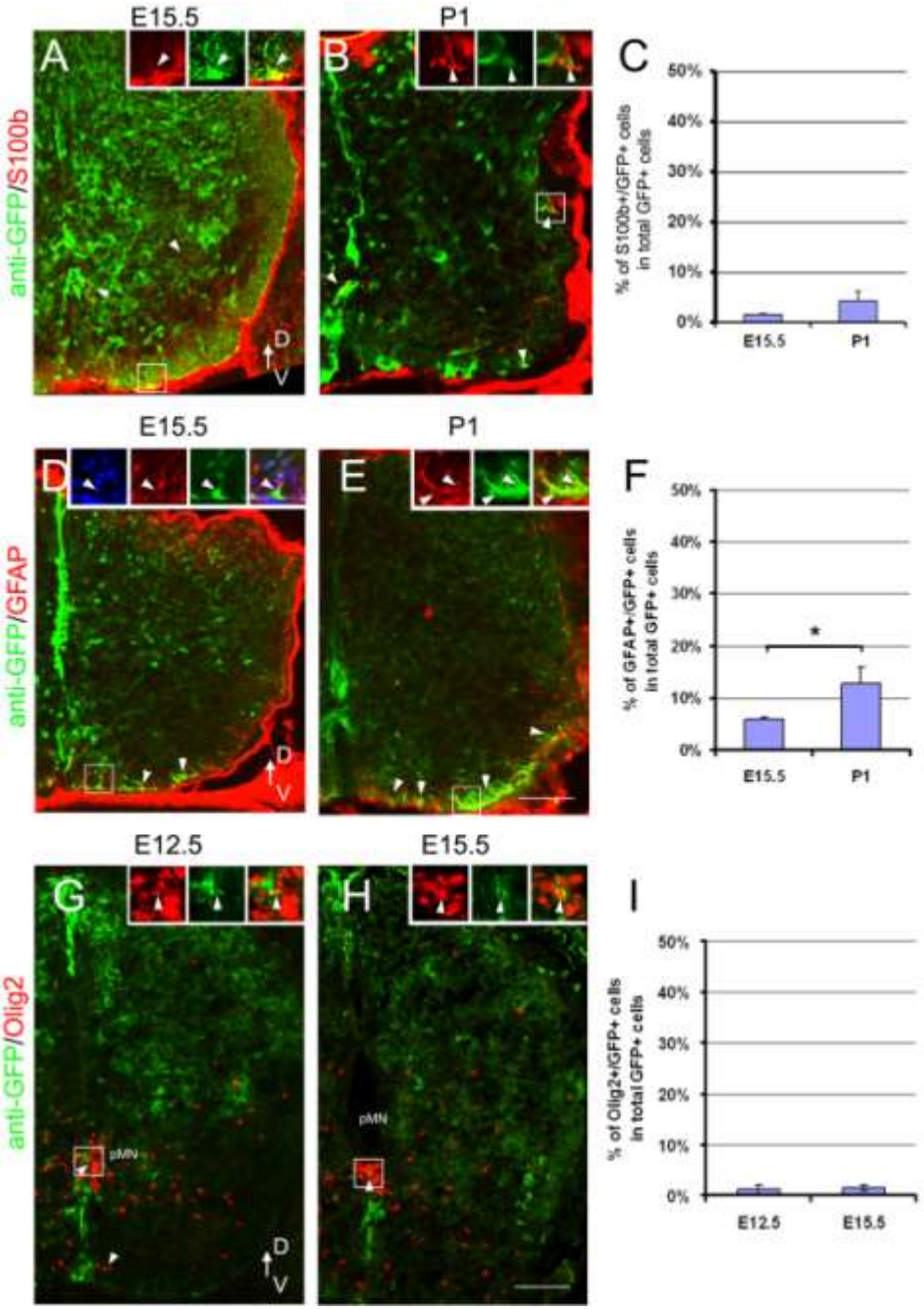

Figure IV.S3. A small portion of CR2-GFP+ cells express S100b, GFAP and Olig2. Cross sections of transgenic spinal cord at various developmental stages were stained with the astrocyte marker S100b (A-D), GFAP (F, G) and oligodendrocyte progenitor/oligodendrocyte marker Olig2 (I-K). S100b+/GFP+ (co-labeled) cells were found in both the grey matter and white matter at E15.5 (A, arrowheads). At P1, a few co-labeled cells can only be found in the white matter (B, arrowheads). (C) Quantification shows the percentages of GFP+/S100b+ cells. GFAP+/GFP+ co-labeled cells were found in white matter at both E15.5 and P1 (D, E, arrowheads). (F) Quantification shows the percentages of GFAP+/GFP+ cells. (G, H) Olig2+/GFP+ cells were found at both E12.5 and E15.5, but only in the pMN domain where oligodendrocyte progenitor originates (arrowheads). No co-labeled cell can be found outside the ventricular zone. (I) Quantification shows the percentage of co-labeled cells is about 1%. Boxed regions are shown in higher magnification with arrowheads

indicating co-labeled cells. Scale bar = 100 μm. T-test * p-value < 0.05, ** p-value < 0.01; n ≥ 3.

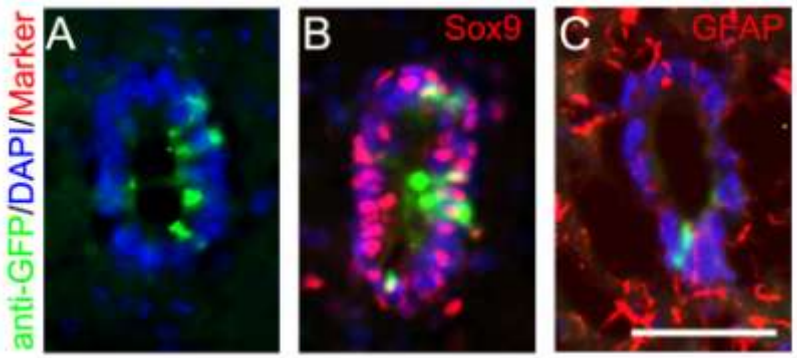

Figure IV.S4. CR2 activity persists in the adult neural stem cells. Cross sections of adult transgenic spinal cord (two-month old) and fluorescently stained with anti-GFP antibody (green). CR2-GFP+ cells were detected in a subset of the ependymal cells lining the central canal (A). GFP+ cells were co-labeled with Sox9 (B) and GFAP (C). Scale bar = 50 μm.

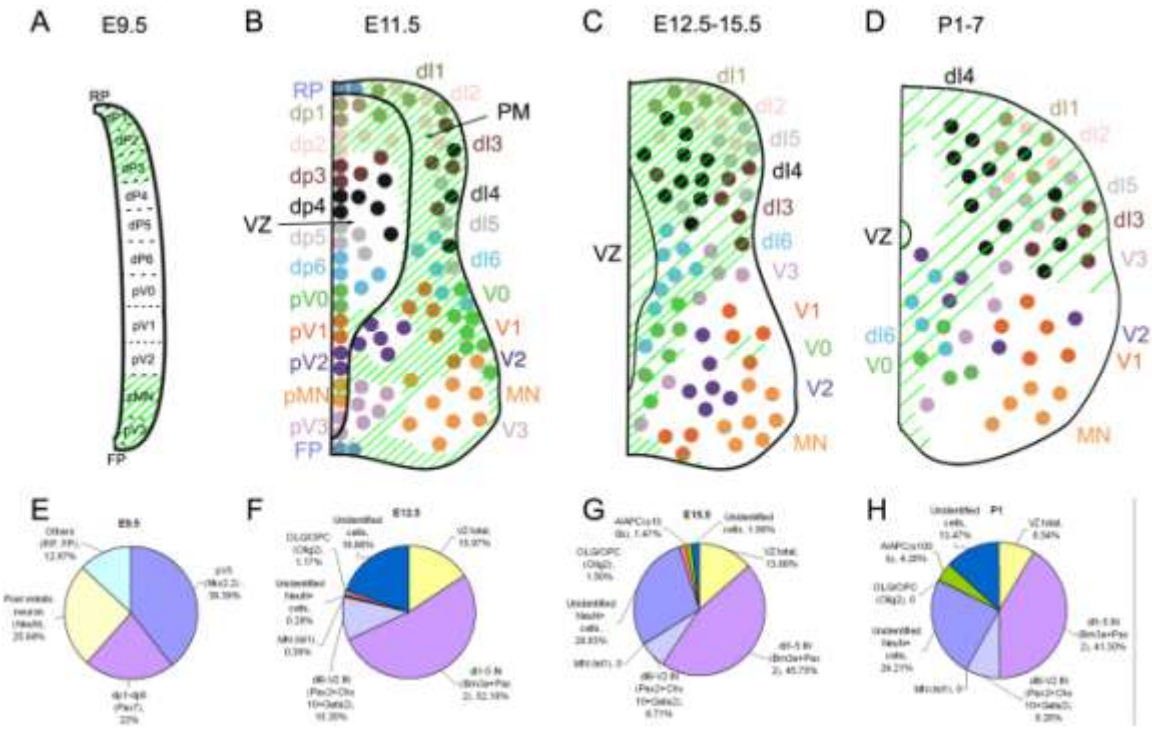

Figure IV.S5. Composition and distribution of CR2-GFP+ cells at various stages during spinal cord development. Schematic diagrams of the right half of the developing spinal cord at various stages (A-D). Pie charts (E-H) summarize the pattern of GFP expression in embryonic and neonatal transgenic mice, respectively. Colored coded circles represent cells from different progenitor domains of the spinal cord. The green shades indicate regions with GFP expression. RP, roof plate; FP, floor plate; dP1-6, dorsal progenitor layer 1-6; pV0-3, ventral progenitor layer 0-3; pMN, motor neuron progenitor layer; dI1-6, dorsal interneuron domain 1-6; V0-3, ventral interneuron 1-3; MN, motor neuron domain/motor neuron; VZ, ventricular zone; OLG, oligodendrocyte; OPC, oligodendrocyte progenitor cell; A, astrocyte; APC, astrocyte progenitor cell; IN, interneuron.

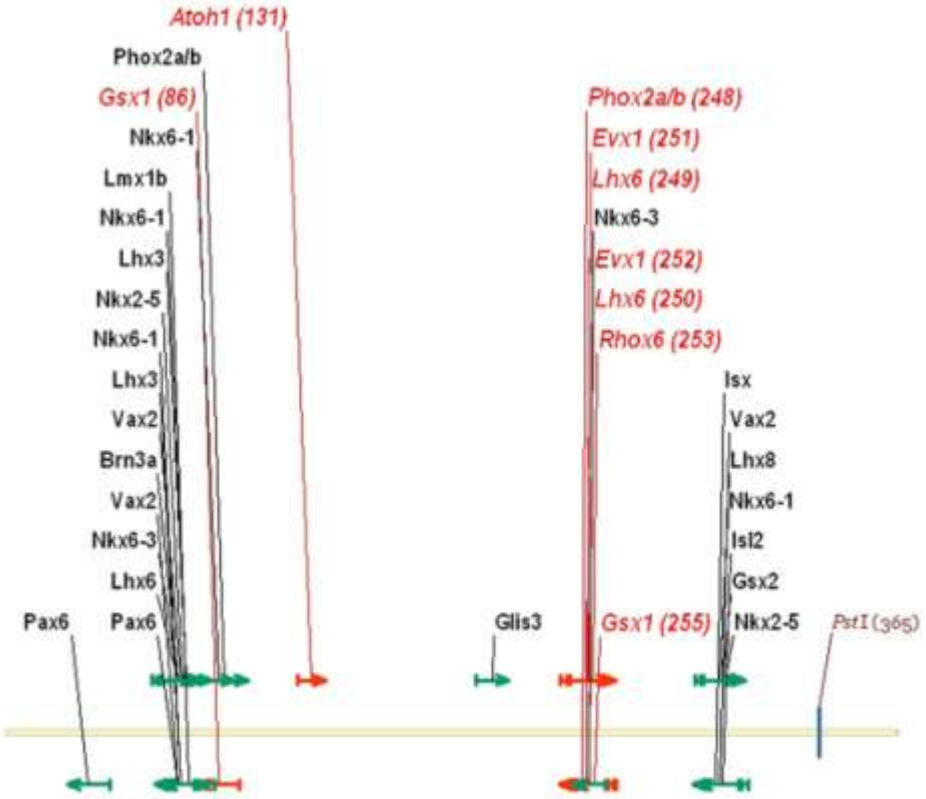

Figure IV.S6. Potential transcription factor binding sites (TFBS) on CR2. Potential TFBSs on CR2 were predicted by MatInspector were represented on the 399 bp CR2 sequence in the second intron of Notch1 (yellow bar). There are 20 factors (arrows represent TFBSs and their relative positions on CR2) with expression in the spinal cord during embryonic and neonatal stages. Of the 20 TFBSs, 9 (TF names and arrows in red) are 100% conserved between mouse and chicken.

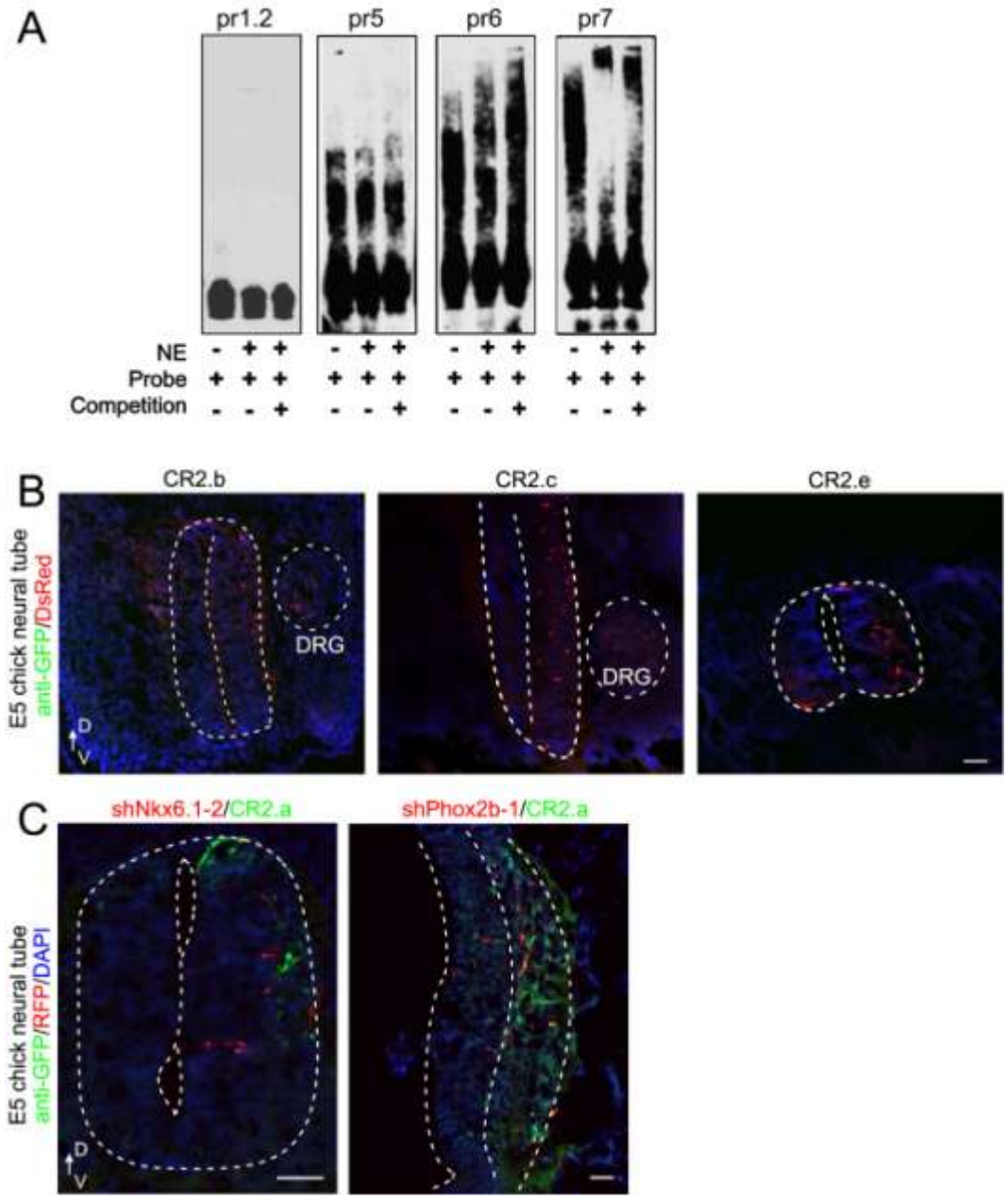

Figure IV.S7. Nuclear protein binding and functional assays of CR2 subregions. A total of 7 probes were designed based on the TFBS analysis and named pr1-7. Sequence specific binding activity was detected with pr1-3 (Fig. IV.4C). Since pr1 contains a cluster of 12 TFBSs and showed multiple bands in EMSA, it was further dissected into pr1.1, pr1.2 and pr1.3. In EMSA, pr1.2, pr5, pr6 and pr7 (Fig. IV.7) were tested with nuclear extract from E15.5 mouse spinal cord and showed no bands (A). Subregions CR2.b, 2.c and 2.e did not allow GFP expression in developing chick neural tube with *in ovo* electroporation of a GFP reporter construct (B). In gene knockdown assay, two sets of shRNA targeting each of Nkx6.1 and Phox2b were tested. Results of one set of constructs are shown in Fig. IV.8, and the 2nd set of constructs in (C). NE, nuclear extract; DRG, dorsal root ganglion; FP, floor plate. Scale bars = 50μm.

Probes	Location (bp)	Sequence (forward strand)
pr1	61-114	TGGGAAGCCACGCATAATTAATCACACAGCATTAATC GCCTCCCAACAATAGCT
pr2	115-170	GCTGCCCTTCTACTGAATCCCAGCTGTCGGCCTCT GAATGGAAGGAAATAAGATTT
pr3	230-287	GCAAAAAAAAAAAAAAAGTAGTGTGCATTCATTAGTG TCTGACAGAGGCACAATCGGC
pr4	171-229	AGGGCATCAAGCGTCCGTGAGGCTTCTGCAAGGGG GAGAAAAGGCCCCCCCCAAAAAAA
pr5	288-340	TTTGTCCAATAAACTGCTCACAGACCTGCTTAATTGG CTTCAGTACAGGGCGG
pr6	341-399	GCCAGCCAGGGAGGTGGGGCTGCAGCCCACAGGC TGGGTACTGGAGGCAGCAGCACCCG
pr7	1-60	CCCTGCCAGTGAGGCAGGCAGACCAAGGAGCACA GAGGCGAGGAAGGGGGTTGTACATTC
pr1.1	60-92	CTGGGAAGCCACGCATAATTAATCACACAGCA
pr1.2	80-100	AATCACACAGCATTAATCGCC
pr1.3	80-114	AATCACACAGCATTAATCGCCTCCCAACAATAGCT
pr2.1	125-148	TACTGAATCCCAGCTGTCGGCCTC

Table IV.S1. Probe design for EMSA.

Name	Region (bp)	Sequence/Primer sequence
CR2.a	52~190	Forward: TGTACATTCTGGGAAGCCACGCAT
		Reverse: TCACGGACGCTTGATGCCCTAAAT
CR2.b	162~341	Forward: ATAAGATTTAGGGCATCAAGCGTCCG
		Reverse: CCCGCCCTGTACTGAAGCCAATTA
CR2.c	52-91	TGTACATTCTGGGAAGCCACGCATAATTAATCACACAGCA
CR2.d	80-114	AATCACACAGCATTAATCGCCTCCCAACAATAGCT
CR2.e	115-164	GCTGCCCTTCTACTGAATCCCAGCTGTCGGCCTCTGAATGG AAGGA

Table IV.S2. Construct design of CR2 subregions for *in ovo* electroporation and reporter assay.

Transcription factor	Binding site(s) (bp)	Expression and Functions	References
Pax6	70-84	Expresses during early neurogenesis and defines the dP4-pV2 progenitor domains in the ventricular zone of spinal cord.	(Ericson et al., 1997; Helms and Johnson, 2003; Liem et al., 2000)
Brn3a	68-86	Expresses both in the pre- and post-mitotic interneurons and defines the dI1-3, dI5 and V0 domains	(Caspary and Anderson, 2003; Helms and Johnson, 2003)
Lhx6	66-88	Expresses in dorsal spinal cord during early neurogenesis. Function in spinal cord is unknown but it mediates the interneuron fate determination and migration during brain development.	(Alifragis et al., 2004; Choi et al., 2005; Gong et al., 2003)
Nkx6.3	70-84	Expresses in ventral spinal cord at E13.5. Function in spinal cord is unknown but it can promote V2 IN production in hindbrain.	(Gray et al., 2004; Hafler et al., 2008)
Vax2	68-86, 69-87	mRNA was found expressed in spinal cord. Function in spinal cord is unknown but it is can define the ventral side of retina.	(Barbieri et al., 1999; LeDoux et al., 2006)
Lhx3	67-89, 70-92	Defines the MN, V2 progenitor domains.	(Sharma et al., 1998; Zhadanov et al., 1995)
Nkx6.1	71-85, 74-88, 88-102	Defines the MN, V2-3 progenitor domains.	(Liem et al., 2000; Sander et al., 2000)
Nkx2.5	70-88	Expresses in brain and cervical spinal cord. No known function in CNS.	Eurexpress (http://www.eurexpress.org/)
Lmx1b	71-93	Defines dI5/dILB progenitor domains. It is required for terminal differentiation of neurons locate in the uppermost layers of dorsal horn.	(Ding et al., 2004)
Gsx1	86-104	Expresses in dI3-5 and dIL progenitors at E10.5-E13.5.	(Mizuguchi et al., 2006; Valerius et al., 1995)
Phox2a/b	88-108	Phox2a co-stain with Lmx1b at E11.5. Forced expression of Phox2b will promote neuronal differentiation and projection.	(Ding et al., 2004; Dubreuil et al., 2000; Pattyn et al., 1997)
Atoh1	131-143	It is involved in dp1/dI1 domain specification in which cells will later develop into commissural interneurons.	(Bermingham et al., 2001; Helms and Johnson, 1998)

Table IV.S3. Known function of the 13 transcription factors with binding sites on CR2.a.

Name	Primer sequence	Transcription factor binding sites (TFBS) involved
CR2.a$^{\Delta 76\text{-}79}$*	F:TGGGAAGCCACGCATAATCACACAGCATTA	Lhx6, Lhx3, Prrx2, Vax2, Nkx6.3, Nkx2.5, Nkx6.1, Pou4f1/2/3, Pax6
	R:TAATGCTGTGTGATTATGCGTGGCTTCCCA	
CR2.a$^{\Delta 75\text{-}82}$*	F:TGGGAAGCCACGCACACACAGCATTA	Lhx6, Lhx3, Prrx2, Vax2, Nkx6.3, Nkx2.5, Nkx6.1, Pou4f1/2/3, Pax6
	R:TAATGCTGTGTGTGCGTGGCTTCCCA	
CR2.a$^{\Delta 91\text{-}94}$	F:CGCATAATTAATCACACAGCATCGCCTCCCAACAATAGCTGCTG	Lhx3, Lmx1b, Nkx6.1, Gsx1, Phox2a/b
	R:CAGCAGCTATTGTTGGGAGGCGATGCTGTGTGATTAATTATGCG	
CR2.a$^{\Delta 95\text{-}96}$	F:CATAATTAATCACACAGCATTACGCCTCCCAACAATAGCTGCTG	Nkx6.1, Phox2a/b, Gsx1
	R:CAGCAGCTATTGTTGGGAGGCGTAATGCTGTGTGATTAATTATG	
CR2.a$^{\Delta 136\text{-}139}$	F:CTGCTGCCCTTCTACTGAATCCCGTCGGCCTCTGAATGGAAG	Atoh1
	R:CTTCCATTCAGAGGCCGACGGGATTCAGTAGAAGGGCAGCAG	
* these two deletion constructs were generated to eliminate TFBSs for Gsx1 and Nkx6.1 on CR2.a.		

Table IV.S4. Primer design of CR2.a for mutagenesis assay and TFBS analysis.

Name	Sequence
shNkx6.1-1F	GATCCGAGGACGACGACGACGACTACAACAATCAAGAGTTGTTGTAGTCGTCGTCGTCGTCCTCTTTTTGGAAA
shNkx6.1-1R	AGCTTTTCCAAAAAGAGGACGACGACGACGACTACAACAACTCTTGATTGTTGTAGTCGTCGTCGTCGTCCTCG
shNkx6.1-2F	GATCCGGAGAAGACTTTCGAGCAGACCATCAAGAGTGGTCTGCTCGAAAGTCTTCTCCTTTTTGGAAA
shNkx6.1-2R	AGCTTTTCCAAAAAGGAGAAGACTTTCGAGCAGACCACTCTTGATGGTCTGCTCGAAAGTCTTCTCCG
shPhox2b-1F	GATCCGCTTCCAGTATAACCCCATAAGGACCACTTCAAGAGAGTGGTCCTTATGGGGTTATACTGGAAGCTTTTTGGAAA
shPhox2b-1R	AGCTTTTCCAAAAAGCTTCCAGTATAACCCCATAAGGACCACTCTCTTGAAGTGGTCCTTATGGGGTTATACTGGAAGCG
shPhox2b-2F	GATCCGGAGACGCACTACCCCGACATTTACATCAAGAGTGTAAATGTCGGGGTAGTGCGTCTCCTTTTTGGAAA
shPhox2b-2R	AGCTTTTCCAAAAAGGAGACGCACTACCCCGACATTTACACTCTTGATGTAAATGTCGGGGTAGTGCGTCTCCG

Table IV.S5. Sequence design of shRNA targeting Nkx6.1 and Phox2b factors in chick.

Name	Sequence
For mouse	
GAPDH-F	5’- ACTCTTCCACCTTCGATGCCG -3’
GAPDH-R	5’- CCGAGTTGGGATAGGGCCTC -3’
GFP-F	5’- CTCGTGACCACCCTGACCTA -3’
GFP-R	5’- CTTGTAGTTGCCGTCGTCCT -3’
Notch1-F	5’- ACAGTGCAACCCCCTGTATG -3’
Notch1-R	5’- AGTTGTTCCGTAGCTGGTCG -3’
For chick	
GAPDH-F	5’- TCAAATGGGCAGATGCAGGT -3’
GAPDH-R	5’- GATGGCATGGACAGTGGTCA -3’
Notch1-F	5’- CAACTGCCAGAACTTGGTGC -3’
Notch1-R	5’- AGAAAGGGCTGCAGTCATCC -3’
Nkx6.1-F	5’- GTCGCTCGTCTCACCTCAC -3’
Nkx6.1-R	5’- TGCCACGCTTTTTCAAGACG -3’
Pax6-F	5’- CCCACCATGCAGAACAGTCA -3’
Pax6-R	5’- CAGACCCCCTCCGAGAGTAA -3’
Lhx3-F	5’- CTGACTACGAGACGGCCAAG -3’
Lhx3-R	5’- GGGCTCGTCTGTGAAGGAGA -3’
GFAP-F	5’- TGGAGAGGTGATCAAGGAGTC -3’
GFAP-R	5’- ATCAACCTGCCTCCCCCTAT -3’
p21-F	5’- ACGAGCAGATCCAGAACGAC -3’
p21-R	5’- TTGGAGCCGTAGAAGTCTTTGA -3’
Foxn4-F	5’- CTGGATAGCTACTGCGTGCG -3’
Foxn4-R	5’- GGGCTGTCTTGAAGTAGGGAAA -3’
Dll4-F	5’- GGGCTGTGTTGTGTTCCTTTG -3’
Dll4-R	5’- GAACGACAGATGCACTCTCCA -3’

Table IV.S6. qRT-PCR primers

Chapter V

Molecular Mechanism of NSC Activation after Spinal Cord Injury

1. Prologue

Approximately 276,000 persons in the US are suffering from SCI by the year of 2014, with an increasing rate of 12,500 new cases each year (The National SCI Statistical Center, 2015). Researchers have been seeking proper treatments to help patient to reduce pain, decrease secondary injury and regain the spinal function. One of the promising direction in promoting the reconstruction of spinal cord and functional recovery is to promote the endogenous neurogenesis from aNSCs (Estrada and Muller, 2014; Picard-Riera et al., 2004). As a source of the aNSCs, ependymal cells in the spinal cord response to injuries by proliferation and differentiation (Meletis et al., 2008; Moreno-Manzano et al., 2009). However, the majority of activated ependymal cells differentiate into the two types of glial cells: most of them become oligodendrocytes that are vulnerable and die fast; a smaller population becomes astrocytes that form the glial scar (Barnabe-Heider et al., 2010; Horky et al., 2006; Meletis et al., 2008; Yang et al., 2006a). Thus, gene therapy can be utilized to promote aNSC proliferation and differentiation into neurons (D'Onofrio et al., 2011). As Notch1 is involved in both glial cell and interneuron fate determination (Cau and Blader, 2009; Yang et al., 2006b) and is up-regulated after CNS injury (Chen et al., 2005), it is a good candidate for gene therapy.

In the previous chapter, an Notch1 enhancer CR2 was found active during the development of ventral interneurons in the spinal cord and maintains low activity in the adult ependymal cells. These studies lead to the hypothesis that CR2 is also involved in the activation of aNSC after injury. To test the hypothesis, CR2 activity in response to injury was examined in the transgenic mice with three injury models. Results show that

in injured spinal cord, there was a dramatic increase in the number of GFP+ cells, which indicates that injury induces CR2 activation and neurogenesis. These GFP+ cells became glia as the injury develops over time. Thus, it is possible to promote the proliferation of aNSCs by enhancing the activation of CR2 with its interacting factors. These findings reveal new hints into the mechanism of NSC activation and neurogenesis after injury. The knowledge gained from this study may facilitate the development of gene therapy for treatment of CNS injuries.

2. Abstract

Only a limited number of aNSCs proliferate and initiate neurogenesis after injury. Even worse, the newly generated neural cells are vulnerable to the unfavorable condition after injury and the majority of them will not survive. To overcome this problem, we need to understand how genes are regulated during the activation of aNSC after SCI. Notch1 serves as a good candidate since it is one of the critical genes for spinal cord development and is up-regulated after SCI. We have determined that enhancer CR2 regulates Notch1expression in interneuron development via its binding with Nkx6.1 and Gsx1. Both of these TFs are up-regulated after CNS injury. Thus, we hypothesize that CR2 is required for the activation of a subset of aNSCs during the post-injury response. To test the hypothesis, CR2-GFP transgenic mice were used to characterize CR2 activity in three injury models with different severity. GFP+ cells were observed throughout the injury site in all three models with different temporal-spatial distribution. The GFP+ cells in the ependymal cells are Sox9+ and GFAP+, and in parenchymal region mostly of them are GFAP+ and Pdgfra+. These results suggest that CR2 activation is triggered in the acute phase post injury and it is involved in the endogenous neurogenesis..

3. Introduction

SCI is the second leading cause of paralysis in US. Approximately 276,000 patients live with SCI in 2014, and in prediction 291,500 in 2015 (The National SCI Statistical Center, 2015). Current treatments of SCI include use of immune-repress drugs and realignment of the spine to prevent further damage, and physical rehabilitation to regain partial function of the spine (Estrada and Muller, 2014). Studies aiming to replace damaged cells, promote neural regeneration and retrain neural circuits are performed throughout the nation. Among them, transplanting cell grafts or synthetic biomaterials into injured site showed some progress in improving spinal cord function (Kobayashi et al., 2012; Lu et al., 2012). However, questions in timely treatment, grafting, axon extending and transplant rejection immune responses remain unsolved. To overcome these difficulties, new focus on treating SCI switched to promotion of the regeneration of patients' own aNSCs including ependymal cells (Moreno-Manzano et al., 2009) and glial cells (Picard-Riera et al., 2004; Su et al., 2014; Yang et al., 2013). aNSCs in parenchymal and ependymal regions of the spinal cord can both be triggered by injury and start to proliferate into neurons, oligodendrocytes and astrocytes (Meletis et al., 2008; Ohori et al., 2006; Yamamoto et al., 2001). Although the majority of aNSC-originated neurons cannot survive the adverse environment after injury (Meletis et al., 2008; Sabelstrom et al., 2013), we see an opportunity of overcome the difficulties by promoting the proliferation of aNSC. This can be accomplished by manipulating the expression of critical genes through transcription regulation.

Many studies have established Notch1 as an important molecule in both embryonic spinal cord development and post-SCI neural regeneration (Chen et al., 2005; Okigawa et al., 2014; Yang et al., 2006b). It is a good gene target for study of neural regeneration. In the previous chapter, we identified a Notch1 regulating mechanism that is specific for

spinal cord ventral interneuron development. It involves the interaction between the Notch1 enhancer CR2 and the TF Nkx6.1 (**Fig. V.6**). Another CR2-interacting TF Gsx1 is also considered as the regulator which is involved in the development of dorsal interneurons (**Fig. V.5**). Moreover, CR2 is found to be quiescent in adult ependymal cells (**Fig. V.S4**). Thus we hypothesize that CR2 will be re-activated in the aNSCs during the neurogenesis after SCI, and Nkx6.1, Gsx1 are involved in this process.

To test the hypothesis, the re-activation of CR2 was studied in three SCI models using the CR2-GFP transgenic mice. GFP+ cells were observed in all models with different temporal-spatial distribution. The GFP+ cells were found in both ependymal and parenchymal regions and tended to take a glial cell fate. Future study will be carried out to examine the mechanism of CR2 activation during post-injury neurogenesis and seek the method to enhance aNSC proliferation and differentiation. .

4. Materials and Methods

Spinal cord injury models

All animal work was conducted following the regulation of the Institutional Animal Care and Use Committee (IACUC) at Rutgers University. The CR2-GFP transgenic mouse (Mus musculus) strain was generated as previously described (Tzatzalos et al., 2012) and maintained in our lab. Adult mice that are 2-6 months old were used in the SCI experiments. Initial anesthetization was performed with 5% isoflurane. Following injury models were introduced to the animals which were maintained anesthetized with 2% Isoflurane.

a). Transection injury (Tx):

Following a laminectomy at T10~11, the dorsal blood vessel was burned with a cauterizer, and the spinal cord was cut transversely using a #10 scalpel.

b). Compression Injury (Cmp):

Following a laminectomy at T10~11, a rod was placed onto the middle of the dural surface of the spinal cord with calculated pressure (5 g/mm^2 for moderate injury, 2 g/mm^2 for mild injury). The rod was left in place for 5 min to create the injury.

c). Compression-on-side Injury (Cmps):

Similar to compression injury, a rod was placed on the surface of the spinal cord that was 1/4 to the right side and left in place for 5 min.

Following induction of injury, the surgical wound was sutured and closed in layers. The mice were returned to their cages for 1 - 4 weeks before harvesting.

Spinal cord tissue preparation

Spinal cords form the injured and sham animals were obtained via microsurgical dissection. They were washed in 1x PBS and fixed with 4% (w/v) paraformaldehyde for

48 hrs. Fixed tissues were washed again and then cryopreserved in 30% (w/v) sucrose for 48 hrs. Afterwards, the spinal cord tissue was embedded in cryo-preserving media (Tissue Tek® OCT compound) and kept frozen at -80ºC.

Immunohistochemistry

Frozen spinal cord tissue was sectioned transversely (10-12 µm in thickness) using a cryostat (ThermoScientific) and air dried. Sections were blocked and permeablized for 1 hr in blocking buffer containing 10% donkey serum, 0.1% TritonX, and 0.1% Tween® 20 at room temperature. Afterwards, they were incubated with primary antibodies overnight at 4ºC. Following three 10-min washes in PBS, sections were incubated in the blocking buffer containing corresponding fluorophore-conjugated secondary antibodies for 1 hr at room temperature. Slides were then washed for three times with PBS (10-min each), and mounted with mounting media (Vector Laboratories) in the presence or absence of DAPI (to label the nuclei). The following primary antibodies were used: Notch1 (1:100, 6014-R) from Santa Cruz Biotechnology, Inc.; Nkx6.1 (1:25, F55A11), Pax6 (1:15) from Developmental Studies Hybridoma Bank (DSHB); NeuN (1:1000, MAB377) and Sox2 (1:500, MAB4343) from Millipore; Sox9 (1:200, AF3075) from R&D System; anti-GFP (1:1000, AB5450) from Abcam; anti-GFP (1:500, a11122) from Invitrogen; S100b (1:1000, S2532) from Sigma; Pax2 (1:250, 71-6000) from Zymed. Slides were incubated with CuSO4 solution for 10 min to reduce autofluorescence. Images were captured using a Zeiss Axio Imager M1 fluorescence microscope and visualized with AxioVision 4.8.

Cell counting and Statistical analysis

Cell counting was performed manually on T8~T10 spinal cord sections basing on the DAPI stained nuclei. For each cellular marker, 3~5 sections from at least 3 animals at each time point were counted. Quantitative data were presented as mean ± standard deviation. Significance (p-value) was determined by Student's t-test.

5. Results

1) Injury induces CR2 reactivation.

In this study, three SCI models were set up on the CR2-GFP transgenic mice for the study of CR2 and its interacting factors: a severe complete transection model (Tx), a moderate compression-on-side model (Cmps) and a mild compression model (Cmp). Two types of control models were also included: naïve animals that are intact without surgery, and sham animals that went through all surgery procedures except the steps causing spinal cord injury. The increase of GFP+ cells were observed in all three injury models comparing to the control models, suggesting reactivation of CR2 in adult animals after injury.

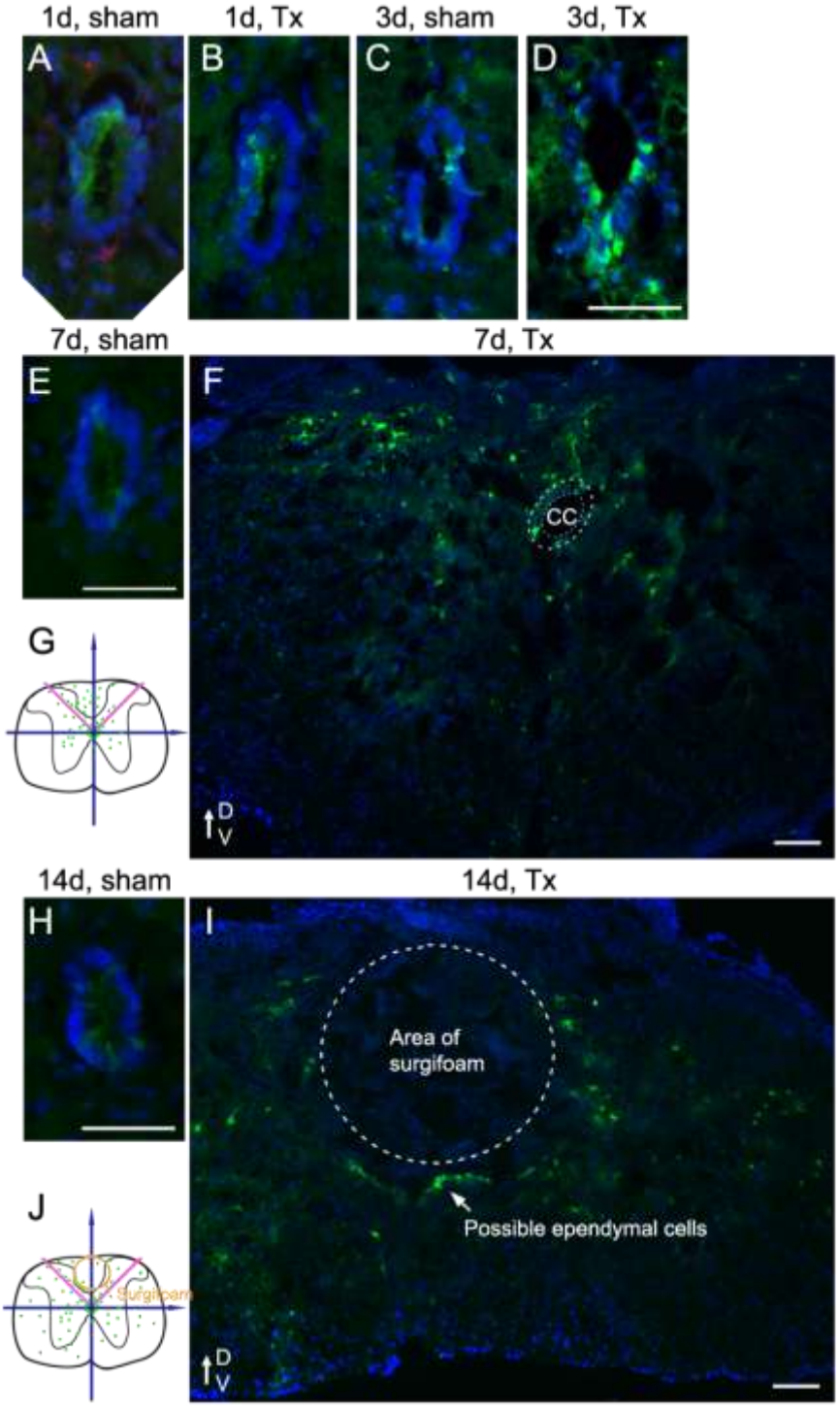

Figure V.1. Transection (Tx) injury on transgenic spinal cord increases the number of GFP+ cells. Spinal cord sections from the CR2-GFP animals in Tx or sham groups were stained with anti-GFP to study the activation pattern of CR2. In sham animals, low GFP expression was found in the ependymal region (A, C, E, H). In Tx animals, increase of GFP+ cells was first found near the ependymal region on 3dpi (D). On 7dpi, they were found in the dorsal half of the spinal cord, and on 14dpi through the entire spinal cord (F, I). A schematic is used to show the distribution of GFP+ cells (G, J). Scale bars in D, E, H = 50 µm; scale bars in F, I = 100 µm.

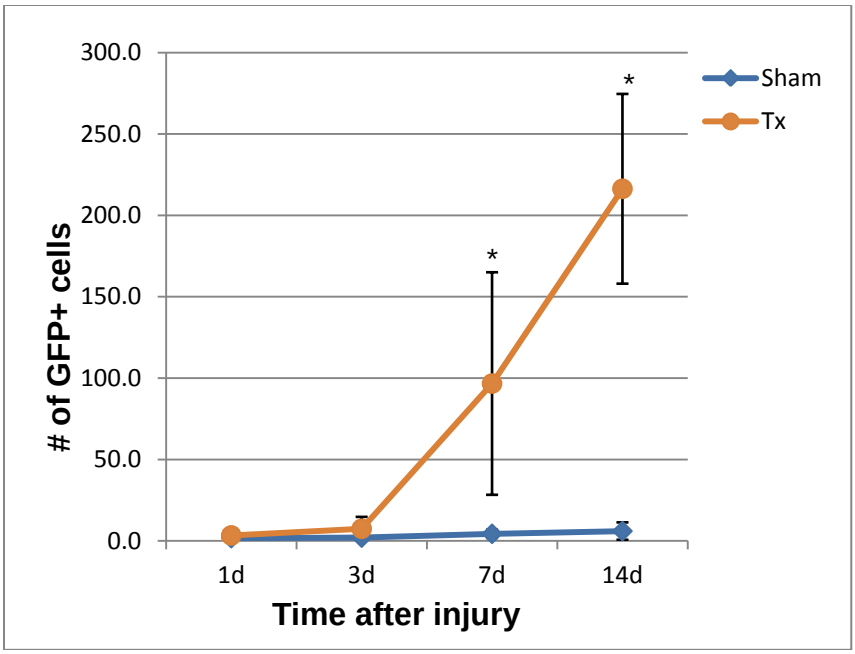

Chart V. 1. The number of GFP+ cells in the spinal cord increases after Tx. The number of GFP+ cells was counted in the spinal cord section that is adjacent to epi-center (< 3 mm) for 1d, 3d, 7d and 14d post injury. This chart is related to Fig. V.1. T-test: * p-value < 0.05.

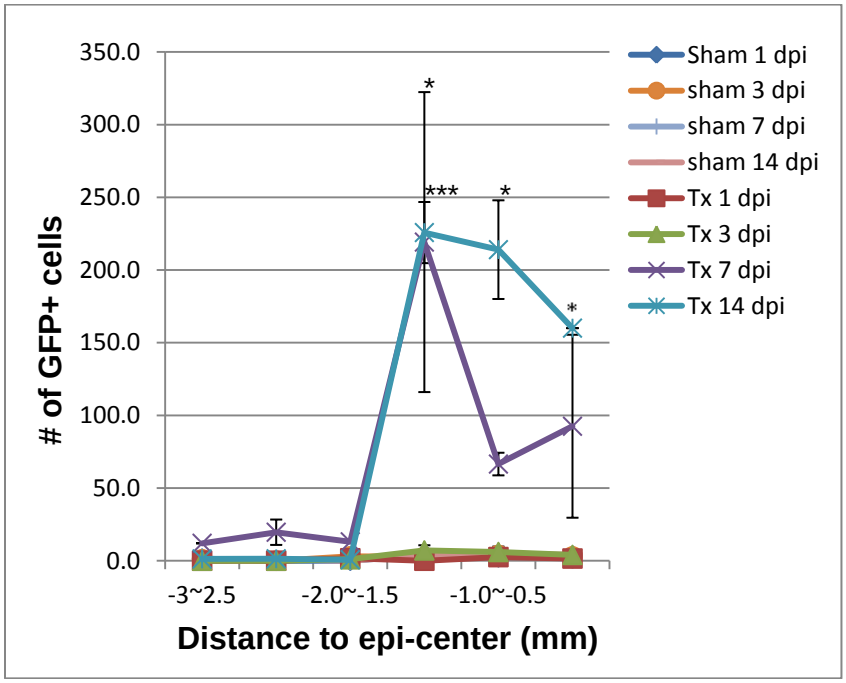

Chart V. 2. Injury-induced GFP+ cells are concentrated near the epi-center. For animals harvested on various stages in Tx and sham groups, spinal cord sections from different distance to epi-center were counted for the number of GFP+ cells. As shown in the plot, significant increases were found within the range of 1.5 mm in the Tx animals harvested on 7dpi or 14dpi. This chart is related to Fig. V.1. T-test: * p-value < 0.05; *** p-value < 0.005.

In Tx model, severe tissue loss was observed in the sections near epi-center, which

was probably the consequence of transection itself or secondary damage such as loss of blood. Ependymal structure was damaged dramatically in this area. However in the adjacent sections, higher GFP expression and increase of number of GFP+ cells were found as early as 3 days post injury (dpi) in the ependymal (**Fig. V.1A-D**), suggesting activation of CR2 in acute response to injury. These GFP+ cells migrated out from ependymal cell layer, first towards the dorsal side where transection initialized (7dpi), then through the entire spinal cord section (14dpi) (**Fig. V.1E-H**). Cell counting was performed on the tissue sections from various distance to epicenter through 1dpi to 14dpi. The results suggest that the increase of GFP+ cells was significant at 7dpi and 14dpi (**Chart V.1**). In addition, the majority of GFP+ cells reside within 2 mm from the epi-center while the peak number is found near 1~1.5 mm (**Chart V.2**).

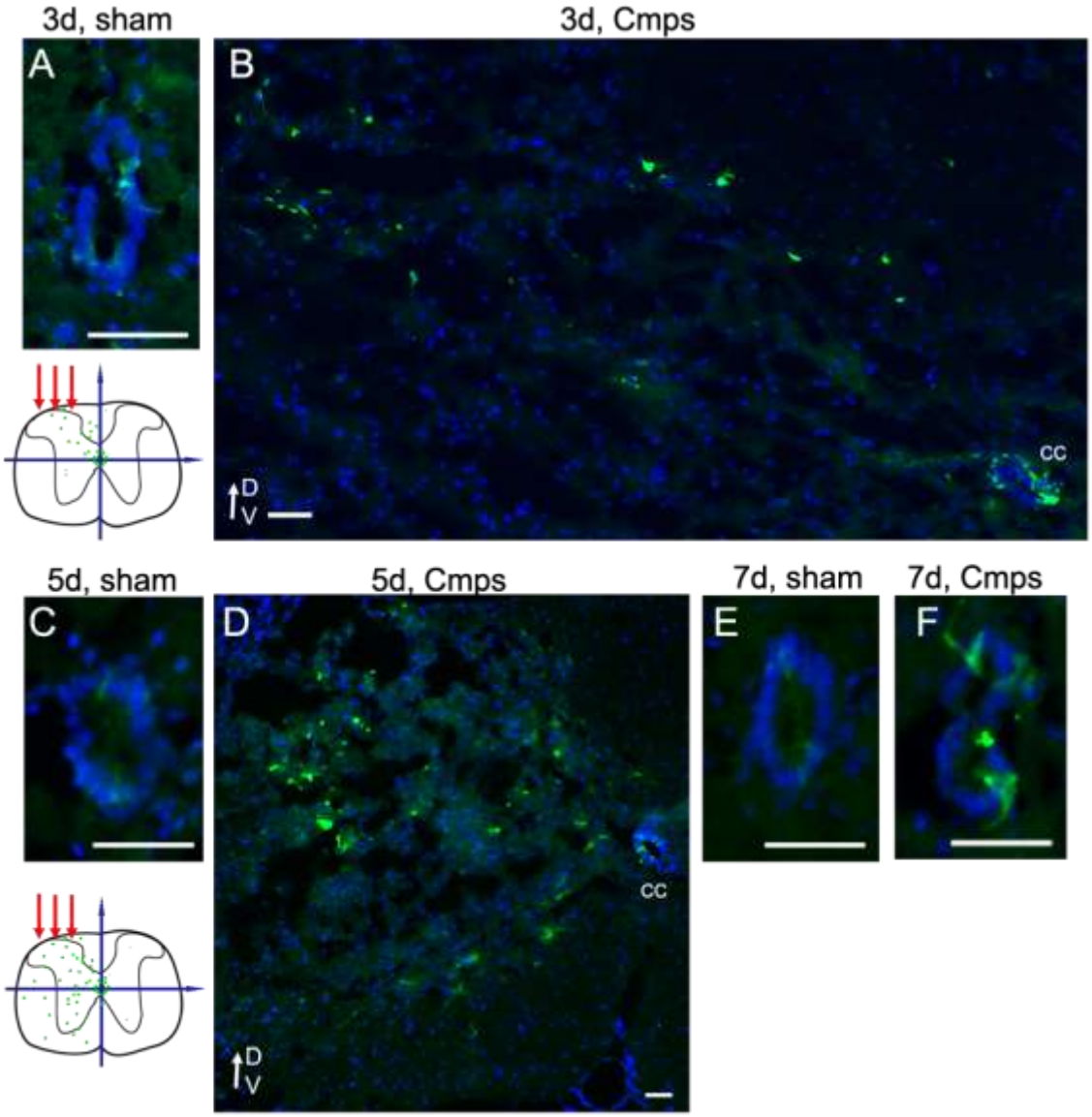

Figure V.2. Compression-on-side (Cmps) injury increases the number of GFP+ cells. Spinal cord sections from the animals in Cmps or sham groups were stained with anti-GFP to study the activation pattern of CR2. In sham animals, a few GFP+ cells were found located in the ependymal region (A, C, E). In Cmps animals, GFP+ cells were found in the dorsal of spinal cord on the injured side on 3dpi (B). On 5dpi, they were found on the entire injured side (D). On 7dpi, GFP+ cells were found only in ependymal region (F). Schematics were used to illustrate the distribution of GFP+ cells. Red arrows indicate the site of injury. Scale bars = 50 μm.

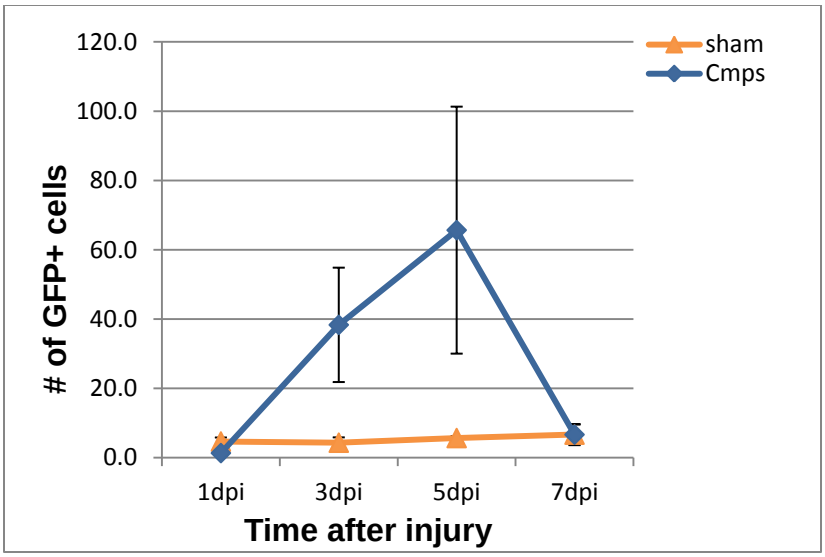

Chart V. 3. The number of GFP+ cells in the spinal cord increases after Cmps. The number of GFP+ cells was counted in the spinal cord section that is adjacent to epi-center (< 3 mm) for 1d, 3d, 5d and 7d post injury. This chart is related to Fig. V.2. T-test: * p-value < 0.05; *** p-value < 0.005.

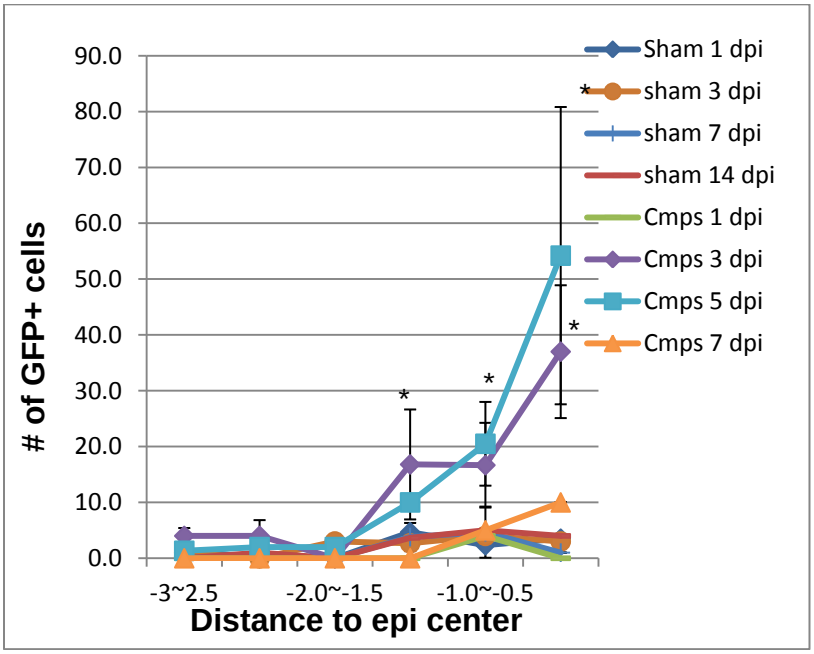

Chart V. 4. Injury induced GFP+ cells concentrate near epi-center in Cmps animals. For animals harvested on various stages in Cmps and sham groups, spinal cord sections from different distance to epi-center were counted for the number of GFP+ cells. As shown in the plot, significant increases were found close to the epi-center (< 1.5 mm) in the animals harvested on 5dpi or 7dpi. This chart is related to Fig. V.2. T-test: * p-value < 0.05; *** p-value < 0.005.

Since the Tx model leads to dramatic tissue damage, a moderate Cmps model was introduced to the transgenic mice. Weight was positioned for 5 min on the side of spinal

cord, approximately on top of the region of dorsal horn to generate the injury. In this model, increase of GFP+ cells was observed on the 3dpi and 5dpi (**Fig. V.2A-D, Chart V.3**), which is the earliest comparing to Tx and cmp model. However, on 7dpi, GFP+ cells in grey and white matter disappeared. They can still be found in the ependymal region, buy only in this region (**Fig. V.2F**). Similar to Tx model, GFP+ cells were first found in the dorsal side of the injured half of spinal cord on 3dpi (**Fig. V.2B**), then spread to the entire injured half of spinal cord on 5dpi (**Fig. V.2D**). From counting the GFP+ cells we found that the majority of GFP+ cells resided within the 1.5 mm range to the epi-center, and the number of GFP+ cells per section increased as it gets closer to the epi-center (**Chart V.3**).

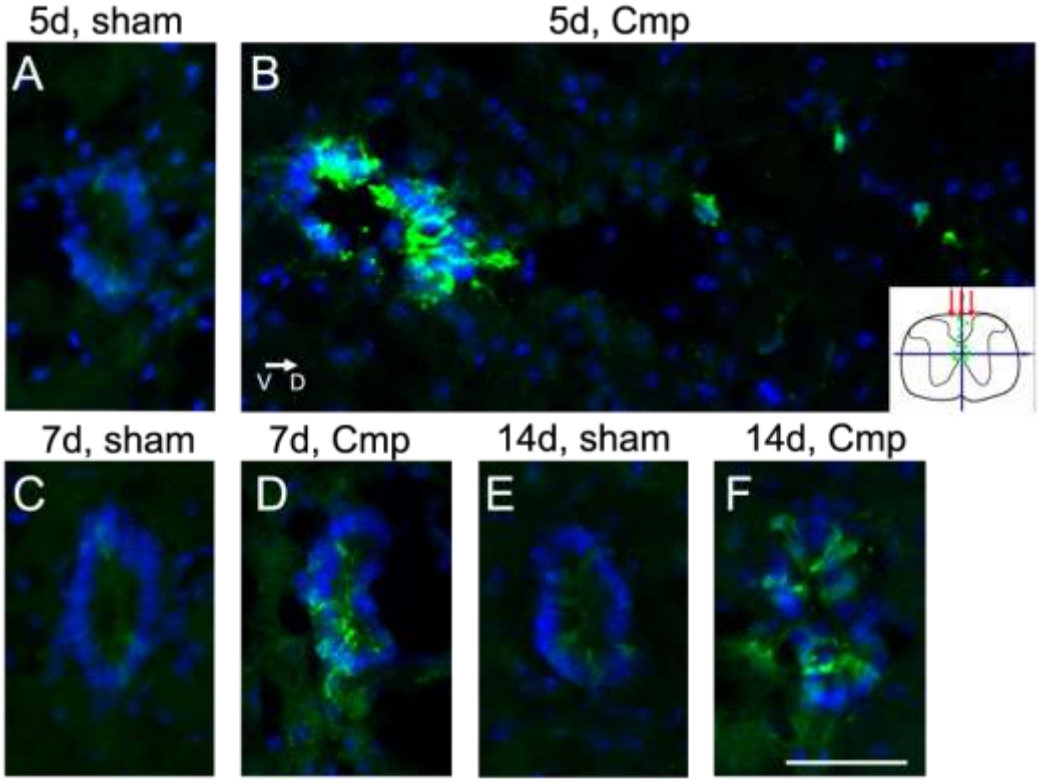

Figure V.3. Compression (Cmp) injury increases the number of GFP+ cells on 5dpi. Spinal cord sections from the animals in Cmp or sham groups were stained with anti-GFP to study the activation pattern of CR2. Compare to sham, GFP+ cells in Cmp animals increased in number on 5dpi (A-B). Additional GFP+ cells were found in the dorsal column. On 7dpi and 14dpi, GFP+ cells were only found in ependymal region (C-F). Schematic was used to illustrate the distribution of GFP+ cells. Red arrows indicate the site of injury. Scale bar = 50 μm.

The mild injury model, Cmp model was also tested in our CR2-GFP transgenic mice. Similarly, we observed increase of GFP+ cells which suggests activation of CR2 with a mild damage to the spinal cord tissue. However the increase was only observed on the 5dpi with a few cells outside the ependymal region (**Fig. V.3B**). Later on 7dpi and 14dpi, GFP+ cells were only found within the ependymal region, similar to the sham animals (**Fig. V.3C-F**). Because of the limited number of GFP+ cells generated in Cmp model, it was eliminated from further studies.

In summary, significant increase in the number of CR2-GFP+ cells was observed in all three SCI models comparing to control groups. These SCI induced CR2-GFP+ cells were counted in spinal cord sections at various distances and stages to determine the temporal and spatial activation pattern of CR2. In general, uprising of GFP+ cells were mostly found in the close range (< 3 mm) of epi-center within the first week post injury., The number of GFP+ cells and the period of CR2 activation is close relative to the severity of injury: the more severe the injury is, the more GFP+ cells are found and the earlier the CR2 is activated.

2) Injury induces GFP expression in aNSCs and glial cells.

To determine the identity of the GFP+ cell presented following injuries, immunohistochemistry was performed with proliferation markers, death markers and various cell type markers.

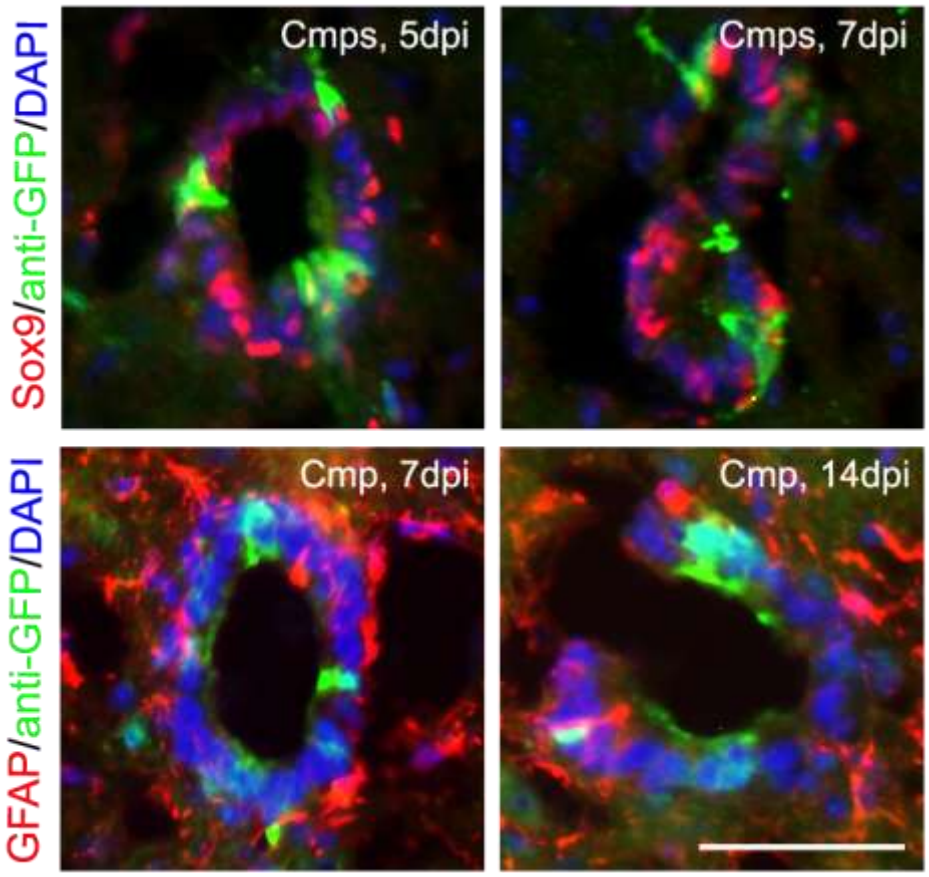

Figure V.4. Injury-induced CR2-GFP+ cells in the ependymal region are aNSC. Spinal cord sections from injured animals were stained with Sox9, which labels the ependymal region; and GFAP, which is intensively active surrounding the ependymal region. GFP+ cells were found co-labeled with Sox9 showing in the top panel. GFP+ cells were also found partially co-labeled with GFAP. Scale bar = 50 µm.

As shown in the previous chapter, CR2 is quiescent in the ependymal cells, which are aNSCs. After injury, CR2 is activated and GFP+ cells were found first in the ependymal region as expected. Staining with Sox9 and GFAP supported the result that these GFP+ cells are stem cells (**Fig. V.4**).

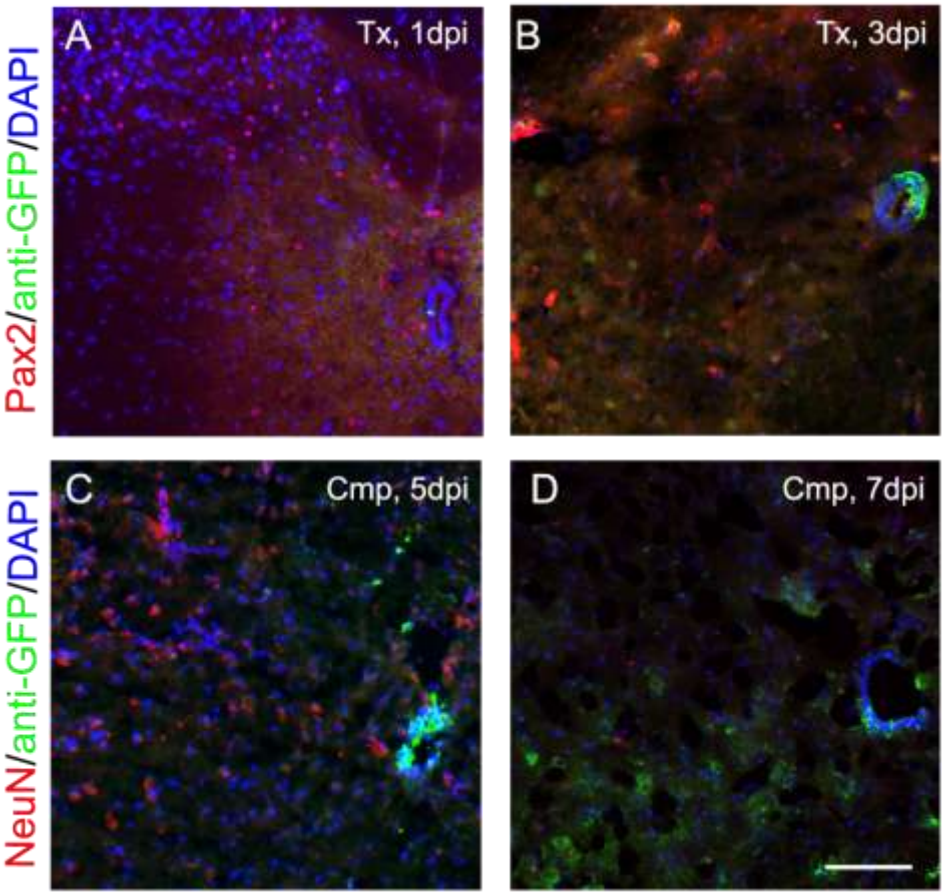

Figure V.5. Injury-induced GFP+ are not neurons or neuronal progenitors. To identify the GFP+ cells, spinal cord sections from various stages after injury were stained with the neuronal marker Pax2 and NeuN. Pax2 was found on 1dpi in the Tx model and disappeared on 3dpi (A, B). NeuN was found on 5dpi in the Cmp model and disappeared on 7dpi (C, D). Neither of the markers co-stained with GFP. Scale bar = 100 μm.

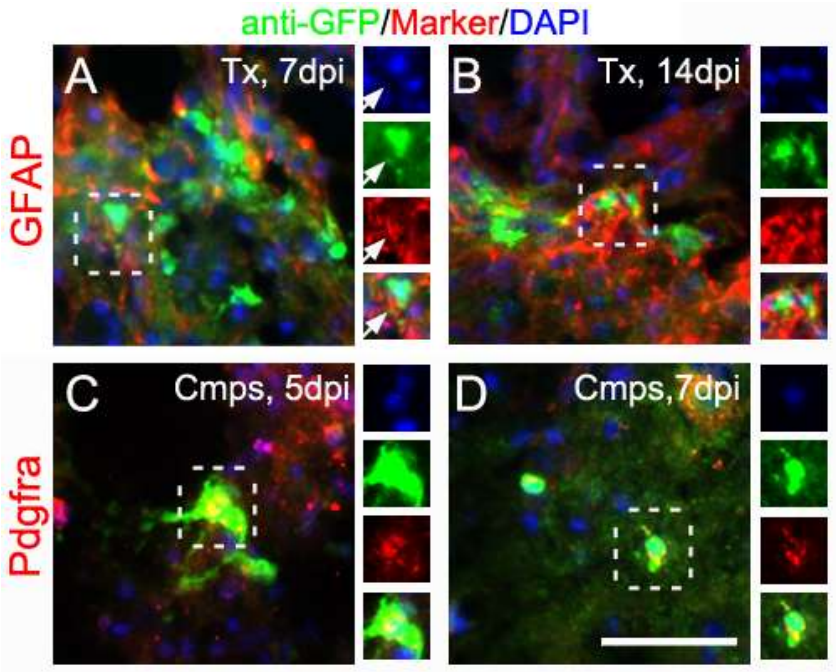

Figure V.6 Injury-induced GFP+ cells in the parenchymal region adopt glial fate. In Tx and Cmps models, spinal cord sections were stained with glial cell marker GFAP and Pdgfra. The results show that GFP+ cells in Tx model co-labeled with GFAP on 7dpi (A) and 14dpi (B). GFP+ cells in Cmps model co-labeled with Pdgfra on 5dpi (C) and 7dpi (D). Scale bar = 50 μm.

Following the above results, the spinal cord samples from Tx and Cmps models were further stained with neural progenitor marker Tuj1, Pax2, neuronal marker NeuN and glial marker GFAP, Pdgfra to determine the identity of the GFP+ cells in parenchymal region. Among these markers, Tuj1 showed no staining in the spinal cord sections (data not shown) after injury. Pax2 and NeuN stained shortly after injury but did not co-stain with GFP+ cells (**Fig. V.5**). Those cells stained by Pax2 and NeuN may be the neurons survived from injury, which died shortly afterwards. In the contrary, major co-staining of GFP+ cells with GFAP and Pdgfra was observed in both Tx and Cmps models at various stages (**Fig. V.6**), suggesting that these GFP+ cells are glial cells or glial progenitor cells. This is consistent with the current knowledge of SCI acute response, in which neural regeneration is limited and most of the aNSCs will develop into oligodendrocytes or astrocytes (Horky et al., 2006; Meletis et al., 2008; Yang et al., 2006a).

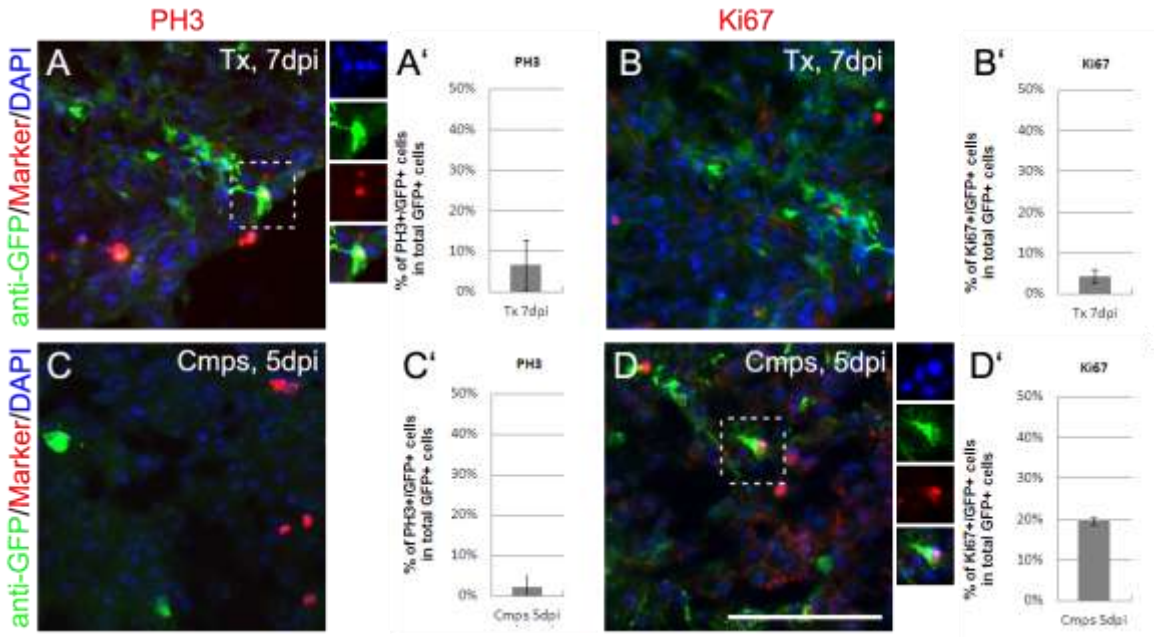

Figure V.7. A small portion of GFP+ cells in parenchymal region are proliferating. In both Tx and Cmps models, the widely spread GFP+ cells were found partially co-labeled with the proliferation markers, either PH3 (A) or Ki67 (D). However, the majority of GFP+ cells were not co-labeled (A-D), which is also shown in the counting (A'-C'). Scale bar = 50 µm.

The proliferation marker PH3 (for cells in M-phase) and Ki67 (for cells in S-phase) were also used to stain spinal cord sections, in order to find out if the GFP+ cells outside ependymal region can proliferate. However, the majority of GFP+ cells were not co-labeled with PH3 or Ki67 (**Fig. V.7**). Only a small portion of GFP+ cells are positive for these proliferation markers, which were usually found in the grey matter near injured area (**Fig. V.7A, D**). These results suggest that most of the GFP+ cells outside ependymal region are no longer proliferating. Combine with the knowledge that most of these GFP+ cells are GFAP+ or Pdgfra+, they may be new progenitor cells that just exit the cell cycle.

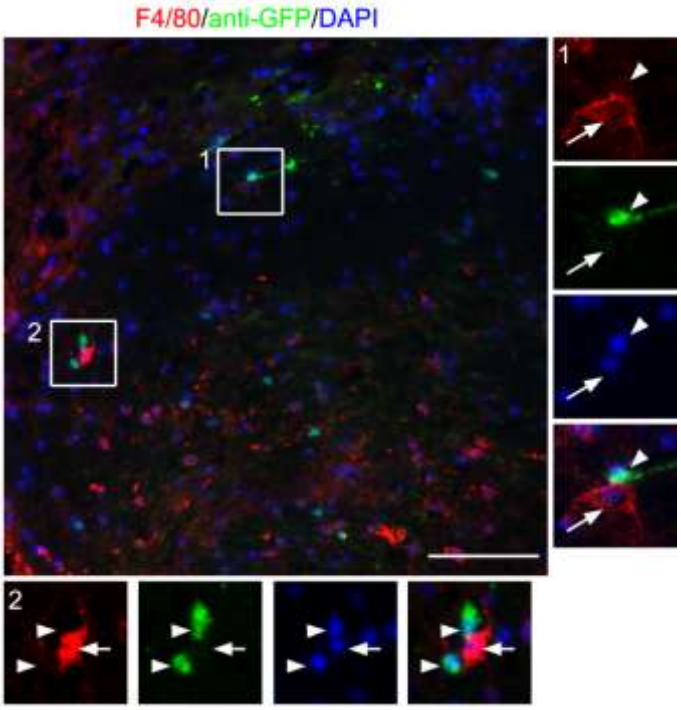

Figure V.8 Injury-induced GFP+ cells are not macrophages. Macrophage marker F4/80 was used to stain spinal cord sections. But no co-labeling was found. Arrowheads represent the GFP+ cells and arrows represent the F4/80+ macrophages. Image shown a sample from Tx model on 3dpi. Scale bar = 50 μm

As a lot of study suggest, inflammatory responses usually occur follow the SCI, in which the infiltration of macrophage is a main event (David and Kroner, 2011). Thus a macrophage marker F4/80 was used to find out if GFP+ cells contain these inflammatory cells. Result show that none of the GFP+ cells is F4/80+ (**Fig. V.8**). Thus GFP+ cells are not macrophages, and CR2 is not activate in macrophages.

In summary, the GFP+ cells reside in ependymal region are aNSCs, while the majority of the GFP+ cells in parenchymal region are GFAP+/Pdgfra+ glial cells. A small portion of these parenchymal GFP+ cells are progenitor/stem-like cells that proliferate. None of the GFP+ cell is neural progenitor or neuron.

6. Discussion

In this chapter, the activation of CR2 and appearance of CR2-GFP cells after SCI

were characterized in three injury models. In mouse spinal cord, CR2 is found to be active in both ependymal and parenchymal neural stem cells which can be labeled with GFAP and Pdgfra.

The CR2-GFP+ cells were found quiescent in the adult ependymal cells (**Fig. IV.S4**) and activated in the three different injury models (**Fig. V.1-3**). They are also positive for Sox9 (**Fig. V.4**), PH3 and Ki67 (**Fig. V.7**). Thus these GFP+ cells are identified as the aNSCs. They were found in both the ependymal and parenchymal regions where aNSCs usually exist (Meletis et al., 2008; Moreno-Manzano et al., 2009; Yamamoto et al., 2001).

The activation of GFP+ cells in three injury models followed different timelines. The mild Cmp injury model only increases the number of GFP+ cells on 5dpi, while the GFP+ cells in moderate Cmps model were found from 3dpi to 7dpi, and in severe Tx model from 3dpi to 14dpi with the number of cells continuing to increase (**Fig. V.1-3**). It is clear that the CR2 activation is in positive correlation to the severity of injury. Furthermore, the range of CR2 activation is relative to both the severity of the injury and the integrity of tissue after injury. In Tx model, GFP+ cells were first found near the ependymal region, but not in the parenchymal region like in Cmps model (**Fig. V.1D, 3B**). A possible explanation is that in Tx model the hemorrhage and massive cell death near the epi-center tampers the activation mechanism of aNSCs. It requires longer time to recruit the molecules needed for aNSC activation. Once these molecules are present, aNSCs in a boarder range are activated, resulting in more GFP+ cells in later stages (**Fig. V.1F, H**).

Moreover, the CR2-GFP+ cells were found distributed throughout the entire injury site (**Fig. V.1, 3**). This suggests that the cells in both grey and white matter are involved in the neurogenesis triggered by injury, and have the potential for the self-repair. The majority of GFP+ cells were co-labeled with GFAP and Pdgfra but not neuronal markers (**Fig. V.5, 6**), suggesting the preference of gliogenesis after injury. It is consistent with the

findings that the neurons and oligodendrocyte generated from aNSC would die while the astrocytes would survive (Barnabe-Heider et al., 2010; Meletis et al., 2008).

Chapter VI

Conclusions and Future Direction

1. General conclusion

The focus of this dissertation is to study the endogenous coordination of the CNS during embryonic development from the aspect of transcription regulation, and extend the observations to the regeneration of neural cells after CNS injury. With each targeting a different mechanism or organ, the four projects described in this dissertation provided new insights in transcription regulation on neural system development and regeneration from chromatin topo-structure remodeling, master TF regulation and specific TF-enhancer interaction.

The first project described in Chapter III demonstrated the importance of Top2b in neural development. Using the retina as a model, conditional Top2b knock out led to not only defects in the dendrite growth and axon guidance as observed in previous publications (Lyu and Wang, 2003a; Nevin et al., 2011a), but also the aberrant cell localization, defects in cell morphology and ultimately, the cell death. Although the mechanism of how Top2b deficiency triggers cell death remains to be determined, it is clear that the cell death was not immediate. Top2b knockout mice do not show any deficiency until late developmental stage. It is possible that the lack of dendritic connections between neighboring neurons causes errors in the system which triggers the pruning-related programmed cell death (Meier et al., 2000; Yuan et al., 2003). Alternatively, the cell death could also be triggered by DNA degradation caused by problematic DNA topo-structure modification (Li et al., 1999).

To focus on the intrinsic regulation of tissue specific genes, Chapter IV illustrated a

network between 15 enhancer sequences that are critical for retinal development and six master TFs including Pou3f2. It was the first time that a group of tissue-specific enhancers was analyzed together to determine their combinatorial effects on development. Typically, the TFmaster regulators are first identified and then their interacting DNA sequences are determined by IP or ChIP-seq analysis (Spitz and Furlong, 2012; Visel et al., 2009). In this chapter, computational method was used to first screen the enhancers retrieved from databases to predict the TFBSs, and then perform cross comparison between the TFBSs of each enhancer for motifs of the master TF. The method was examined in predicting a retinal regulatory network, in which tissue all neural cells were originated from the retinal progenitor cells (Young, 1985b). Such single-origin cells fits best with our hypothesis of the existence of master TF. This method can be used in any other tissues that contain cells originate from one progenitor cell source.

Further in Chapter IV and V, the enhancer CR2 was studied in depth for its regulatory function in Notch1 expression during spinal cord development and after injury. Notch1 is an important gene that has multiple roles during neural development and regeneration, including maintaining stem cells in cell cycle, determine glial cell fate and axon guidance (Alexson et al., 2006; Grandbarbe et al., 2003; Kawaguchi et al., 2008; Mason et al., 2006; Pierfelice et al., 2011; Redmond et al., 2000; Yang et al., 2006b). In this study, the mechanism of Notch1 regulation in interneurons was investigated. CR2 activity was found to be specific to interneurons progenitors (**Fig. IV.3**) and was activated after SCI (**Fig. V.1-3**). With the understanding of CR2 function and the mechanism of how it regulates Notch1 for interneuron differentiation, we hypothesize CR2 activity is involved in the neural regeneration after injury. In Chapter IV, Nkx6.1 was found to be interacting CR2 during ventral interneuron development (**Fig. IV.6**) and Gsx1 was a

potential factor that may interact with CR2 during dorsal interneuron development. In Chapter V, CR2 was found re-activated in both ependymal and parenchymal regions in the injured spinal cord. And the CR2-GFP+ cells were identified as aNSCs and glial progenitors. Further experiments will be performed to characterize the influence of Nkx6.1 and Gsx1 on aNSCs.

2. Future direction

1) Gene regulation network during CNS development

In this dissertation I studied the gene regulation of both one single gene (Notch1) and group of retinal specific genes, using both traditional experimental methods (e.g. reporter assay and *in ovo* electroporation) and computational methods (e.g. screening for TFBS with MatInspector, analyzing RNA-seq data from Top2b knockout animal). The questions proposed were answered, however also led to many more questions, such as the mechanism behind regulation of Top2b in retinal specific genes, how transcription regulatory network function during retinal development, what are the other components in the transcription initializing complex for Notch1 expression, and how we can utilize Nkx6.1 and Gsx1 to promote post injury neurogenesis. Among all these questions, I will focus on building a transcription regulatory network for spinal cord development, which will expand our understanding of the development of spinal cord, and provide insights in the treatment of developmental diseases and injuries.

Computational methods have been used for the prediction of gene regulatory elements for almost two decades (Brazma et al., 1998; Wasserman and Sandelin, 2004), and the widely used next-generation sequencing have largely changed our methods of identifying *cis*-regulatory sequence and *trans*-interacting factors (Morozova and Marra,

2008). Now researchers study the transcription regulation in a network manner. Beyond the interaction of single TF-regulator sequence, network is more close to how genes are regulated in nature. The excessive variability of gene expression is usually controlled in some feedback loops that are robust enough to maintain proper phenotypes (Felix and Wagner, 2008). Many methods have been used to study transcription binding sites in large scales, including ChIPseq or microarray (Johnson et al., 2007; Ren et al., 2000). With such methods the master TFs in a specific tissue can be identified, though with high expenses. In addition, with the developed tools, we are also able to profile transcriptome for the entire tissue, including alternative transcripts, non-coding RNAs, etc. Databases are built with sequencing data that is contributed from scientists all over the world, such as NCBI, Ensembl, ENCODE and NHGRIGSP. Such databases make it possible for researchers to save the time and effort of generating their own data. Instead we can find the datasets that are needed, pool the datasets together and use computational tools to analyze them together. The concept of Big Data was introduced to the biological and medical research in the past few years (Bender, 2015). With the fast development of programs for data analysis, we will be able to handle the large amount of data gathered for our target tissue, the spinal cord, and build the transcription regulatory network.

2) Gene regulation after SCI

In Chapter VI, the re-activation of Notch1 enhancer CR2 was characterized using SCI mouse model. We were able to determine the identity of CR2-GFP+ cells as aNSCs since they express NSC and progenitor markers, e.g., Sox9, GFAP and Pdgfra. However, there was no significant difference between these GFP+ cells and the rest of the

ependymal cells (**Fig. V.4**). Thus, as future direction, we plan to perform a single-cell RNA-seq on a) the spinal cord ependymal cell after injury. Profile of the transcriptome in GFP+ ependymal cells, GFP-ependymal cells and control naive ependymal cells will be studied to identify gene signatures that mark the different subgroups of the NSCs before and after injury. The use of single-cell RNA-seq instead of traditional RNA-seq aids to reveal the molecular profile of cell population of small amount (Stegle et al., 2015) such as ependymal cells. Several recent studies have been reported to use single-cell RNA-seq in analyzing NSCs in adult mammalian brain (Llorens-Bobadilla et al., 2015; Luo et al., 2015; Shin et al., 2015) which yields good resolution. We will adopt this technique and apply on our SCI study. By comparing the GFP+ ependymal cells to the GFP- ones we should be able to find out if these cells belong to different sub-types of stem cells and why they both differentiate into astrocytes.

Chapter VII

Appendix: The 173 TFBS that are predicted to have binding site on CR2.

Transcription factor <-> matrix family assignment				Position			Strand
Matrix Family	Detailed Family Information	Matrix	Detailed Matrix Information	from	to	anchor	
V$EREF	Estrogen response elements	V$ER.03	Estrogen response elements, IR3 sites	6	28	17	(+)
V$SMAD	Vertebrate SMAD family of transcription factors	V$SMAD.01	Sma- and Mad-related proteins	16	26	21	(-)
V$PAX5	PAX-2/5/8 binding sites	V$PAX5.01	B-cell-specific activator protein	23	51	37	(+)
V$PAX6	PAX-4/PAX-6 paired domain binding sites	V$PAX6.04	PAX6 paired domain binding site	28	46	37	(-)
V$PAX9	PAX-9 binding sites	V$PAX9.01	Zebrafish PAX9 binding sites	29	49	39	(+)
V$PLAG	Pleomorphic adenoma gene	V$PLAG1.01	Pleomorphic adenoma gene (PLAG) 1, a developmentally regulated C2H2 zinc finger protein	33	55	44	(+)
V$E2FF	E2F-myc activator/cell cycle regulator	V$E2F1_DP1.01	E2F-1/DP-1 heterodimeric complex	33	49	41	(+)
V$ETSF	Human and murine ETS1 factors	V$ETV1.02	Ets variant 1	34	54	44	(+)
V$KLFS	Krueppel like transcription factors	V$BTEB3.01	Basic transcription element (BTE) binding protein, BTEB3, FKLF-2	40	56	48	(+)
V$PLAG	Pleomorphic adenoma gene	V$PLAG1.02	Pleomorphic adenoma gene 1	44	66	55	(+)
V$STAF	Selenocysteine tRNA activating factor	V$STAF.01	Se-Cys tRNA gene transcription activating factor	46	68	57	(-)
V$FAST	FAST-1 SMAD interacting proteins	V$FAST1.01	FAST-1 SMAD interacting protein	47	63	55	(+)
V$HEAT	Heat shock factors	V$HSF1.01	Heat shock factor 1	49	73	61	(-)
V$STAT	Signal transducer and activator of transcription	V$STAT5.01	STAT5: signal transducer and activator of transcription 5	52	70	61	(-)
V$BCL6	POZ domain zinc finger expressed in B-Cells	V$BCL6.04	B-cell CLL/lymphoma 6, member B (BCL6B)	53	69	61	(-)
V$STAT	Signal transducer and activator of transcription	V$STAT.01	Signal transducers and activators of transcription	54	72	63	(+)
V$AHRR	AHR-arnt heterodimers and AHR-related factors	V$AHRARNT.02	Aryl hydrocarbon / Arnt heterodimers, fixed core	59	83	71	(-)
V$PAX5	PAX-2/5/8 binding sites	V$PAX5.02	B-cell-specific activator protein	60	88	74	(-)
V$CART	Cart-1 (cartilage homeoprotein 1)	V$S8.01	Binding site for S8 type homeodomains	65	85	75	(-)

V$SORY	SOX/SRY-sex/testis determinig and related HMG box factors	V$HMGA.01	HMGA family of architectural transcription factors (HMGA1, HMGA2)	66	90	78	(-)
V$DLXF	Distal-less homeodomain transcription factors	V$DLX1.01	DLX-1, -2, and -5 binding sites	66	84	75	(+)
V$LHXF	Lim homeodomain factors	V$LHX6.01	LIM homeobox 6	66	88	77	(+)
V$PDX1	Pancreatic and intestinal homeodomain transcription factor	V$IPF1.01	Insulin promoter factor 1, pancreatic and duodenal homeobox 1 (Pdx1)	66	84	75	(+)
V$OCT1	Octamer binding protein	V$POU3F3.01	POU class 3 homeobox 3 (POU3F3), OTF8	67	81	74	(+)
V$HOXF	Paralog hox genes 1-8 from the four hox clusters A, B, C, D	V$HOXC8.01	Homeobox C8 / Hox-3alpha	67	85	76	(-)
V$BRN5	Brn-5 POU domain factors	V$BRN5.01	Brn-5, POU-VI protein class (also known as emb and CNS-1)	67	89	78	(+)
V$LHXF	Lim homeodomain factors	V$LHX3.01	Homeodomain binding site in LIM/Homeodomain factor LHX3	67	89	78	(-)
V$BRNF	Brn POU domain factors	V$BRN3.02	Brn-3, POU-IV protein class	68	86	77	(+)
V$HBOX	Homeobox transcription factors	V$VAX2.01	Ventral anterior homeobox 2	68	86	77	(-)
V$HOMF	Homeodomain transcription factors	V$MSX1.01	Muscle-segment homeobox 1, msh homeobox 1	68	86	77	(+)
V$HOMF	Homeodomain transcription factors	V$BARX2.01	Barx2, homeobox transcription factor that preferentially binds to paired TAAT motifs	69	87	78	(-)
V$HBOX	Homeobox transcription factors	V$VAX2.01	Ventral anterior homeobox 2	69	87	78	(+)
V$NKX1	NK1 homeobox transcription factors	V$NKX12.01	NK1 homeobox 2, Sax1-like	69	85	77	(-)
V$OCT1	Octamer binding protein	V$OCT1.03	Octamer-binding transcription factor-1, POU class 2 homeobox 1 (POU2F1)	69	83	76	(+)
V$BRNF	Brn POU domain factors	V$BRN3.03	POU class 4 homeobox 3 (POU4F3), BRN3C	69	87	78	(-)
V$CART	Cart-1 (cartilage homeoprotein 1)	V$S8.01	Binding site for S8 type homeodomains	70	90	80	(+)
V$LHXF	Lim homeodomain factors	V$LHX3.01	Homeodomain binding site in LIM/Homeodomain factor LHX3	70	92	81	(+)
V$NKX6	NK6 homeobox transcription factors	V$NKX63.01	NK6 homeobox 3	70	84	77	(+)
V$PAXH	PAX homeodomain binding sites	V$PAX6_HD.01	Paired box 6, homeodomain binding site	70	84	77	(-)
V$HOXF	Paralog hox genes 1-8 from the four hox clusters A, B, C, D	V$HOXC8.01	Homeobox C8 / Hox-3alpha	70	88	79	(+)

V$NKXH	NKX homeodomain factors	V$NKX25.02	Homeo domain factor Nkx-2.5/Csx, tinman homolog low affinity sites	70	88	79	(+)
V$ABDB	Abdominal-B type homeodomain transcription factors	V$HOXC9.01	Homeobox C9 / Hox-3beta	70	86	78	(+)
V$DLXF	Distal-less homeodomain transcription factors	V$DLX2.01	Distal-less homeobox 2	71	89	80	(-)
V$PAXH	PAX homeodomain binding sites	V$PAX4.02	Paired box 4, homeodomain binding site	71	85	78	(+)
V$HOXF	Paralog hox genes 1-8 from the four hox clusters A, B, C, D	V$HOXB8.01	Homeobox B8 / Hox-2delta	71	89	80	(-)
V$PDX1	Pancreatic and intestinal homeodomain transcription factor	V$IPF1.01	Insulin promoter factor 1, pancreatic and duodenal homeobox 1 (Pdx1)	71	89	80	(-)
V$LHXF	Lim homeodomain factors	V$LMX1B.01	LIM-homeodomain transcription factor	71	93	82	(-)
V$NKX6	NK6 homeobox transcription factors	V$NKX61.01	NK6 homeobox 1	71	85	78	(-)
V$HOXC	HOX - PBX complexes	V$HOXA9.01	Member of the vertebrate HOX - cluster of homeobox factors	72	88	80	(-)
V$OCT1	Octamer binding protein	V$OCT1.03	Octamer-binding transcription factor-1, POU class 2 homeobox 1 (POU2F1)	72	86	79	(-)
V$PIT1	GHF-1 pituitary specific pou domain transcription factor	V$PIT1.02	POU domain, class 1, transcription factor 1 (POU1F1) / Pituitary transcription factor-1	72	86	79	(-)
V$ARID	AT rich interactive domain factor	V$BRIGHT.01	Bright, B cell regulator of IgH transcription	72	92	82	(+)
V$BRNF	Brn POU domain factors	V$BRN3.03	POU class 4 homeobox 3 (POU4F3), BRN3C	72	90	81	(+)
V$LEFF	LEF1/TCF	V$LEF1.04	TCF/LEF-1 (secondary DNA binding preference)	72	88	80	(+)
V$ABDB	Abdominal-B type homeodomain transcription factors	V$HOXC9.01	Homeobox C9 / Hox-3beta	73	89	81	(-)
V$ATBF	AT-binding transcription factor	V$ATBF1.01	AT-binding transcription factor 1	73	89	81	(-)
V$PIT1	GHF-1 pituitary specific pou domain transcription factor	V$PIT1.02	POU domain, class 1, transcription factor 1 (POU1F1) / Pituitary transcription factor-1	73	87	80	(+)
V$NKX6	NK6 homeobox transcription factors	V$NKX61.01	NK6 homeobox 1	74	88	81	(+)
V$BCDF	Bicoid-like homeodomain transcription factors	V$CRX.01	Cone-rod homeobox-containing transcription factor / otx-like homeobox gene	74	90	82	(+)

V$HOXF	Paralog hox genes 1-8 from the four hox clusters A, B, C, D	V$HOXC8.01	Homeobox C8 / Hox-3alpha	74	92	83	(+)
V$HOXF	Paralog hox genes 1-8 from the four hox clusters A, B, C, D	V$HOX1-3.01	Hox-1.3, vertebrate homeobox protein	81	99	90	(-)
V$BRNF	Brn POU domain factors	V$BRN3.03	POU class 4 homeobox 3 (POU4F3), BRN3C	83	101	92	(-)
V$HOMF	Homeodomain transcription factors	V$BARX2.01	Barx2, homeobox transcription factor that preferentially binds to paired TAAT motifs	83	101	92	(-)
V$HOXF	Paralog hox genes 1-8 from the four hox clusters A, B, C, D	V$HOXB8.01	Homeobox B8 / Hox-2delta	85	103	94	(-)
V$HBOX	Homeobox transcription factors	V$GSH1.01	Homeobox transcription factor Gsh-1	86	104	95	(-)
V$HOMF	Homeodomain transcription factors	V$HMX1.01	H6 family homeobox 1 / NKX5-3	86	104	95	(+)
V$ABDB	Abdominal-B type homeodomain transcription factors	V$HOXC9.01	Homeobox C9 / Hox-3beta	87	103	95	(-)
V$NKX6	NK6 homeobox transcription factors	V$NKX61.02	NK6 homeobox 1	88	102	95	(+)
V$CART	Cart-1 (cartilage homeoprotein 1)	V$PHOX2.01	Phox2a (ARIX) and Phox2b	88	108	98	(+)
V$BCDF	Bicoid-like homeodomain transcription factors	V$CRX.01	Cone-rod homeobox-containing transcription factor / otx-like homeobox gene	88	104	96	(+)
O$TF2D	General transcription factor IID, GTF2D	O$INR_DPE.01	Initiator (INR) and downstream promoter element (DPE) with strictly maintained spacing	92	130	111	(-)
V$MAZF	Myc associated zinc fingers	V$MAZ.01	Myc associated zinc finger protein (MAZ)	94	106	100	(-)
V$ZF01	C2H2 zinc finger transcription factors 1	V$ZBRK1.01	Transcription factor with 8 central zinc fingers and an N-terminal KRAB domain	100	124	112	(-)
V$FKHD	Fork head domain factors	V$FHXB.01	Fork head homologous X binds DNA with a dual sequence specificity (FHXA and FHXB)	100	116	108	(+)
V$SORY	SOX/SRY-sex/testis determinig and related HMG box factors	V$SOX5.01	Sox-5	101	125	113	(+)
V$STAT	Signal transducer and activator of transcription	V$STAT6.01	STAT6: signal transducer and activator of transcription 6	117	135	126	(-)
V$PLAG	Pleomorphic adenoma gene	V$PLAG1.01	Pleomorphic adenoma gene (PLAG) 1, a developmentally regulated C2H2 zinc finger protein	128	150	139	(-)
V$AP4R	AP4 and related	V$AP4.02	Activator protein 4	129	145	137	(-)

	proteins						
V$MYOD	Myoblast determining factors	V$MYOGENIN.02	Myogenic bHLH protein myogenin (myf4)	129	145	137	(+)
V$AP4R	AP4 and related proteins	V$AP4.01	Activator protein 4	130	146	138	(+)
V$MYOD	Myoblast determining factors	V$MYOGENIN.02	Myogenic bHLH protein myogenin (myf4)	130	146	138	(-)
V$NEUR	NeuroD, Beta2, HLH domain	V$ATOH1.01	Atonal homolog 1, HATH1, MATH-1	131	143	137	(+)
V$HOXF	Paralog hox genes 1-8 from the four hox clusters A, B, C, D	V$NANOG.01	Homeobox transcription factor Nanog	144	162	153	(+)
V$SORY	SOX/SRY-sex/testis determinig and related HMG box factors	V$HBP1.02	HMG box-containing protein 1	144	168	156	(+)
V$NFAT	Nuclear factor of activated T-cells	V$NFAT.01	Nuclear factor of activated T-cells	153	171	162	(+)
V$FKHD	Fork head domain factors	V$FHXB.01	Fork head homologous X binds DNA with a dual sequence specificity (FHXA and FHXB)	156	172	164	(+)
V$BRNF	Brn POU domain factors	V$TST1.01	POU-factor Tst-1/Oct-6	156	174	165	(+)
V$EVI1	EVI1-myleoid transforming protein	V$MEL1.01	MEL1 (MDS1/EVI1-like gene 1) DNA-binding domain 1	159	175	167	(+)
V$HOXC	HOX - PBX complexes	V$HOXC9.02	Member of the vertebrate HOX - cluster of homeobox factors	161	177	169	(+)
V$RORA	v-ERB and RAR-related orphan receptor alpha	V$RORA2.01	RAR-related orphan receptor alpha2	163	185	174	(+)
V$PAX5	PAX-2/5/8 binding sites	V$PAX2.02	Paired box protein 2	163	191	177	(-)
V$HICF	Krueppel-like C2H2 zinc finger factors hypermethylated in cancer	V$HIC1.02	Hypermethylated in cancer 1 (secondary DNA binding preference)	167	179	173	(-)
V$SIXF	Sine oculis (SIX) homeodomain factors	V$SIX6.01	Sine oculis homeobox homolog 6, optic homeobox 2 (OPTX2)	168	182	175	(+)
V$HEAT	Heat shock factors	V$HSF1.04	Heat shock factor 1	176	200	188	(+)
V$WHNF	Winged helix binding sites	V$WHN.01	Winged helix protein, involved in hair keratinization and thymus epithelium differentiation	177	187	182	(-)
V$HNFP	Histone nuclear factor P	V$MIZF.01	MBD2 (methyl-CpG-binding protein)-interacting zinc finger protein, histone nuclear factor P (HiNF-P)	177	189	183	(-)
V$HEAT	Heat shock factors	V$HSF2.02	Heat shock factor 2	185	209	197	(-)
V$PLAG	Pleomorphic adenoma gene	V$PLAG1.01	Pleomorphic adenoma gene (PLAG) 1, a developmentally regulated C2H2 zinc finger protein	187	209	198	(+)

V$CEBP	Ccaat/Enhancer Binding Protein	V$CEBP.02	CCAAT/enhancer binding protein	190	204	197	(+)
V$MOKF	Mouse Krueppel like factor	V$MOK2.01	Ribonucleoprotein associated zinc finger protein MOK-2 (mouse)	196	216	206	(-)
V$ZF02	C2H2 zinc finger transcription factors 2	V$ZBP89.01	Zinc finger transcription factor ZBP-89	197	219	208	(-)
V$INSM	Insulinoma associated factors	V$INSM1.01	Zinc finger protein insulinoma-associated 1 (IA-1) functions as a transcriptional repressor	197	209	203	(+)
V$NR2F	Nuclear receptor subfamily 2 factors	V$HPF1.01	HepG2-specific P450 2C factor-1, DR1 sites	199	223	211	(+)
V$PLAG	Pleomorphic adenoma gene	V$PLAG1.02	Pleomorphic adenoma gene 1	200	222	211	(+)
V$ZF02	C2H2 zinc finger transcription factors 2	V$ZF9.01	Core promoter-binding protein (CPBP) with 3 Krueppel-type zinc fingers	204	226	215	(+)
V$ZF02	C2H2 zinc finger transcription factors 2	V$ZBTB7.01	Zinc finger and BTB domain containing 7, Proto-oncogene FBI-1, Pokemon	207	229	218	(+)
V$MOKF	Mouse Krueppel like factor	V$MOK2.02	Ribonucleoprotein associated zinc finger protein MOK-2 (human)	207	227	217	(-)
V$GLIF	GLI zinc finger family	V$GLIS3.01	GLIS family zinc finger 3, Gli-similar 3	211	225	218	(+)
V$SP1F	GC-Box factors SP1/GC	V$GC.01	GC box elements	211	227	219	(-)
V$MAZF	Myc associated zinc fingers	V$MAZR.01	MYC-associated zinc finger protein related transcription factor	212	224	218	(-)
V$RREB	Ras-responsive element binding protein	V$RREB1.01	Ras-responsive element binding protein 1	219	233	226	(+)
V$BARB	Barbiturate-inducible element box from pro+eukaryotic genes	V$BARBIE.01	Barbiturate-inducible element	240	254	247	(+)
V$BRN5	Brn-5 POU domain factors	V$BRN5.03	Brn-5, POU-VI protein class (also known as emb and CNS-1)	242	264	253	(-)
V$SORY	SOX/SRY-sex/testis determinig and related HMG box factors	V$HBP1.01	HMG box-containing protein 1	242	266	254	(-)
V$MTF1	Metal induced transcription factor	V$MTF-1.02	Metal-regulatory transcription factor 1	245	259	252	(-)
V$HESF	Vertebrate homologues of enhancer of split complex	V$HES1.01	Drosophila hairy and enhancer of split homologue 1 (HES-1)	245	259	252	(+)
V$FAST	FAST-1 SMAD interacting proteins	V$FAST1.02	Forkhead box H1 (Foxh1)	246	262	254	(+)
V$HOXF	Paralog hox genes 1-8 from the four hox clusters A, B, C, D	V$NANOG.01	Homeobox transcription factor Nanog	247	265	256	(-)

V$STEM	Motif composed of binding sites for pluripotency or stem cell factors	V$OCT3_4.02	POU domain, class 5, transcription factor 1	247	265	256	(+)
V$CART	Cart-1 (cartilage homeoprotein 1)	V$PHOX2.01	Phox2a (ARIX) and Phox2b	248	268	258	(-)
V$LHXF	Lim homeodomain factors	V$LHX6.01	LIM homeobox 6	249	271	260	(+)
V$HOXF	Paralog hox genes 1-8 from the four hox clusters A, B, C, D	V$HOXA3.01	Homeobox A3	250	268	259	(-)
V$LHXF	Lim homeodomain factors	V$LHX6.01	LIM homeobox 6	250	272	261	(-)
V$HBOX	Homeobox transcription factors	V$EVX1.01	Even-skipped homeobox 1	251	269	260	(-)
V$BRNF	Brn POU domain factors	V$BRN3.03	POU class 4 homeobox 3 (POU4F3), BRN3C	252	270	261	(-)
V$HBOX	Homeobox transcription factors	V$EVX1.01	Even-skipped homeobox 1	252	270	261	(+)
V$HOXF	Paralog hox genes 1-8 from the four hox clusters A, B, C, D	V$HOXB3.01	Homeobox B3 / Hox 2-gamma	253	271	262	(+)
V$CART	Cart-1 (cartilage homeoprotein 1)	V$RHOX6.01	Reproductive homeobox 6, placenta specific homeobox 1	253	273	263	(+)
V$NKX6	NK6 homeobox transcription factors	V$NKX63.01	NK6 homeobox 3	254	268	261	(-)
V$PDX1	Pancreatic and intestinal homeodomain transcription factor	V$PDX1.01	Pdx1 (IDX1/IPF1) pancreatic and intestinal homeodomain TF	254	272	263	(-)
V$HBOX	Homeobox transcription factors	V$GSH1.01	Homeobox transcription factor Gsh-1	255	273	264	(-)
V$TALE	TALE homeodomain class recognizing TG motifs	V$TGIF.01	TG-interacting factor belonging to TALE class of homeodomain factors	264	280	272	(-)
V$NR2F	Nuclear receptor subfamily 2 factors	V$HNF4.01	Hepatic nuclear factor 4, DR1 sites	277	301	289	(-)
V$DEAF	Homolog to deformed epidermal autoregulatory factor-1 from D. melanogaster	V$NUDR.01	NUDR (nuclear DEAF-1 related transcriptional regulator protein)	280	298	289	(+)
V$RXRF	RXR heterodimer binding sites	V$VDR_RXR.03	Bipartite binding site of VDR/RXR heterodimers, DR1 sites	286	310	298	(-)
V$CLOX	CLOX and CLOX homology (CDP) factors	V$CDP.02	Transcriptional repressor CDP	288	306	297	(+)
V$ABDB	Abdominal-B type homeodomain transcription factors	V$HOXC13.01	Homeodomain transcription factor HOXC13	288	304	296	(+)
V$CAAT	CCAAT binding factors	V$NFY.04	Nuclear factor Y (Y-box binding factor)	289	303	296	(+)
V$CDXF	Vertebrate caudal related homeodomain protein	V$CDX2.03	Caudal type homeobox transcription factor 2	289	307	298	(-)
V$FAST	FAST-1 SMAD interacting proteins	V$FAST1.01	FAST-1 SMAD interacting protein	291	307	299	(-)

V$AP1R	MAF and AP1 related factors	V$MAFK.01	V-maf musculoaponeurotic fibrosarcoma oncogene homolog K (half site)	295	315	305	(+)
V$FXRE	Farnesoid X - activated receptor response elements	V$FXRE.01	Farnesoid X - activated receptor (RXR/FXR dimer), IR1 sites	302	314	308	(-)
V$ARID	AT rich interactive domain factor	V$BRIGHT.01	Bright, B cell regulator of IgH transcription	306	326	316	(-)
V$BRNF	Brn POU domain factors	V$BRN4.01	POU domain transcription factor brain 4	307	325	316	(+)
V$HOMF	Homeodomain transcription factors	V$HHEX.01	Hematopoietically expressed homeobox, proline-rich homeodomain protein	307	325	316	(+)
V$CART	Cart-1 (cartilage homeoprotein 1)	V$ISX.01	Intestine-specific homeobox	308	328	318	(-)
V$BRNF	Brn POU domain factors	V$TST1.01	POU-factor Tst-1/Oct-6	308	326	317	(-)
V$LHXF	Lim homeodomain factors	V$LHX8.01	LIM homeobox 8	309	331	320	(+)
V$DLXF	Distal-less homeodomain transcription factors	V$DLX3.01	Distal-less 3 homeodomain transcription factor	309	327	318	(+)
V$HOXF	Paralog hox genes 1-8 from the four hox clusters A, B, C, D	V$HOXA3.02	Homeobox A3	310	328	319	(-)
V$LHXF	Lim homeodomain factors	V$ISL2.01	ISL LIM homeobox 2	310	332	321	(-)
V$CLOX	CLOX and CLOX homology (CDP) factors	V$CDP.02	Transcriptional repressor CDP	311	329	320	(-)
V$HBOX	Homeobox transcription factors	V$VAX2.01	Ventral anterior homeobox 2	311	329	320	(-)
V$HOMF	Homeodomain transcription factors	V$NOBOX.01	Homeobox containing germ cell-specific transcription factor NOBOX	311	329	320	(+)
V$HBOX	Homeobox transcription factors	V$GSH2.01	Homeodomain transcription factor Gsh-2	312	330	321	(+)
V$HOMF	Homeodomain transcription factors	V$NOBOX.02	NOBOX oogenesis homeobox	312	330	321	(-)
V$NKX6	NK6 homeobox transcription factors	V$NKX61.01	NK6 homeobox 1	313	327	320	(+)
V$BCDF	Bicoid-like homeodomain transcription factors	V$PCE1.01	Photoreceptor conserved element 1	313	329	321	(+)
V$CART	Cart-1 (cartilage homeoprotein 1)	V$S8.01	Binding site for S8 type homeodomains	313	333	323	(+)
V$HOXF	Paralog hox genes 1-8 from the four hox clusters A, B, C, D	V$HOXA3.01	Homeobox A3	313	331	322	(+)
V$NKXH	NKX homeodomain factors	V$NKX25.02	Homeo domain factor Nkx-2.5/Csx, tinman homolog low affinity sites	313	331	322	(+)
V$CAAT	CCAAT binding factors	V$CAAT.01	Cellular and viral CCAAT box	314	328	321	(-)
V$DLXF	Distal-less homeodomain transcription factors	V$DLX5.01	Distal-less homeobox 5	314	332	323	(-)

O$VTBP	Vertebrate TATA binding protein factor	O$ATATA.01	Avian C-type LTR TATA box	319	335	327	(-)
V$GREF	Glucocorticoid responsive and related elements	V$ARE.03	Androgene receptor binding site, IR3 sites	327	345	336	(-)
V$SP1F	GC-Box factors SP1/GC	V$SP1.03	Stimulating protein 1, ubiquitous zinc finger transcription factor	330	346	338	(+)
V$E2FF	E2F-myc activator/cell cycle regulator	V$E2F3.01	E2F transcription factor 3	332	348	340	(+)
V$PAX5	PAX-2/5/8 binding sites	V$PAX5.01	B-cell-specific activator protein	339	367	353	(+)
V$SP1F	GC-Box factors SP1/GC	V$GC.01	GC box elements	347	363	355	(+)
V$ZF02	C2H2 zinc finger transcription factors 2	V$ZKSCAN3.01	Zinc finger with KRAB and SCAN domains 3	348	370	359	(-)
V$MAZF	Myc associated zinc fingers	V$MAZR.01	MYC-associated zinc finger protein related transcription factor	350	362	356	(+)
V$KLFS	Krueppel like transcription factors	V$KLF6.01	Kruppel-like factor 6	350	366	358	(+)
V$NRSF	Neuron-restrictive silencer factor	V$NRSF.03	Neuron-restrictive silencer factor (17 bp spacer between half sites)	357	387	372	(-)
V$AP2F	Activator protein 2	V$TCFAP2C.02	Transcription factor AP-2, gamma	363	377	370	(-)
V$RU49	Zinc finger transcription factor RU49, zinc finger proliferation 1 - Zipro1	V$RU49.01	Zinc finger transcription factor RU49 (zinc finger proliferation 1 - Zipro 1). RU49 exhibits a strong preference for binding to tandem repeats of the minimal RU49 consensus binding site.	377	383	380	(-)

References

Alaynick, W. A., Jessell, T. M., Pfaff, S. L., 2011. SnapShot: spinal cord development. Cell. 146**,** 178-178 e1.

Alexson, T. O., Hitoshi, S., Coles, B. L., Bernstein, A., van der Kooy, D., 2006. Notch signaling is required to maintain all neural stem cell populations--irrespective of spatial or temporal niche. Developmental neuroscience. 28**,** 34-48.

Arai, Y., Pulvers, J. N., Haffner, C., Schilling, B., Nusslein, I., Calegari, F., Huttner, W. B., 2011. Neural stem and progenitor cells shorten S-phase on commitment to neuron production. Nat Commun. 2**,** 154.

Bae, S., Bessho, Y., Hojo, M., Kageyama, R., 2000. The bHLH gene Hes6, an inhibitor of Hes1, promotes neuronal differentiation. Development. 127**,** 2933-2943.

Bagnoli, P., Dal Monte, M., Casini, G., 2003. Expression of neuropeptides and their receptors in the developing retina of mammals. Histol Histopathol. 18**,** 1219-42.

Bannister, A. J., Kouzarides, T., 2011. Regulation of chromatin by histone modifications. Cell Res. 21**,** 381-95.

Barnabe-Heider, F., Goritz, C., Sabelstrom, H., Takebayashi, H., Pfrieger, F. W., Meletis, K., Frisen, J., 2010. Origin of new glial cells in intact and injured adult spinal cord. Cell Stem Cell. 7**,** 470-82.

Bassett, E. A., Wallace, V. A., 2012. Cell fate determination in the vertebrate retina. Trends Neurosci. 35**,** 565-73.

Bender, E., 2015. Big data in biomedicine. Nature. 527**,** S1.

Berger, J. M., Gamblin, S. J., Harrison, S. C., Wang, J. C., 1996. Structure and mechanism of DNA topoisomerase II. Nature. 379**,** 225-32.

Bhanu, M. U., Mandraju, R. K., Bhaskar, C., Kondapi, A. K., 2010. Cultured cerebellar granule neurons as an in vitro aging model: topoisomerase IIbeta as an additional biomarker in DNA repair and aging. Toxicol In Vitro. 24**,** 1935-45.

Bonasio, R., Tu, S., Reinberg, D., 2010. Molecular signals of epigenetic states. Science. 330**,** 612-6.

Brazma, A., Jonassen, I., Eidhammer, I., Gilbert, D., 1998. Approaches to the automatic discovery of patterns in biosequences. J Comput Biol. 5**,** 279-305.

Briscoe, J., Pierani, A., Jessell, T. M., Ericson, J., 2000. A homeodomain protein code specifies progenitor cell identity and neuronal fate in the ventral neural tube. Cell. 101**,** 435-45.

Brohl, D., Strehle, M., Wende, H., Hori, K., Bormuth, I., Nave, K. A., Muller, T., Birchmeier, C., 2008. A transcriptional network coordinately determines transmitter and peptidergic fate in the dorsal spinal cord. Dev Biol. 322**,** 381-93.

Brooks, M. J., Rajasimha, H. K., Roger, J. E., Swaroop, A., 2011. Next-generation sequencing facilitates quantitative analysis of wild-type and Nrl(-/-) retinal transcriptomes. Mol Vis. 17**,** 3034-54.

Brzezinski, J. A., Reh, T. A., 2015. Photoreceptor cell fate specification in vertebrates. Development. 142**,** 3263-73.

Bucher, P., 1999. Regulatory elements and expression profiles. Curr Opin Struct Biol. 9**,** 400-7.

Catalani, E., Dal Monte, M., Gangitano, C., Lucattelli, M., Fineschi, S., Bosco, L., Bagnoli, P., Casini, G., 2006. Expression of substance P, neurokinin 1 receptors (NK1) and neurokinin 3 receptors in the developing mouse retina and in the retina of

NK1 knockout mice. Neuroscience. 138**,** 487-99.
Cau, E., Blader, P., 2009. Notch activity in the nervous system: to switch or not switch? Neural development. 4**,** 36.
Chang, F., Steelman, L. S., Lee, J. T., Shelton, J. G., Navolanic, P. M., Blalock, W. L., Franklin, R. A., McCubrey, J. A., 2003. Signal transduction mediated by the Ras/Raf/MEK/ERK pathway from cytokine receptors to transcription factors: potential targeting for therapeutic intervention. Leukemia. 17**,** 1263-93.
Chen, J., Leong, S. Y., Schachner, M., 2005. Differential expression of cell fate determinants in neurons and glial cells of adult mouse spinal cord after compression injury. The European journal of neuroscience. 22**,** 1895-906.
Chenn, A., McConnell, S. K., 1995. Cleavage orientation and the asymmetric inheritance of Notch1 immunoreactivity in mammalian neurogenesis. Cell. 82**,** 631-41.
Conaway, R. C., Conaway, J. W., 2011. Function and regulation of the Mediator complex. Curr Opin Genet Dev. 21**,** 225-30.
Corbo, J. C., Lawrence, K. A., Karlstetter, M., CRX ChIP-seq reveals the cis-regulatory architecture of mouse photoreceptors. Vol. 20, 2010, pp. 1512-1525.
Core, L. J., Waterfall, J. J., Lis, J. T., 2008. Nascent RNA sequencing reveals widespread pausing and divergent initiation at human promoters. Science. 322**,** 1845-8.
Coulon, A., Chow, C. C., Singer, R. H., Larson, D. R., 2013. Eukaryotic transcriptional dynamics: from single molecules to cell populations. Nat Rev Genet. 14**,** 572-84.
Cristiani, R., Petrucci, C., Dal Monte, M., Bagnoli, P., 2002. Somatostatin (SRIF) and SRIF receptors in the mouse retina. Brain Res. 936**,** 1-14.
D'Onofrio, P. M., Thayapararajah, M., Lysko, M. D., Magharious, M., Spratt, S. K., Lee, G., Ando, D., Surosky, R., Fehlings, M. G., Koeberle, P. D., 2011. Gene therapy for traumatic central nervous system injury and stroke using an engineered zinc finger protein that upregulates VEGF-A. J Neurotrauma. 28**,** 1863-79.
David, S., Kroner, A., 2011. Repertoire of microglial and macrophage responses after spinal cord injury. Nat Rev Neurosci. 12**,** 388-99.
Del Barrio, M. G., Taveira-Marques, R., Muroyama, Y., Yuk, D. I., Li, S., Wines-Samuelson, M., Shen, J., Smith, H. K., Xiang, M., Rowitch, D., Richardson, W. D., 2007. A regulatory network involving Foxn4, Mash1 and delta-like 4/Notch1 generates V2a and V2b spinal interneurons from a common progenitor pool. Development. 134**,** 3427-36.
Dingledine, R., Borges, K., Bowie, D., Traynelis, S. F., 1999. The glutamate receptor ion channels. Pharmacol Rev. 51**,** 7-61.
Dudek, H., Datta, S. R., Franke, T. F., Birnbaum, M. J., Yao, R., Cooper, G. M., Segal, R. A., Kaplan, D. R., Greenberg, M. E., 1997. Regulation of neuronal survival by the serine-threonine protein kinase Akt. Science. 275**,** 661-5.
Ericson, J., Briscoe, J., Rashbass, P., van Heyningen, V., Jessell, T. M., 1997. Graded sonic hedgehog signaling and the specification of cell fate in the ventral neural tube. Cold Spring Harb Symp Quant Biol. 62**,** 451-66.
Estrada, V., Muller, H. W., 2014. Spinal cord injury - there is not just one way of treating it. F1000Prime Rep. 6**,** 84.
Fariss, R. N., Molday, R. S., Fisher, S. K., Matsumoto, B., 1997. Evidence from normal and degenerating photoreceptors that two outer segment integral membrane proteins have separate transport pathways. J Comp Neurol. 387**,** 148-56.
Farooque, M., 2000. Spinal cord compression injury in the mouse: presentation of a model including assessment of motor dysfunction. Acta neuropathologica. 100**,**

13-22.
Felix, M. A., Wagner, A., 2008. Robustness and evolution: concepts, insights and challenges from a developmental model system. Heredity (Edinb). 100**,** 132-40.
Fischer, A. J., Scott, M. A., Zelinka, C., Sherwood, P., 2010. A novel type of glial cell in the retina is stimulated by insulin-like growth factor 1 and may exacerbate damage to neurons and Muller glia. Glia. 58**,** 633-49.
Fisher, S. K., Lewis, G. P., Linberg, K. A., Barawid, E., Verardo, M. R., Cellular Remodeling in Mammalian Retina Induced by Retinal Detachment. In: H. Kolb, E. Fernandez, R. Nelson, Eds.), Webvision: The Organization of the Retina and Visual System, Salt Lake City (UT), 1995.
Flicek, P., Amode, M. R., Barrell, D., Beal, K., Brent, S., Carvalho-Silva, D., Clapham, P., Coates, G., Fairley, S., Fitzgerald, S., Gil, L., Gordon, L., Hendrix, M., Hourlier, T., Johnson, N., Kahari, A. K., Keefe, D., Keenan, S., Kinsella, R., Komorowska, M., Koscielny, G., Kulesha, E., Larsson, P., Longden, I., McLaren, W., Muffato, M., Overduin, B., Pignatelli, M., Pritchard, B., Riat, H. S., Ritchie, G. R., Ruffier, M., Schuster, M., Sobral, D., Tang, Y. A., Taylor, K., Trevanion, S., Vandrovcova, J., White, S., Wilson, M., Wilder, S. P., Aken, B. L., Birney, E., Cunningham, F., Dunham, I., Durbin, R., Fernandez-Suarez, X. M., Harrow, J., Herrero, J., Hubbard, T. J., Parker, A., Proctor, G., Spudich, G., Vogel, J., Yates, A., Zadissa, A., Searle, S. M., 2012. Ensembl 2012. Nucleic Acids Res. 40**,** D84-90.
Francke, M., Faude, F., Pannicke, T., Bringmann, A., Eckstein, P., Reichelt, W., Wiedemann, P., Reichenbach, A., 2001. Electrophysiology of rabbit Muller (glial) cells in experimental retinal detachment and PVR. Invest Ophthalmol Vis Sci. 42**,** 1072-9.
Frey, E., Valakh, V., Karney-Grobe, S., Shi, Y., Milbrandt, J., DiAntonio, A., 2015. An in vitro assay to study induction of the regenerative state in sensory neurons. Exp Neurol. 263**,** 350-63.
Gamsiz, E. D., Ouyang, Q., Schmidt, M., Nagpal, S., Morrow, E. M., 2012. Genome-wide transcriptome analysis in murine neural retina using high-throughput RNA sequencing. Genomics. 99**,** 44-51.
Godinho, L., Williams, P. R., Claassen, Y., Provost, E., Leach, S. D., Kamermans, M., Wong, R. O., 2007. Nonapical symmetric divisions underlie horizontal cell layer formation in the developing retina in vivo. Neuron. 56**,** 597-603.
Grandbarbe, L., Bouissac, J., Rand, M., Hrabe de Angelis, M., Artavanis-Tsakonas, S., Mohier, E., 2003. Delta-Notch signaling controls the generation of neurons/glia from neural stem cells in a stepwise process. Development. 130**,** 1391-402.
Guerin, C. J., Anderson, D. H., Fisher, S. K., 1990. Changes in intermediate filament immunolabeling occur in response to retinal detachment and reattachment in primates. Invest Ophthalmol Vis Sci. 31**,** 1474-82.
Harada, H., Andersen, J. S., Mann, M., Terada, N., Korsmeyer, S. J., 2001. p70S6 kinase signals cell survival as well as growth, inactivating the pro-apoptotic molecule BAD. Proc Natl Acad Sci U S A. 98**,** 9666-70.
Harada, T., Harada, C., Parada, L. F., 2007. Molecular regulation of visual system development: more than meets the eye. Genes Dev. 21**,** 367-78.
Hatakeyama, J., Tomita, K., Inoue, T., Kageyama, R., 2001. Roles of homeobox and bHLH genes in specification of a retinal cell type. Development. 128**,** 1313-1322.
Hebert, J. M., McConnell, S. K., 2000. Targeting of cre to the Foxg1 (BF-1) locus mediates loxP recombination in the telencephalon and other developing head structures. Dev Biol. 222**,** 296-306.

Heng, X., Jin, G., Zhang, X., Yang, D., Zhu, M., Fu, S., Li, X., Le, W., 2012. Nurr1 regulates Top IIbeta and functions in axon genesis of mesencephalic dopaminergic neurons. Mol Neurodegener. 7**,** 4.

Horky, L. L., Galimi, F., Gage, F. H., Horner, P. J., 2006. Fate of endogenous stem/progenitor cells following spinal cord injury. J Comp Neurol. 498**,** 525-38.

Horner, P. J., Power, A. E., Kempermann, G., Kuhn, H. G., Palmer, T. D., Winkler, J., Thal, L. J., Gage, F. H., 2000. Proliferation and differentiation of progenitor cells throughout the intact adult rat spinal cord. J Neurosci. 20**,** 2218-28.

Hsiau, T. H. C., Diaconu, C., Myers, C. A., Lee, J., Cepko, C. L., Corbo, J. C., 2007. The Cis-regulatory Logic of the Mammalian Photoreceptor Transcriptional Network. PLoS ONE. 2**,** e643.

Hu, J., Wan, J., Hackler, L., Jr., Zack, D. J., Qian, J., 2010. Computational analysis of tissue-specific gene networks: application to murine retinal functional studies. Bioinformatics. 26**,** 2289-97.

Iulianella, A., Sharma, M., Vanden Heuvel, G. B., Trainor, P. A., 2009. Cux2 functions downstream of Notch signaling to regulate dorsal interneuron formation in the spinal cord. Development. 136**,** 2329-2334.

Jacob, F., Monod, J., 1961. Genetic regulatory mechanisms in the synthesis of proteins. J Mol Biol. 3**,** 318-56.

Jin, K., Zhu, Y., Sun, Y., Mao, X. O., Xie, L., Greenberg, D. A., 2002. Vascular endothelial growth factor (VEGF) stimulates neurogenesis in vitro and in vivo. Proc Natl Acad Sci U S A. 99**,** 11946-50.

Johnson, D. S., Mortazavi, A., Myers, R. M., Wold, B., 2007. Genome-wide mapping of in vivo protein-DNA interactions. Science. 316**,** 1497-502.

Ju, B. G., Lunyak, V. V., Perissi, V., Garcia-Bassets, I., Rose, D. W., Glass, C. K., Rosenfeld, M. G., 2006. A topoisomerase IIbeta-mediated dsDNA break required for regulated transcription. Science. 312**,** 1798-802.

Kawaguchi, D., Yoshimatsu, T., Hozumi, K., Gotoh, Y., 2008. Selection of differentiating cells by different levels of delta-like 1 among neural precursor cells in the developing mouse telencephalon. Development. 135**,** 3849-58.

Kim, D. S., Matsuda, T., Cepko, C. L., 2008. A Core Paired-Type and POU Homeodomain-Containing Transcription Factor Program Drives Retinal Bipolar Cell Gene Expression. Journal of Neuroscience. 28**,** 7748-7764.

King, I. F., Yandava, C. N., Mabb, A. M., Hsiao, J. S., Huang, H. S., Pearson, B. L., Calabrese, J. M., Starmer, J., Parker, J. S., Magnuson, T., Chamberlain, S. J., Philpot, B. D., Zylka, M. J., 2013. Topoisomerases facilitate transcription of long genes linked to autism. Nature. 501**,** 58-62.

Kinner, A., Wu, W., Staudt, C., Iliakis, G., 2008. Gamma-H2AX in recognition and signaling of DNA double-strand breaks in the context of chromatin. Nucleic Acids Res. 36**,** 5678-94.

Kobayashi, Y., Okada, Y., Itakura, G., Iwai, H., Nishimura, S., Yasuda, A., Nori, S., Hikishima, K., Konomi, T., Fujiyoshi, K., Tsuji, O., Toyama, Y., Yamanaka, S., Nakamura, M., Okano, H., 2012. Pre-evaluated safe human iPSC-derived neural stem cells promote functional recovery after spinal cord injury in common marmoset without tumorigenicity. PLoS One. 7**,** e52787.

Kouzine, F., Gupta, A., Baranello, L., Wojtowicz, D., Ben-Aissa, K., Liu, J., Przytycka, T. M., Levens, D., 2013a. Transcription-dependent dynamic supercoiling is a short-range genomic force. Nat Struct Mol Biol. 20**,** 396-403.

Kouzine, F., Wojtowicz, D., Yamane, A., Resch, W., Kieffer-Kwon, K. R., Bandle, R.,

Nelson, S., Nakahashi, H., Awasthi, P., Feigenbaum, L., Menoni, H., Hoeijmakers, J., Vermeulen, W., Ge, H., Przytycka, T. M., Levens, D., Casellas, R., 2013b. Global regulation of promoter melting in naive lymphocytes. Cell. 153**,** 988-99.

Krivega, I., Dean, A., 2012. Enhancer and promoter interactions-long distance calls. Curr Opin Genet Dev. 22**,** 79-85.

Kumar, J. P., 2009. The molecular circuitry governing retinal determination. Biochimica et biophysica acta. 1789**,** 306-14.

Kungel, M., Piechotta, K., Rietzel, H. J., Friauf, E., 1997. Influence of the neuropeptide somatostatin on the development of dendritic morphology: a cysteamine-depletion study in the rat auditory brainstem. Brain Res Dev Brain Res. 101**,** 107-14.

Kuo, L. J., Yang, L. X., 2008. Gamma-H2AX - a novel biomarker for DNA double-strand breaks. In Vivo. 22**,** 305-9.

Kuribayashi, K., Mayes, P. A., El-Deiry, W. S., 2006. What are caspases 3 and 7 doing upstream of the mitochondria? Cancer Biol Ther. 5**,** 763-5.

Lahlou, H., Saint-Laurent, N., Esteve, J. P., Eychene, A., Pradayrol, L., Pyronnet, S., Susini, C., 2003. sst2 Somatostatin receptor inhibits cell proliferation through Ras-, Rap1-, and B-Raf-dependent ERK2 activation. The Journal of biological chemistry. 278**,** 39356-71.

Langmead, B., Trapnell, C., Pop, M., Salzberg, S. L., 2009. Ultrafast and memory-efficient alignment of short DNA sequences to the human genome. Genome Biology. 10**,** R25.

Lee, T. I., Young, R. A., 2013. Transcriptional regulation and its misregulation in disease. Cell. 152**,** 1237-51.

Li, T. K., Chen, A. Y., Yu, C., Mao, Y., Wang, H., Liu, L. F., 1999. Activation of topoisomerase II-mediated excision of chromosomal DNA loops during oxidative stress. Genes Dev. 13**,** 1553-60.

Li, Y., Hao, H., Tzatzalos, E., Lin, R. K., Doh, S., Liu, L. F., Lyu, Y. L., Cai, L., 2014. Topoisomerase IIbeta is required for proper retinal development and survival of postmitotic cells. Biol Open. 3**,** 172-184.

Li, Y., Huang, H., Cai, L., Prediction of Transcriptional Regulatory Networks for Retinal Development. In: H. S. Lopes, L. M. Cruz, Eds.), Computational Biology and Applied Bioinformatics. InTech, 2011, pp. 357-374.

Lin, R. K., Ho, C. W., Liu, L. F., Lyu, Y. L., 2013. Topoisomerase IIbeta deficiency enhances camptothecin-induced apoptosis. J Biol Chem. 288**,** 7182-92.

Llorens-Bobadilla, E., Zhao, S., Baser, A., Saiz-Castro, G., Zwadlo, K., Martin-Villalba, A., 2015. Single-Cell Transcriptomics Reveals a Population of Dormant Neural Stem Cells that Become Activated upon Brain Injury. Cell Stem Cell. 17**,** 329-40.

London, A., Benhar, I., Schwartz, M., 2013. The retina as a window to the brain-from eye research to CNS disorders. Nat Rev Neurol. 9**,** 44-53.

Louie, C. M., Caridi, G., Lopes, V. S., Brancati, F., Kispert, A., Lancaster, M. A., Schlossman, A. M., Otto, E. A., Leitges, M., Grone, H. J., Lopez, I., Gudiseva, H. V., O'Toole, J. F., Vallespin, E., Ayyagari, R., Ayuso, C., Cremers, F. P., den Hollander, A. I., Koenekoop, R. K., Dallapiccola, B., Ghiggeri, G. M., Hildebrandt, F., Valente, E. M., Williams, D. S., Gleeson, J. G., 2010. AHI1 is required for photoreceptor outer segment development and is a modifier for retinal degeneration in nephronophthisis. Nat Genet. 42**,** 175-80.

Lu, P., Wang, Y., Graham, L., McHale, K., Gao, M., Wu, D., Brock, J., Blesch, A., Rosenzweig, E. S., Havton, L. A., Zheng, B., Conner, J. M., Marsala, M.,

Tuszynski, M. H., 2012. Long-distance growth and connectivity of neural stem cells after severe spinal cord injury. Cell. 150**,** 1264-73.

Luo, Y., Coskun, V., Liang, A., Yu, J., Cheng, L., Ge, W., Shi, Z., Zhang, K., Li, C., Cui, Y., Lin, H., Luo, D., Wang, J., Lin, C., Dai, Z., Zhu, H., Zhang, J., Liu, J., Liu, H., deVellis, J., Horvath, S., Sun, Y. E., Li, S., 2015. Single-cell transcriptome analyses reveal signals to activate dormant neural stem cells. Cell. 161**,** 1175-86.

Lupo, R., Breiling, A., Bianchi, M. E., Orlando, V., 2001. Drosophila chromosome condensation proteins Topoisomerase II and Barren colocalize with Polycomb and maintain Fab-7 PRE silencing. Mol Cell. 7**,** 127-36.

Lyu, Y. L., Kerrigan, J. E., Lin, C. P., Azarova, A. M., Tsai, Y. C., Ban, Y., Liu, L. F., 2007. Topoisomerase IIbeta mediated DNA double-strand breaks: implications in doxorubicin cardiotoxicity and prevention by dexrazoxane. Cancer Res. 67**,** 8839-46.

Lyu, Y. L., Lin, C. P., Azarova, A. M., Cai, L., Wang, J. C., Liu, L. F., 2006. Role of topoisomerase IIbeta in the expression of developmentally regulated genes. Mol Cell Biol. 26**,** 7929-41.

Lyu, Y. L., Wang, J. C., 2003a. Aberrant lamination in the cerebral cortex of mouse embryos lacking DNA topoisomerase IIbeta. Proceedings of the National Academy of Sciences of the United States of America. 100**,** 7123-8.

Lyu, Y. L., Wang, J. C., 2003b. Aberrant lamination in the cerebral cortex of mouse embryos lacking DNA topoisomerase IIbeta. Proc Natl Acad Sci U S A. 100**,** 7123-8.

Marquardt, T., Ashery-Padan, R., Andrejewski, N., Scardigli, R., Guillemot, F., Gruss, P., 2001. Pax6 is required for the multipotent state of retinal progenitor cells. Cell. 105**,** 43-55.

Marquardt, T., Gruss, P., 2002. Generating neuronal diversity in the retina: one for nearly all. Trends Neurosci. 25**,** 32-8.

Mason, H. A., Rakowiecki, S. M., Gridley, T., Fishell, G., 2006. Loss of notch activity in the developing central nervous system leads to increased cell death. Developmental neuroscience. 28**,** 49-57.

McConnell, S. K., 1991. The generation of neuronal diversity in the central nervous system. Annu Rev Neurosci. 14**,** 269-300.

McConnell, S. K., Kaznowski, C. E., 1991. Cell cycle dependence of laminar determination in developing neocortex. Science. 254**,** 282-5.

Meier, P., Finch, A., Evan, G., 2000. Apoptosis in development. Nature. 407**,** 796-801.

Meletis, K., Barnabe-Heider, F., Carlen, M., Evergren, E., Tomilin, N., Shupliakov, O., Frisen, J., 2008. Spinal cord injury reveals multilineage differentiation of ependymal cells. PLoS Biology. 6**,** e182.

Merico, D., Isserlin, R., Stueker, O., Emili, A., Bader, G. D., 2010. Enrichment map: a network-based method for gene-set enrichment visualization and interpretation. PLoS ONE. 5**,** e13984.

Meyer-Ficca, M. L., Lonchar, J. D., Ihara, M., Meistrich, M. L., Austin, C. A., Meyer, R. G., 2011. Poly(ADP-ribose) polymerases PARP1 and PARP2 modulate topoisomerase II beta (TOP2B) function during chromatin condensation in mouse spermiogenesis. Biol Reprod. 84**,** 900-9.

Meyer-Franke, A., Kaplan, M. R., Pfrieger, F. W., Barres, B. A., 1995. Characterization of the signaling interactions that promote the survival and growth of developing retinal ganglion cells in culture. Neuron. 15**,** 805-19.

Millan, C., Lujan, R., Shigemoto, R., Sanchez-Prieto, J., 2002. The inhibition of

glutamate release by metabotropic glutamate receptor 7 affects both [Ca2+]c and cAMP: evidence for a strong reduction of Ca2+ entry in single nerve terminals. J Biol Chem. 277**,** 14092-101.

Moreno-Manzano, V., Rodriguez-Jimenez, F. J., Garcia-Rosello, M., Lainez, S., Erceg, S., Calvo, M. T., Ronaghi, M., Lloret, M., Planells-Cases, R., Sanchez-Puelles, J. M., Stojkovic, M., 2009. Activated spinal cord ependymal stem cells rescue neurological function. Stem Cells. 27**,** 733-43.

Morozova, O., Marra, M. A., 2008. Applications of next-generation sequencing technologies in functional genomics. Genomics. 92**,** 255-64.

Naughton, C., Avlonitis, N., Corless, S., Prendergast, J. G., Mati, I. K., Eijk, P. P., Cockroft, S. L., Bradley, M., Ylstra, B., Gilbert, N., 2013. Transcription forms and remodels supercoiling domains unfolding large-scale chromatin structures. Nat Struct Mol Biol. 20**,** 387-95.

Nevin, L. M., Xiao, T., Staub, W., Baier, H., 2011a. Topoisomerase II{beta} is required for lamina-specific targeting of retinal ganglion cell axons and dendrites. Development. 138**,** 2457-65.

Nevin, L. M., Xiao, T., Staub, W., Baier, H., 2011b. Topoisomerase IIbeta is required for lamina-specific targeting of retinal ganglion cell axons and dendrites. Development. 138**,** 2457-65.

Nitiss, J. L., 2009. DNA topoisomerase II and its growing repertoire of biological functions. Nat Rev Cancer. 9**,** 327-37.

Nur, E. K. A., Meiners, S., Ahmed, I., Azarova, A., Lin, C. P., Lyu, Y. L., Liu, L. F., 2007. Role of DNA topoisomerase IIbeta in neurite outgrowth. Brain Res. 1154**,** 50-60.

Ogawa, Y., Sawamoto, K., Miyata, T., Miyao, S., Watanabe, M., Nakamura, M., Bregman, B. S., Koike, M., Uchiyama, Y., Toyama, Y., Okano, H., 2002. Transplantation of in vitro-expanded fetal neural progenitor cells results in neurogenesis and functional recovery after spinal cord contusion injury in adult rats. J Neurosci Res. 69**,** 925-33.

Ohori, Y., Yamamoto, S., Nagao, M., Sugimori, M., Yamamoto, N., Nakamura, K., Nakafuku, M., 2006. Growth factor treatment and genetic manipulation stimulate neurogenesis and oligodendrogenesis by endogenous neural progenitors in the injured adult spinal cord. J Neurosci. 26**,** 11948-60.

Okigawa, S., Mizoguchi, T., Okano, M., Tanaka, H., Isoda, M., Jiang, Y. J., Suster, M., Higashijima, S., Kawakami, K., Itoh, M., 2014. Different combinations of Notch ligands and receptors regulate V2 interneuron progenitor proliferation and V2a/V2b cell fate determination. Dev Biol. 391**,** 196-206.

Peng, C. Y., Yajima, H., Burns, C. E., Zon, L. I., Sisodia, S. S., Pfaff, S. L., Sharma, K., 2007. Notch and MAML signaling drives Scl-dependent interneuron diversity in the spinal cord. Neuron. 53**,** 813-27.

Picard-Riera, N., Nait-Oumesmar, B., Baron-Van Evercooren, A., 2004. Endogenous adult neural stem cells: limits and potential to repair the injured central nervous system. J Neurosci Res. 76**,** 223-31.

Pierfelice, T., Alberi, L., Gaiano, N., 2011. Notch in the vertebrate nervous system: an old dog with new tricks. Neuron. 69**,** 840-55.

Pinzon-Guzman, C., Zhang, S. S., Barnstable, C. J., 2011. Specific protein kinase C isoforms are required for rod photoreceptor differentiation. The Journal of neuroscience : the official journal of the Society for Neuroscience. 31**,** 18606-17.

Poitry, S., Poitry-Yamate, C., Ueberfeld, J., MacLeish, P. R., Tsacopoulos, M., 2000. Mechanisms of glutamate metabolic signaling in retinal glial (Muller) cells. J

Neurosci. 20**,** 1809-21.
Redmond, L., Oh, S. R., Hicks, C., Weinmaster, G., Ghosh, A., 2000. Nuclear Notch1 signaling and the regulation of dendritic development. Nat Neurosci. 3**,** 30-40.
Ren, B., Robert, F., Wyrick, J. J., Aparicio, O., Jennings, E. G., Simon, I., Zeitlinger, J., Schreiber, J., Hannett, N., Kanin, E., Volkert, T. L., Wilson, C. J., Bell, S. P., Young, R. A., 2000. Genome-wide location and function of DNA binding proteins. Science. 290**,** 2306-9.
Reynolds, B. A., Rietze, R. L., 2005. Neural stem cells and neurospheres--re-evaluating the relationship. Nat Methods. 2**,** 333-6.
Rice, D. S., Curran, T., 2001. Role of the reelin signaling pathway in central nervous system development. Annu Rev Neurosci. 24**,** 1005-39.
Rice, D. S., Nusinowitz, S., Azimi, A. M., Martinez, A., Soriano, E., Curran, T., 2001. The reelin pathway modulates the structure and function of retinal synaptic circuitry. Neuron. 31**,** 929-41.
Robinson, G. S., Ju, M., Shih, S. C., Xu, X., McMahon, G., Caldwell, R. B., Smith, L. E., 2001. Nonvascular role for VEGF: VEGFR-1, 2 activity is critical for neural retinal development. FASEB J. 15**,** 1215-7.
Rowland, J. W., Hawryluk, G. W., Kwon, B., Fehlings, M. G., 2008. Current status of acute spinal cord injury pathophysiology and emerging therapies: promise on the horizon. Neurosurg Focus. 25**,** E2.
Sabelstrom, H., Stenudd, M., Frisen, J., 2013. Neural stem cells in the adult spinal cord. Exp Neurol.
Salic, A., Mitchison, T. J., 2008. A chemical method for fast and sensitive detection of DNA synthesis in vivo. Proc Natl Acad Sci U S A. 105**,** 2415-20.
Sano, K., Miyaji-Yamaguchi, M., Tsutsui, K. M., Tsutsui, K., 2008. Topoisomerase IIbeta activates a subset of neuronal genes that are repressed in AT-rich genomic environment. PLoS One. 3**,** e4103.
Sato, S., Inoue, T., Terada, K., Matsuo, I., Aizawa, S., Tano, Y., Fujikado, T., Furukawa, T., 2007. Dkk3-Cre BAC transgenic mouse line: a tool for highly efficient gene deletion in retinal progenitor cells. genesis. 45**,** 502-7.
Shin, J., Berg, D. A., Zhu, Y., Shin, J. Y., Song, J., Bonaguidi, M. A., Enikolopov, G., Nauen, D. W., Christian, K. M., Ming, G. L., Song, H., 2015. Single-Cell RNA-Seq with Waterfall Reveals Molecular Cascades underlying Adult Neurogenesis. Cell Stem Cell. 17**,** 360-72.
Spitz, F., Furlong, E. E., 2012. Transcription factors: from enhancer binding to developmental control. Nat Rev Genet. 13**,** 613-26.
Stegle, O., Teichmann, S. A., Marioni, J. C., 2015. Computational and analytical challenges in single-cell transcriptomics. Nat Rev Genet. 16**,** 133-45.
Su, Z., Niu, W., Liu, M. L., Zou, Y., Zhang, C. L., 2014. In vivo conversion of astrocytes to neurons in the injured adult spinal cord. Nat Commun. 5**,** 3338.
Subramanian, A., Tamayo, P., Mootha, V. K., Mukherjee, S., Ebert, B. L., Gillette, M. A., Paulovich, A., Pomeroy, S. L., Golub, T. R., Lander, E. S., Mesirov, J. P., 2005. Gene set enrichment analysis: a knowledge-based approach for interpreting genome-wide expression profiles. Proc Natl Acad Sci U S A. 102**,** 15545-50.
Swaroop, A., Kim, D., Forrest, D., 2010. Transcriptional regulation of photoreceptor development and homeostasis in the mammalian retina. Nature reviews. Neuroscience. 11**,** 563-76.
The National SCI Statistical Center, Spinal Cord Injury (SCI) Facts and Figures at a Glance. University of Alabama at Birmingham, Birmingham, Alabama, 2015.

Tiwari, V. K., Burger, L., Nikoletopoulou, V., Deogracias, R., Thakurela, S., Wirbelauer, C., Kaut, J., Terranova, R., Hoerner, L., Mielke, C., Boege, F., Murr, R., Peters, A. H., Barde, Y. A., Schubeler, D., 2012. Target genes of Topoisomerase IIbeta regulate neuronal survival and are defined by their chromatin state. Proc Natl Acad Sci U S A. 109**,** E934-43.

Tomita, S., Ueno, M., Sakamoto, M., Kitahama, Y., Ueki, M., Maekawa, N., Sakamoto, H., Gassmann, M., Kageyama, R., Ueda, N., Gonzalez, F. J., Takahama, Y., 2003. Defective brain development in mice lacking the Hif-1alpha gene in neural cells. Mol Cell Biol. 23**,** 6739-49.

Trapnell, C., Roberts, A., Goff, L., Pertea, G., Kim, D., Kelley, D. R., Pimentel, H., Salzberg, S. L., Rinn, J. L., Pachter, L., 2012. Differential gene and transcript expression analysis of RNA-seq experiments with TopHat and Cufflinks. Nat Protoc. 7**,** 562-78.

Trapnell, C., Williams, B. A., Pertea, G., Mortazavi, A., Kwan, G., van Baren, M. J., Salzberg, S. L., Wold, B. J., Pachter, L., 2010. Transcript assembly and quantification by RNA-Seq reveals unannotated transcripts and isoform switching during cell differentiation. Nature Biotechnology. 28**,** 511-5.

Tsutsui, K., Hosoya, O., Sano, K., Tokunaga, A., 2001a. Immunohistochemical analyses of DNA topoisomerase II isoforms in developing rat cerebellum. J. Comp. Neurol. 431**,** 228-239.

Tsutsui, K., Okada, S., Watanabe, M., Shohmori, T., Seki, S., Inoue, Y., 1993. Molecular cloning of partial cDNAs for rat DNA topoisomerase II isoforms and their differential expression in brain development. Journal of Biological Chemistry. 268**,** 19076-19083.

Tsutsui, K., Sano, K., Kikuchi, A., Tokunaga, A., 2001b. Involvement of DNA topoisomerase IIbeta in neuronal differentiation. The Journal of biological chemistry. 276**,** 5769-78.

Tsutsui, K., Tsutsui, K., Sano, K., Kikuchi, A., Tokunaga, A., 2001c. Involvement of DNA topoisomerase IIbeta in neuronal differentiation. J Biol Chem. 276**,** 5769-78.

Tzatzalos, E., Smith, S. M., Doh, S. T., Hao, H., Li, Y., Wu, A., Grumet, M., Cai, L., 2012. A cis-element in the Notch1 locus is involved in the regulation of gene expression in interneuron progenitors. Dev Biol. 372**,** 217-28.

Uemura, T., Lee, S. J., Yasumura, M., Takeuchi, T., Yoshida, T., Ra, M., Taguchi, R., Sakimura, K., Mishina, M., 2010. Trans-synaptic interaction of GluRdelta2 and Neurexin through Cbln1 mediates synapse formation in the cerebellum. Cell. 141**,** 1068-79.

Vavouri, T., Walter, K., Gilks, W. R., Lehner, B., Elgar, G., 2007. Parallel evolution of conserved non-coding elements that target a common set of developmental regulatory genes from worms to humans. Genome Biology. 8**,** R15.

Visel, A., Blow, M. J., Li, Z., Zhang, T., Akiyama, J. A., Holt, A., Plajzer-Frick, I., Shoukry, M., Wright, C., Chen, F., Afzal, V., Ren, B., Rubin, E. M., Pennacchio, L. A., 2009. ChIP-seq accurately predicts tissue-specific activity of enhancers. Nature. 457**,** 854-858.

Visel, A., Minovitsky, S., Dubchak, I., Pennacchio, L. A., 2007. VISTA Enhancer Browser—a database of tissue-specific human enhancers. Nucleic Acids Research. 35**,** D88-D92.

Wang, J. C., 1998. Moving one DNA double helix through another by a type II DNA topoisomerase: the story of a simple molecular machine. Q Rev Biophys. 31**,** 107-44.

Wang, J. C., 2002. Cellular roles of DNA topoisomerases: a molecular perspective. Nat Rev Mol Cell Biol. 3**,** 430-40.

Wasserman, W. W., Sandelin, A., 2004. Applied bioinformatics for the identification of regulatory elements. Nat Rev Genet. 5**,** 276-87.

Xiang, M., 1998. Requirement for Brn-3b in early differentiation of postmitotic retinal ganglion cell precursors. Dev Biol. 197**,** 155-69.

Xiang, M., Zhou, L., Macke, J. P., Yoshioka, T., Hendry, S. H., Eddy, R. L., Shows, T. B., Nathans, J., 1995. The Brn-3 family of POU-domain factors: primary structure, binding specificity, and expression in subsets of retinal ganglion cells and somatosensory neurons. J Neurosci. 15**,** 4762-85.

Xiang, M., Zhou, L., Peng, Y. W., Eddy, R. L., Shows, T. B., Nathans, J., 1993. Brn-3b: a POU domain gene expressed in a subset of retinal ganglion cells. Neuron. 11**,** 689-701.

Yamamoto, S., Yamamoto, N., Kitamura, T., Nakamura, K., Nakafuku, M., 2001. Proliferation of parenchymal neural progenitors in response to injury in the adult rat spinal cord. Exp Neurol. 172**,** 115-27.

Yang, H., Lu, P., McKay, H. M., Bernot, T., Keirstead, H., Steward, O., Gage, F. H., Edgerton, V. R., Tuszynski, M. H., 2006a. Endogenous neurogenesis replaces oligodendrocytes and astrocytes after primate spinal cord injury. J Neurosci. 26**,** 2157-66.

Yang, N., Zuchero, J. B., Ahlenius, H., Marro, S., Ng, Y. H., Vierbuchen, T., Hawkins, J. S., Geissler, R., Barres, B. A., Wernig, M., 2013. Generation of oligodendroglial cells by direct lineage conversion. Nat Biotechnol. 31**,** 434-9.

Yang, X., Li, W., Prescott, E. D., Burden, S. J., Wang, J. C., 2000. DNA topoisomerase IIbeta and neural development. Science. 287**,** 131-4.

Yang, X., Tomita, T., Wines-Samuelson, M., Beglopoulos, V., Tansey, M. G., Kopan, R., Shen, J., 2006b. Notch1 signaling influences v2 interneuron and motor neuron development in the spinal cord. Developmental neuroscience. 28**,** 102-17.

Yin, J., Morrissey, M. E., Shine, L., Kennedy, C., Higgins, D. G., Kennedy, B. N., 2014. Genes and signaling networks regulated during zebrafish optic vesicle morphogenesis. BMC Genomics. 15**,** 825.

Yiu, G., He, Z., 2006. Glial inhibition of CNS axon regeneration. Nat Rev Neurosci. 7**,** 617-27.

Young, R. W., 1985a. Cell differentiation in the retina of the mouse. Anat Rec. 212**,** 199-205.

Young, R. W., 1985b. Cell differentiation in the retina of the mouse. The Anatomical record. 212**,** 199-205.

Young, R. W., 1985c. Cell proliferation during postnatal development of the retina in the mouse. Brain research. 353**,** 229-39.

Yuan, J., Lipinski, M., Degterev, A., 2003. Diversity in the mechanisms of neuronal cell death. Neuron. 40**,** 401-13.

Zalutsky, R. A., Miller, R. F., 1990. The physiology of substance P in the rabbit retina. J Neurosci. 10**,** 394-402.